UiT
THE ARCTIC UNIVERSITY OF NORWAY

Faculty of science and technology

Department of geology

Triassic Channel Systems on the northern Loppa High, SW Barents Sea

Marit Arntzen

Master's thesis in Geology, GEO-3900
June 2018

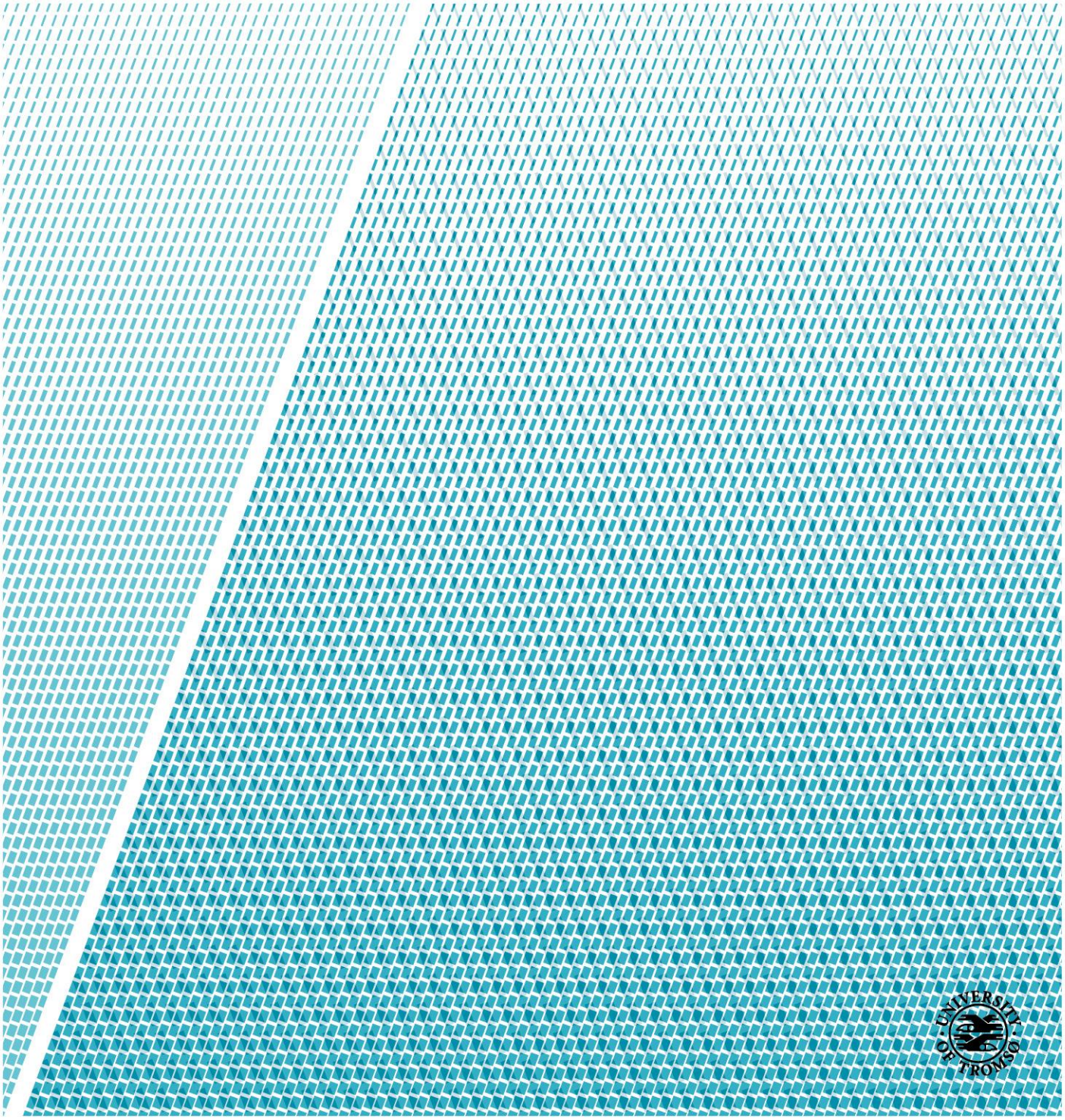

Abstract

During the Triassic, the Barents Sea Basin was filled with sediments from the Uralian and Caledonian mountain belts. High sediment yield and large river systems made progradation possible, resulting in an alluvial to deltaic plain stretching from the mountain belts in the south east to Spitsbergen in the north.

This thesis focuses on the northwestern part of the Loppa High area, SW Barents Sea. The aim of this study is to further understand channel development in the Triassic, which is of great importance in hydrocarbon exploration. Channel systems can act as a repository for coarse-grained sediments, and hence represent promising hydrocarbon reservoirs.

This study is based on the 3D seismic dataset WIN12003 together with logs from exploration well 7224/2-1. In the focus area, several channel systems are present in the middle to late Triassic succession. By identifying, mapping and visualizing Triassic channel bodies from the 3D dataset, increased knowledge of the evolution of these fluvial depositional systems are achieved, including river geomorphology, depositional mechanisms and the controlling factors.

Two channels is further analyzed, interpreted and described, classified as meandering and braiding rivers. A brief theory of why these two rivers from various parts of the channel system (distal and proximal) are present in the same area is presented.

The interpretation of the two fluvial channels show consistency with the westward propagation of siliclastic sediments sourced from Caledonian and Uralian orogeny during Triassic.

Acknowledgements

Da er masteroppgaven endelig levert. Det har vært noen flotte og innholdsrike år på universitetet, men jeg hadde ikke klart det uten all tålmodighet og støtte fra familie og kjæreste. Takk for at dere har gjort en til dels krevende studiehverdag litt enklere!

Takk til studieveileder Stefan Bünz for en interessant og spennende oppgave, og for gode tilbakemeldinger fra andre siden av verden. Det har vært en lærerik prosess!

En stor takk rettes også til Aker BP i Harstad, for kontorplass og uvurderlig hjelp med programvaren GeoTeric.

Til slutt vil jeg takke alle studievenner og hele kontoret på rødbrakka for faglige og mindre faglige diskusjoner, og alle venner utenfor studiet for å alltid stille opp hvis det skulle være noe.

Table of Contents

1. Introduction

The Barents Sea comprises a massive, widespread fluvial system in the Snadd Formation from Middle to Late Triassic times, characterized by channel bodies of varying size and extent. This system can be revealed for hundreds of kilometers, adding valuable information about the development and characteristics of these channels, which can act as conduits for sediment transport (Klausen, et al., 2014). In exploration, the Snadd Formation has been of substantial interest, because of the reservoir potential of channel sandstones. Understanding the sedimentology of the fluvial part of the study area is therefore of high relevance. The Barents Sea Basin was in the Triassic period gradually filled by sediments, sourced from the Uralian and Caledonian mountain belts, by prograding alluvial to deltaic plain (Glørstad-Clark, et al., 2010).

This study is based on the 3D seismic dataset WIN12003, and exploration well 7224/2-1, located in the north-eastern part of the Loppa High in the South-Western Barents Sea *(Figure 1-1)*. The objective is to increase knowledge about the distribution and evolution of fluvial depositional systems of the Snadd Formation in the study area. By preparing and interpreting the seismic volume, channel dimensions, geomorphology and sediment deposition mechanisms are revealed to better understand the fluvial part of the Snadd succession. The thesis describes observed fluvial geomorphological features, such as point bars, concave-banks, channel fills and levee deposits in the study area, linking them to sedimentology and river system classifications.

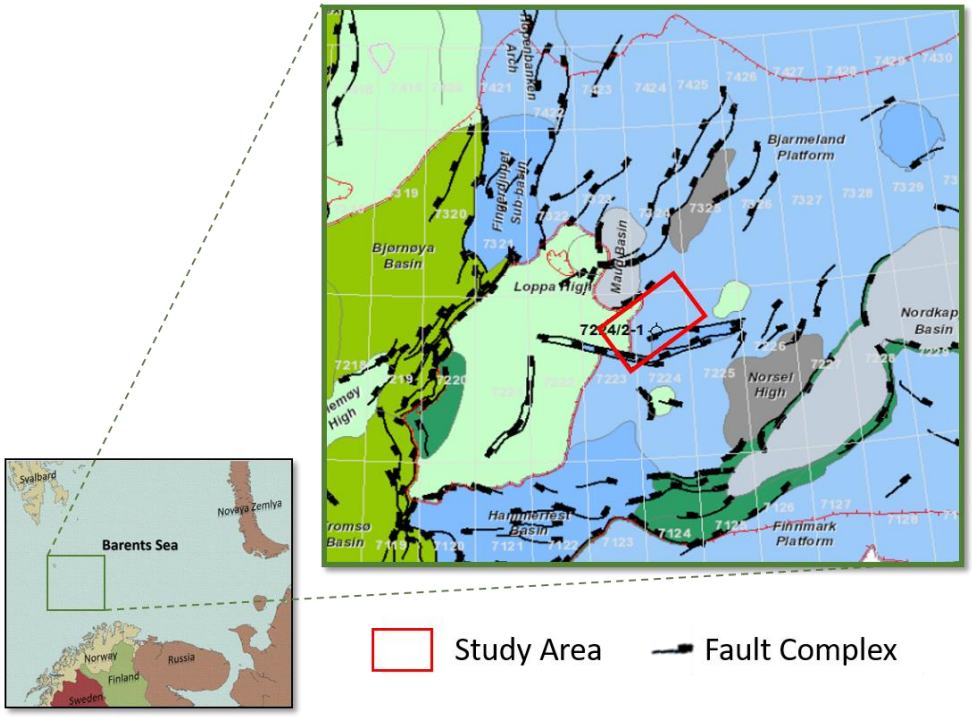

Figure 1-1 *Location of study area (red rectangle) in the southwest Barents Sea, with surrounding platforms and highs. Location of the Barents Sea in the bottom left corner. Modified from fact maps NPD (NPD, u.d.).*

2. Theoretical framework

2.1 River channels

River channels ability to erode, transport and deposit fluvial sediments have been one of the main drivers for shaping the Earth's landscape throughout times. They are major agents for the biogeochemical cycling of materials, and influence global climate (Hudson-Edwards, 2007). Studies of sediment transport processes, ancient sequences and features of different river channel types recognize that the lateral migration of a channel generates fining-upwards sequence (Collinson, 1996). Fluvial deposits could potentially contain economically important resources such as water, oil, gas, placer minerals, coal, building stone, sand and gravel (Bridge & Demicco, 2008). Fluvial deposits could also be important hydrocarbon reservoirs. They are sensitive paleo-environment indicators, as they reflect tectonic slope changes and source area geology. Such deposits also contain an important record of the morphology, flow and sedimentary processes of the rivers and floodplains in the past (Bridge, 1999).

According to Miall (1992), fluvial deposits occur in a wide range of tectonic settings, and are important components of stratigraphic structure. They serve as sensitive indicators of events like tectonic processes and sea level change (Hubbard, et al., 2011).

Channels are defined as surface scours, or depressions that contain water flows, such as rivers and other streams. Floodplains is explained as the overbank area, the area of land between or beyond channels, that receives water (except for rain) only when the river is in flood state *(Figure 2-1).* The fluvial environment is the channel and the overbank settings, often referred to as the alluvial. This is a general term for land surface processes that involve water flows. An alluvial plain is a low-relief continental area where sediments are accumulating. It includes not only sediments from rivers, but could also be fans of detritus, caused by other, not river related flows (Nichols, 2009).

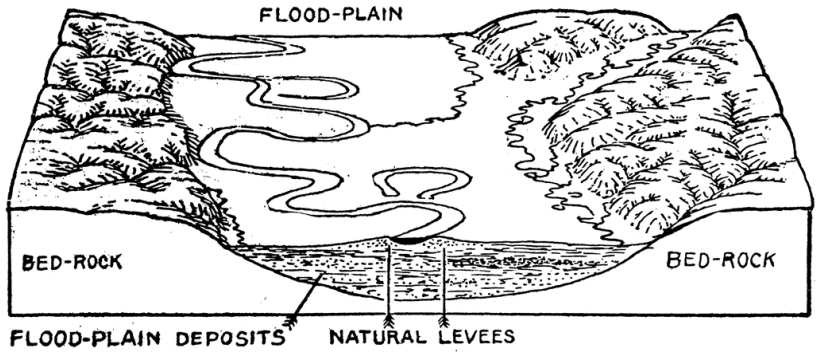

Figure 2-1. *Floodplain of a meandering river with levees, oxbow lakes and floodplain deposits (Grabau, 1920).*

Climate and geology are the primary forces shaping the Earth's landscape. The combination of these processes control water discharge, sediment supply and channel slope, which determine the pattern of a river channel (Wooster, 2002). Recent deposited sediments can be fully or partly removed and transported by turbulent and rapid surface flows. Such flow will often follow river channels, formed by scouring. Similar confined flows can also occur in other depositional settings on the seafloor, at different depths. Scours could generally be recognized in a wide range of depths and widths, from small, meter-deep features to large structures, tens of meters deep and several kilometers wide.

Scours confining a flow, is commonly recognized and distinguished as channels (Nichols, 2009). Fluvial deposits are predominantly clastic, ranging in grain size from finest mud to coarsest boulder conglomerates, deposited at river channels, banks, fluvial fans or floodplains (Miall, 1992).

2.2 Geomorphic zones

There are three geomorphological zones recognized within alluvial and fluvial systems. These are the erosional zone, the transport zone and the depositional zone (*Figure 2-2a)*. How these zones are represented in an area, depend on the interaction between uplift and exposure, weathering and erosion, and the amount of energy in the river *(Figure 2-2b*) (Bennett, n.d.; Nichols, 2009).

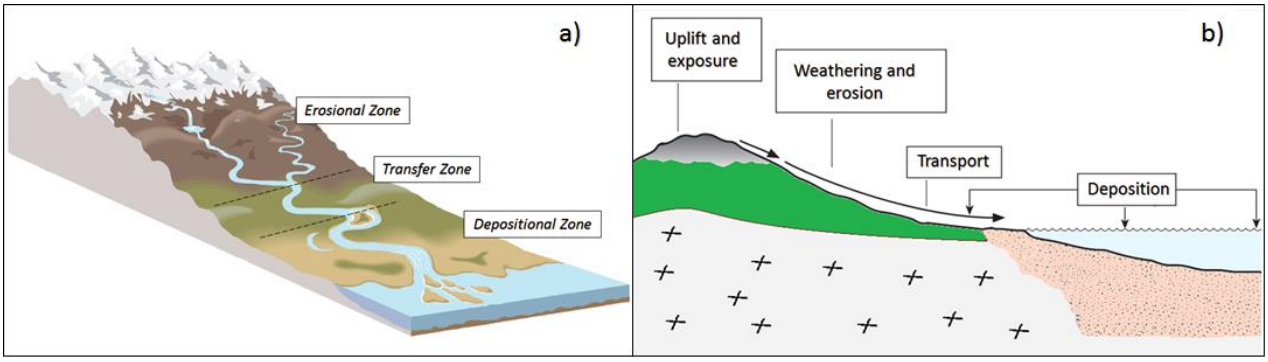

Figure 2-2 a) *Geomorphic zones within alluvial and fluvial systems. Erosional-, transfer-, and depositional zones. Modified from (Hayes, n.d.).* ***b)*** *The processes involved in the rock cycle at the Earth´s surface. The pathway from the uplift and exposure of underlying rocks, transportation, burial and starting metamorphic process of the sediments. Modified from (Nichols, 2009).*

2.2.1 Erosional Zone

The erosional zone is located at the top of the river system *(Figure 2-2a)*, and is the area where the stream is actively eroding the bedrock, removing materials from the valley. This zone contributes a substantial proportion of the clastic sediments that is deposited in other sedimentary environments. River erosion is the process where the force of the river erodes away the bed and banks of its channel,

vertically and laterally. It can be divided into three different parts, depending on the type of erosion that takes place; headward, vertical and lateral erosion. The headward erosion occur near its source and makes the river longer. The vertical erosion often takes place in the upper stages of the river, and makes it deeper. The lateral erosion occurs mostly in the middle and lower stages of the river, making it wider (Bennett, n.d.). Rain and melt water from the catchment area of the river is flowing across the erosional zone, leaving behind very few organisms. This is mainly due to the limited nutritional content in this part of the river, and the force of the water in this zone.

In any zone of the river, there are four ways the river can erode the bed and the river bank (Bennett, n.d.). *Hydraulic action* is one of these, meaning that the force of the river flow helps to break the rock and drag the sediments away from the bed and the banks of the river. *Corrosion/abrasion* is the process when the rock fragments carried by the river velocity are grinding against the banks and bed of the channel. This grinding process widens and deepens the channel. *Attrition* means that rock fragments in the water are knocking against each other. The fragments become rounded or broken into smaller and smoother pebbles. *Solution/corrosion* is the last process, where the water react chemically with soluble minerals in the rocks and dissolve them. Carbonate rocks, such as limestone and chalk are among these, dissolving in the river, forming a weak acid (Bennett, n.d.).

2.2.2 Transfer Zone

In the middle of the river, the transfer zone is located *(Figure 2-2a).* In this part, the gradient is lower, and very limited erosion or sedimentation takes place (Nichols, 2009). When the friction in the river overcomes the force of the flow, the transportation of the material, torn loose by erosion, starts (Bennett, n.d.). These particles can be transported in several ways; by rolling, saltation and suspension. In the transportation zone, the nutrition content of the water is much higher than in the erosional zone, and the highest biodiversity is found in this zone.

2.2.3 Depositional Zone

The depositional zone *(Figure 2-2a),* is the lowest part of the system. This is the part where the river loses its moment, and the deposition takes place. Where the transported material ends up, depends on the local settings. It could be deposited in the river channel, on the surface of an alluvial fan or on the floodplain of a fluvial system. The loss of energy in the river occurs for several reasons, for example with reduction in rainfall, increase in evaporation or increased friction in the flow. The sediments are transported down the river and deposited further down the terrain, where the river no longer has enough power to hold the particles in the stream (Nichols, 2009).

In the depositional zone, sediments from organic and non-organic materials are settled when the velocity is low enough. The amount, type of material and size of transported sediments is dependent on the contribution from the different controlling factors in any particular river system. Sediments transported in rivers with headwaters from a mountain range will often include glacial silt, while a body of water surrounded by swampland will be inundated with decomposing organic material.

All of these three geomorphic zones are not necessarily present simultaneous in all systems. Some may not display a transfer zone at all, while others may be entirely erosional (Nichols, 2009).

2.3 Sediment transport and flow regimes

When investigating how the sediments are distributed in an area, water transportation is the main mechanism. Both in established channel systems and in water that flows over land for different reasons, like heavy rainfall over time or rapid melting of snow (*Figure 2-3*). In the ocean, sediments are carried away by currents driven by wind, tides and sea water circulation (Nichols, 2009). These mechanisms can be strong enough to carry coarse material with significant grain size, as well as finer material over great distances, deposited far away from the original sediment source.

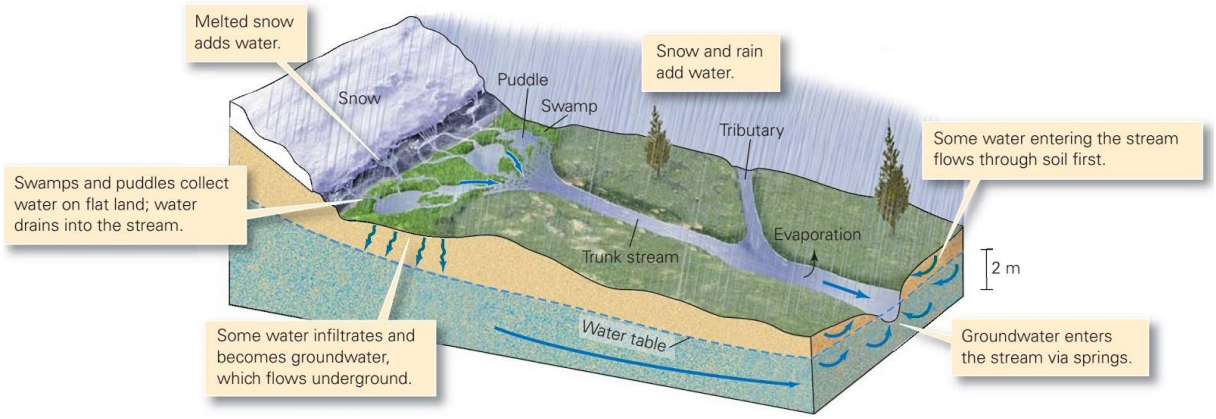

Figure 2-3. *Excess surface water, in form of melting snow or ice, ground water springs and rainfall (Marshak, 2005).*

2.3.1 Fluid flows: laminar and turbulent flow

Molecules in a fluid can be transported in different ways, both by laminar and turbulent flow (Nichols, 2009) *(Figure 2-4).* Laminar fluid flows occur when the fluid molecules internally move in parallel, with the same direction as the flow itself. For a heterogeneous fluid, this means that there will be nearly no mixing of molecules. On the other hand, turbulent flow occurs when the molecules in the fluid move in all directions. This mixes all the molecules in heterogeneous fluids. The higher velocity,

the more turbulent the flow becomes (Nichols, 2009). To measure whether a fluid flow is laminar or turbulent, the Reynolds number is applied. This is defined as:

$$RE = \frac{u \times l}{v} \qquad \textit{(Equation 1)}$$

Where *u* is the velocity flow, *v* is the fluid kinematic viscosity of the fluid and *l* is the characteristic length, meaning the diameter of a pipe or depth of a flow in an open channel (Nichols, 2009).

The flow is considered to be laminar if the Reynolds number is less than 500, and becomes tubular at higher values, RE > 2000) (Nichols, 2009). In between these values, the flow goes from laminar do turbulent with increasing flow velocity. When this happens, is depending of the fluid composition viscosity. When investigating how water flows, the flow is laminar only at very low velocities or at shallow depths (Nichols, 2009). For water sediment transportation and deposition to occur, turbulent water flows are more far more common, due to the power it generates.

2.3.2 Transport mechanisms

According to Nichols (2009), there are three ways the particles in a river can be transported; rolling, saltation and suspension *(Figure 2-4b).* By rolling, the particles are transported on the bottom of the river floor without losing contact with the bed surface. By saltation, the particles move in a series of jumps, periodically leaving the bed surface and carried short distances within the body of the fluid before returning to the bed again. By suspension, the turbulence within the flow produces sufficient upward motion to keep particles in the moving fluid more-or-less continually.

Particles being carried by rolling and saltation are referred to as bedload, while the material in suspension is called suspended load. At low current velocities in water, only fine particles (fine silt and clay) and low density particles are kept in suspension, while sand-size particles move by rolling and some by saltation. At higher flow rates, silt and some sand may be kept in suspension, with granules and fine pebbles in saltation, and coarser material rolling (Nichols, 2009).

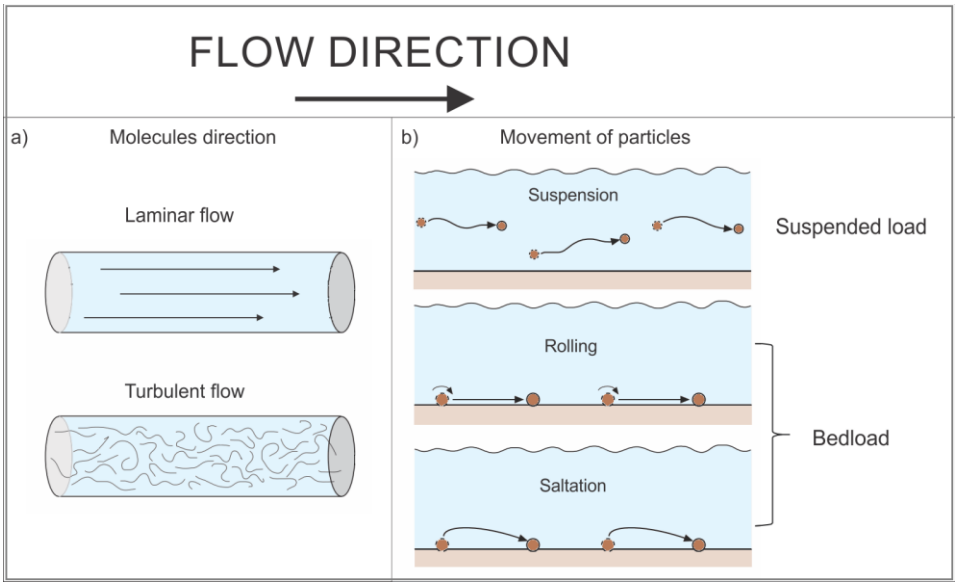

Figure 2-4. a) *Flow direction of molecules within a laminar and turbulent flow.* ***b)*** *Particle movement methods in a stream. Suspended load (suspension) and bedload (rolling and saltation). Modified from Nichols (2009).*

The Hjülstroms Diagram *(Figure 2-5)* shows the relation between flow velocity and particle size by erosion, transport and sedimentation. It shows the required velocities to transport, erode and deposit sediments with different grain size (Nichols, 2009). It illustrates that higher velocities are required to entrain fine particles of clay and silt than coarse sand. However, once the fine sediment is in suspension, a much lower velocity is required to keep it in suspension (Keylock, 2014). That is why significant volumes of silts and sands are found in channels, on levees and on fan surfaces. They are accumulated at periods of flooding, even on low velocities.

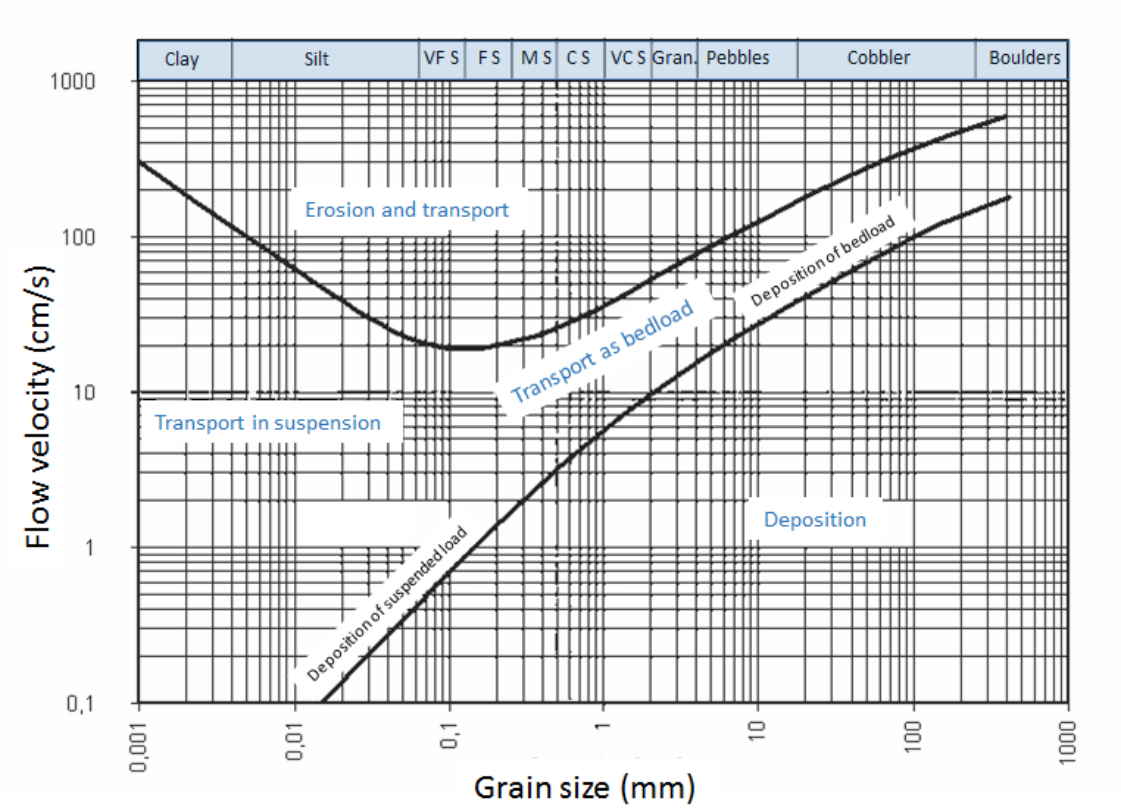

Figure 2-5. *The relation between the velocity of a water flow and the transport of loose grains, illustrated in Hjülstroms Diagram. Modified from (Press & Siever, 1986), in Nichols (2009).*

2.4 Bedforms

When the fluid stream in a river is strong enough to move the particles of the bed material, the bed changes into a series of bedforms. According to Collinson (1996), these alluvial deposits are governed by different accumulation conditions in the fluvial settings, which results in bedforms in a wide range of forms and scales. For siliclastic sediments, variations in sediment transport rate and sediment size control the sediment transport behavior, and are the most fundamental properties of these sediments.

A bedform is a morphological feature, formed by the interaction between a flow and cohesionless sediment on a bed (Nichols, 2009). When a river flows, the mechanisms and processes of sediment movement change with flow velocity. At low flow velocity (lower flow regime), current ripples, dunes, small-scale trough cross-bedding, wavy and horizontal lamination are generated. The occurrence of both ripples and dunes are limited by critical values of grain size. As flow velocity increases, and reaches required level to move sediment particles, the sediment particles start to move by rolling and saltation (Perry & Taylor, 2007). With increasing flow velocities, sediment bedforms are smoothed out to planar beds and eventually antidunes, which are generated at upper flow regime.

According to Nichols (2007), it is possible to show the bedform that will occur for a given grain size and velocity in a bedform stability diagram. The upper boundary of the ripple field is considered as sharp, but the boundaries between the other fields are gradational and could be overlapped. The diagram in *Figure 2-6* shows two identified regimes: a lower flow regime where ripples, dunes and lower plane beds are stable, and an upper flow regime where plane beds and antidunes form.

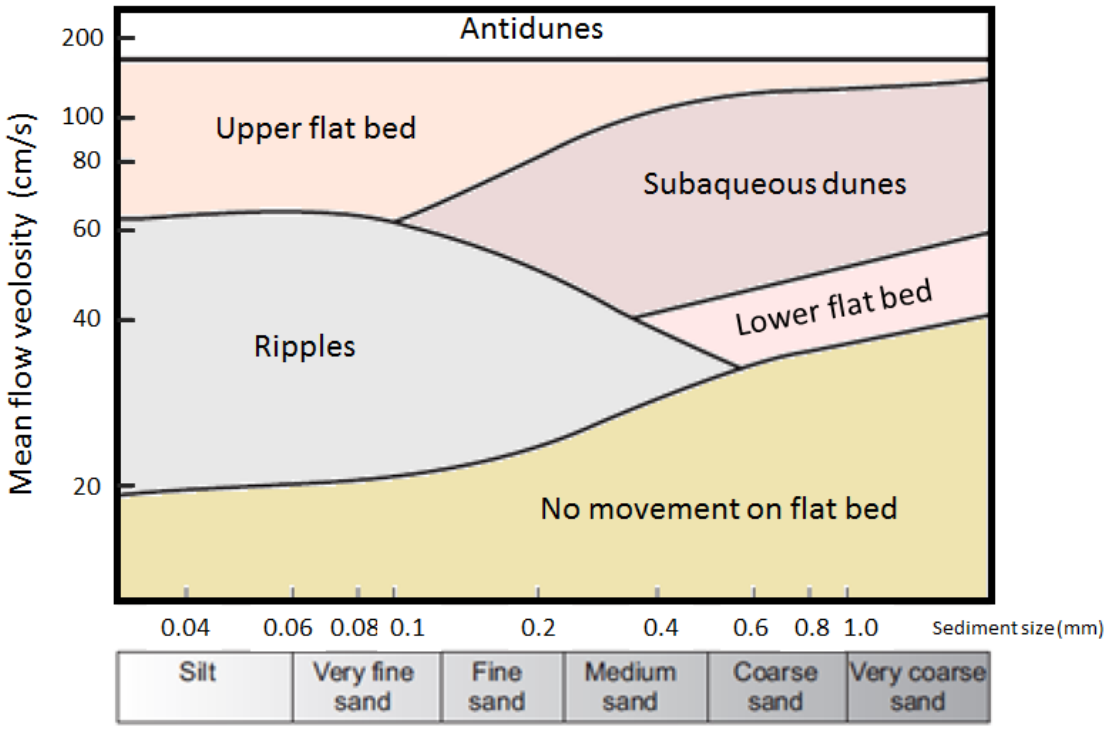

Figure 2-6. *Current-generated bedform stability diagram which shows how the stable type of bedform varies with both the grain size of the sediment and the velocity of the flow (logarithmic scale). Modified from Nichols (2009).*

2.5 Fluvial and alluvial systems

2.5.1 Rivers and channels

According to Leopold & Wolman (1957), a number of different channel types can fall within the definition of rivers. Braided, meandering and straight channels can all be categorized as rivers, but since one channel type often can be found within another, attempting to classify one entire channel into one category, becomes difficult (Duncan & Harding, 2007). Therefore, it is beneficial to instead regard one channel pattern as a continuum with these three general characteristic morphologies; straight, meandering and braided. The threshold between meandering and braiding represents a primary subdivision of channel patterns into single and multiple channel forms (Wooster, 2002) .

2.5.2 Alluvial fans and alluvial delta

Alluvial fans are conical or fan-shaped accumulations of sediments (e.g. *Figure 2-7a*) that have a focused source of sediment supply, usually from an incised canyon or a mountain front channel (Galloway & Hodbay, 1996). They form in areas where there is a break in topography between the high ground of the drainage basin and the significant flatter sedimentary basin floor (Nichols, 2009). Alluvial fans are deposited along highland margins in response to the high rate of sediment supply and a sudden fall in stream velocity, as the gradient flattens onto the basin floor (Galloway & Hodbay, 1996). Such fans are found where high energy streams are reaching a plain. When no longer confined to a channel, the energy level of the water drops, which makes the water unable to transport larger sediments like cobbles or gravel. If the water is no longer able to carry those sediments, they drop out and are deposited. Alluvial deposits are often poorly sorted.

A typical alluvial fan represents several types of depositional geomorphic features (*Figure 2-7b*). The fan apex is defined as the highest, most proximal point adjacent to the feeder canyon. From this point, the fan form radiates. A fan-head canyon may be present in the fan surface near the apex. Alluvial fans can be divided into different parts that show significant changes downwards (*Figure 2-7c*). The depositional slope will usually be steepest in the proximal area, where you have proximal debris flow deposits. In the middle of the fan, braided stream deposits dominate, and in the distal fan sheet, there are flow deposits beyond the fan toe. The fan toe grades gradually into a basin floor environment (Leeder, 2011). The slope over most of the fan may be only a degree or so, but it is a distinct break in slope at the fan toe, which is the limit of the deposition of coarse detritus at the edge of the alluvial fan. The fan deposits are thickest at the apex and develop as a conical wedge towards the toe (Nichols, 2009).

According to Einslie (1992), fan deltas are deposited in a lake or in the sea, with characteristic progradational geometries, in a coarsening-upwards succession, meaning a vertical change in the facies where the grain size increases upwards. When deposited, the sediments are modified by current waves (Galloway & Hodbay, 1996). The sedimentation on alluvial fans starts where the streams loose some of the transport energy. As flow channels migrate laterally, they generate a broad, low angle fan-shaped body of sediments (Leeder, 2011). This structure is commonly referred to as a fluvial distributary system (Nichols, et al., 2007). In alluvial fans, major depositional episodes correspond to the periods where it is controlled by local rainfall amount and the availability of detritus (Leeder, 2011).

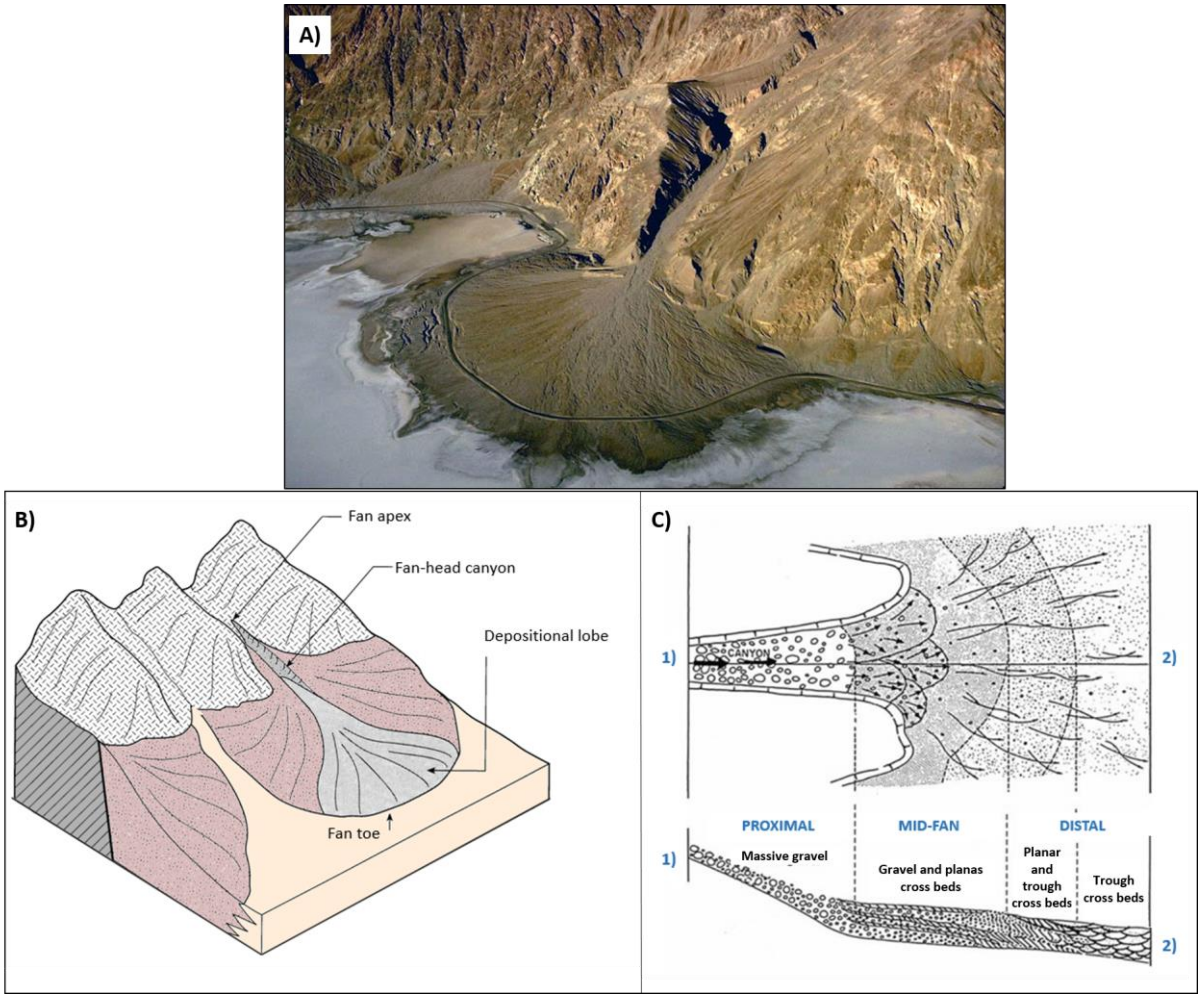

Figure 2-7 a) *Example of an alluvial fan in Death Valley, California (Marshak, 2005).* ***b)*** *Alluvial fan consisting depositional geomorphic features modified from (Miller, u.d.).* ***c)*** *Plan view of an alluvial fan showing general deposition throughout a fan. Modified from (Steel, 1980).*

There are two main types of alluvial fans. First, *debris-flow-dominated* alluvial fans, established in high mountain areas in humid as well as in semiarid climates. These are triggered by floods on steep surfaces of unconsolidated clay-rich sediment (Galloway & Hodbay, 1996). In many of these fans, a rockhead confined valley continues into a distributive network of fan channels and midfan lobes. Second, the s*tream-flow-dominated* alluvial fans, created by perennial or seasonal stream flows. The migration of these channel streams dominate the produced sequences in such fans. Stream-flow-dominated fans show proximal to distal change from coarse depositions in rapidly shifting braided channels, to fine sediments occurring from meandering rivers and overbank flood deposits.

2.5.3 Braided rivers

Many different attempts to define braided rivers *(Figure 2-8)* have been made, most of them with focus on the distinct physical characteristics as multiple surface-flowing channels.

"*Braided stream is characterized by having a number of alluvial channels with bars or Islands between meeting and dividing again, and presenting from the air the intertwining effect of a braid*" (Lane, 1957)

"*A braided river is one which flows in two or more channels around alluvial islands."* (Leopold & Wolman, 1957).

Figure 2-8. *Example of a braided river in Alaska (Mosaselim, 2015).*

According to Leopold & Wolman (1957), there are two primary controlling variables on channel pattern, discharge and slope: 1) For a given discharge and bed material, there are threshold slopes between which channels will braid. 2) The critical slope decreases with increasing discharge or decreasing sediment size. Both slope and bed material change naturally and predictably down the length of a river. Generally, according to Browne (2004), rivers are steeper in their headwaters and bed materials are coarser, but as rivers flow away from their headwaters, slope decreases and bed materials become finer. This suggests that the channel form changes in a relative predictable way as we go downstream. But changes in slope and in bed material, in connection with intermediate changes in discharge, can make braiding and other channel patterns to occur irregularly along the length of the river. Times with high discharges may produce a distinctly braided channel pattern, as much as different periods of climatic stability may produce a single, straight channel (Bridge, 1993; Whited, et al., 2007).

Ferguson (1993) focuses on the important features of braided rivers when it comes to deposition and channel charging effects. *"Braided rivers are distinctive because of their high stream power (product of specific gravity of water, slope, and discharge) and subsequent high rates of erosion, deposition,*

and channel change compared to other river types" (Ferguson, 1993). Braiding is commonly associated with high values of factors like valley slope, stream power, sediment supply, shear stress, width to depth and bedload transport rates. Shear stress is the product of specific gravity of water, slope, and water depth (Ferguson, 1993). In rivers, coarse sediments attached to the channel base are mid-channel bars, also called braid bars. Such bars are primary common for braiding stream deposits (*Figure 2-9a*) (Collinson, 1996).

In terms of flow dynamics, a mid-channel bar is a double sided point bar, but the important difference is that the mid-channel bar is constantly moving downstream (Leeder, 2011), and separates the flow into distinct braid channels, oriented parallel or sub-parallel to the main flow (Schumm & Germanoski, 1993). At low flow stages, the bars in a braided river channel are exposed, but they are covered when the flow is at full level. Generally, flow is strongest between the bars. The coarsest material in transportation will then be deposited on the channel floor, forming an accumulation of larger clasts, or coarse lag (*Figure 2-9b*) (Nichols, 2009). Within a channel, a variation of bars can be present. Longitudinal, elongate bars occur along the axis of the channel. Transverse bars are wider, spreading across the channel, and lingouid bars have a crescentic shape, with their apex pointing downstream (Nichols, 2009).

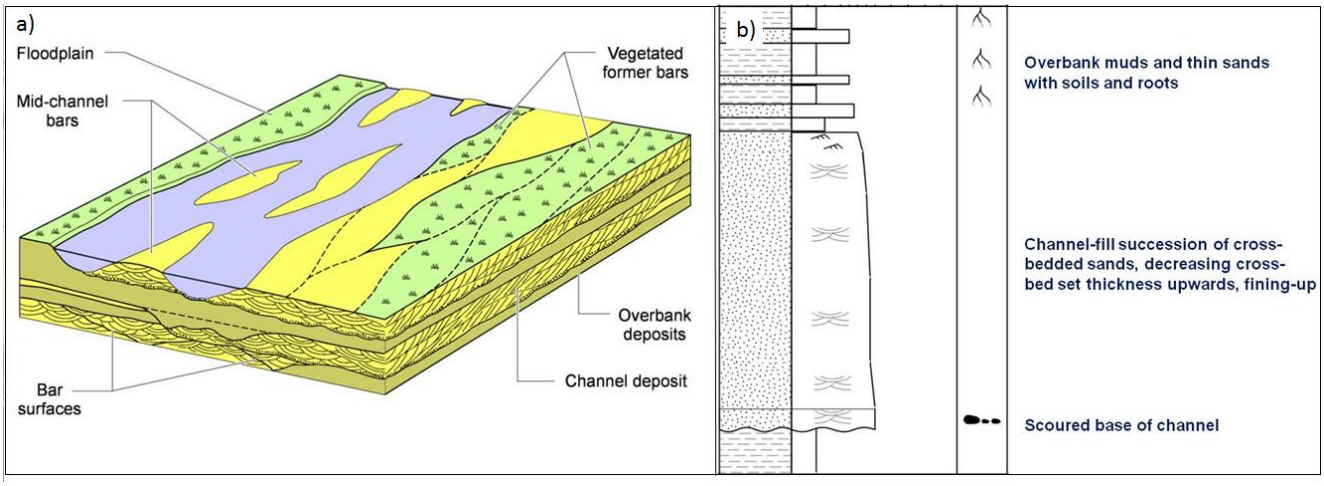

Figure 2-9 a) *Morphological features of a braided river, showing an active river with mid-channel bars and floodplains. Ancient, abandonment bars and subsurface channel banks and deposits are also included (Nichols, 2009).* ***b)*** *Vertical section of braided river deposits (Nichols, 2009).*

According to (Bridge & Lunt, 2006), braided rivers and their deposition mechanisms are important components of the Earth´s surface, as the deposits of ancient braided rivers are indicators of past Earth surface environments. Braded rivers have through times and in different areas of the Earth deposited sedimentary sequences that form valuable water or hydrocarbon reservoirs and important mineral accumulation.

2.5.4 Meandering rivers

Meandering rivers (*Figure 2-10*) are commonly found in lowland alluvial plains, and are rivers with a distinct sinuous pattern, without large longitudinal width variations. Meanders develop through erosion of the bank closest to the thalweg, followed by deposition on the opposite side of the channel, where the flow is sluggish and the bedload can no longer be carried. With continued erosion of the outer bank and deposition of bedload on the inner bank, the channel develops a bend and meander loops are formed (Nichols, 2009). As the outer bank progressively retreats and the inner bank accretes, due to sedimentation, (Grenfell, 2012), states that the term "meandering" should be used only to actively migrating channels of high-sinuosity in alluvial floodplains. According to (Collinson, 1996), meandering rivers characteristically occur on alluvial plains, but also on valley floors and between terraces at relatively lower slopes. They are carrying predominantly fine grained sediments, and are generally single-thread, as they follow a sinuous path, moving from one side to another along the channel path.

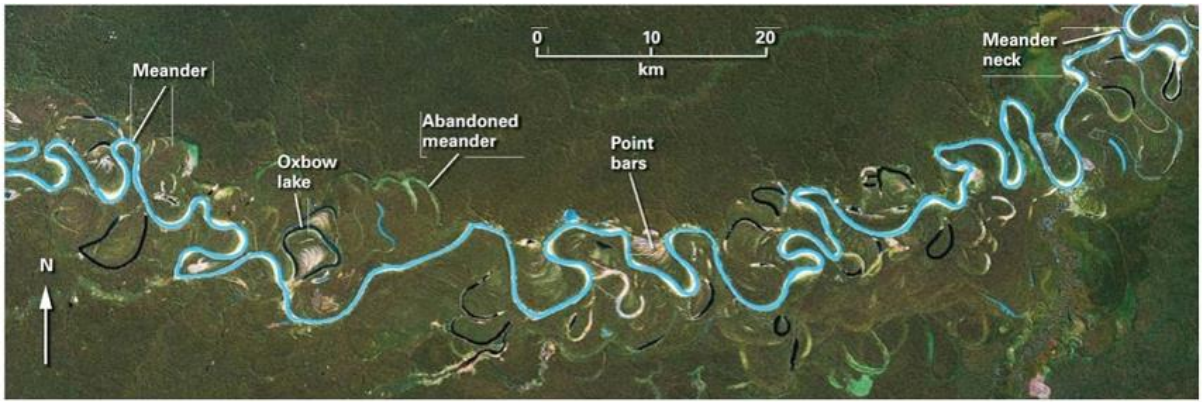

Figure 2-10 *Example of a meandring river in Brazil with corresponding cutoffs, oxbow lakes and point bars (Marshak, 2005).*

To theoretically understand the meanders formation, one must study the unstable straight channel configuration. That includes the study of planimetrically unstable configuration, bend instability and altimetrically instability (Van Djiik, et al., 2012). As a result, initially straight channels grow to form meandering patterns. Maximum velocities and depth occur close to the outer bank so that the channel has an asymmetric cross-section (Collinson, 1996).

The length and the width of the meanders grow as the river discharge, and the slope of the river valley or fluvial plain increases (Einsele, 1992). The deposition of meandering rivers consists of fine-grained sediments as sand and small proportions of silts and muds. Also locally back swamp carbonaceous muds and clays occur (Einsele, 1992). The physical processes operating within these channels are particularly associated with turbidity current flow (Clark & Pickering, 1996).

When a river flows, the water flow may also take a short-cut between meanders, resulting in a new section of channels developing, and the longer loop of the meander built becomes abandoned. Point bars on the inside bends of the meandering river are exposed during periods of low flow, while abandoned meander loops are isolated as oxbow lakes. These will remain as an area of standing water until they are filled up by deposition from floods and/or choked by vegetation. The deposits of an oxbow lake may be recognized in ancient fluvial sediments, as channel fills made up of fine-grained, sometimes carbonaceous sediments (Nichols, 2009). Avulsion is the process where bars move until the channel moves sideways, leaving the bar out of the main flow of the water, or resulting in the point bar being cut-off by a chute. Such point bar deposition begins with medium to fine trough cross-beds with rippled surface, and ends with fine sand and silt that contains climbing ripples and cross-laminae (Leeder, 2011). After the moving of the channel, flood plain muds with mud cracks and roots starts to accumulate. This sequence would normally be formed within a single pass of a meander loop.

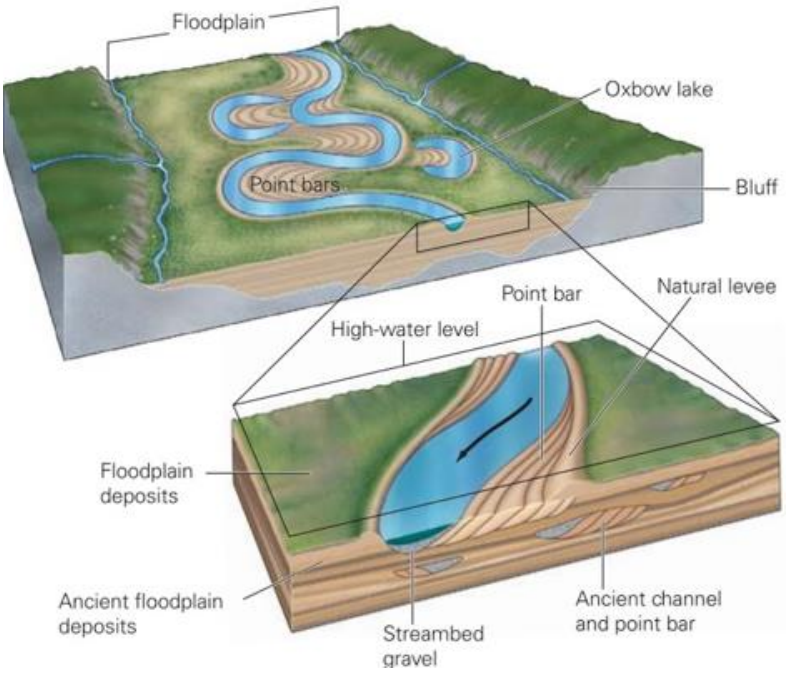

Figure 2-11 *Landform along a typical meandering river, including floodplain, oxbow lake, point bars and levees. Notice the older, subsurface channels, being the main objective of this study (Marshak, 2005).*

2.5.5 Anastomosing rivers

According to Makaske (2000), an anastomosing river is a type of river with multiple, interconnected coexisting channel belts on alluvial plains (*Figure 2-12*), which most often seem to form under relatively low-energetic conditions near a local base level. This type of rivers develop in areas of rapid aggregation, for example where rapid base-level rise is matched by an abundant sediment supply, or in basins that is confined and rapidly subsiding. Anastomosing rivers have a tendency of being stable in position, and are characterized by channels that are relatively narrow.

Figure 2-12. *Yukon anastomosing river in the central Alaska (Ellen Wohl, 2013).*

Masake (2000), also states that anastomosing rivers are composed of two or more interconnected channels that enclose floodbasins. This means that the terms ”straight”, ”meandering” and ”braided” rivers, all can be a part of an anastomosing river system (*Figure 2-13).* This includes environments like bars, crevasse splays, levees and abandoned channel segments. Anastomosing rivers are usually formed by avulsions, which means that flow diversions cause the formation of new channels on the floodplain.

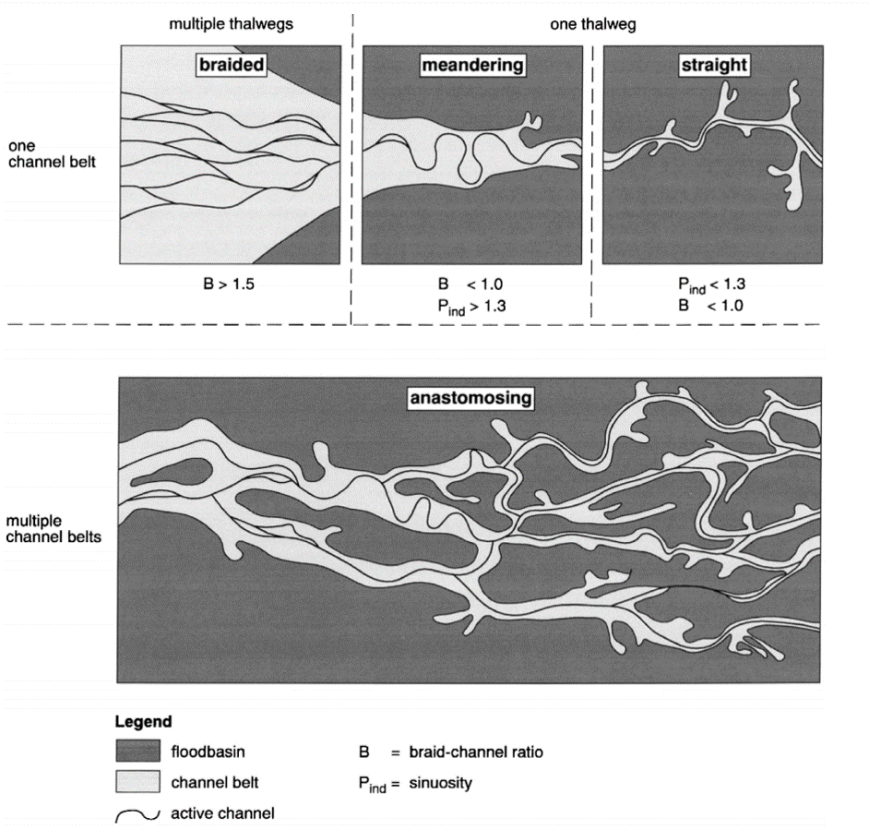

Figure 2-13 *Classification of alluvial river types based on channel pattern and floodplain geomorphology (Makaske, 2000).*

2.5.6 River classification

The river classification system by (Rosgen & Silvey, 1996) *(Figure 2-14)* promotes a better understanding of river processes, and is an important input when studying the paleo-environment. In this thesis, the common river classification system is used to relate the observed paleo-channels to the morphological properties of corresponding river channels. Measured hydraulic variabilities of the discussed channel systems can be directly compared with the morphological features of the proposed classification (Technical Supplement, 2007). This is based on measurable physical parameters such as entrenchment, channel gradient, width-to depth ratio, sinuosity and bed material in a river segment.

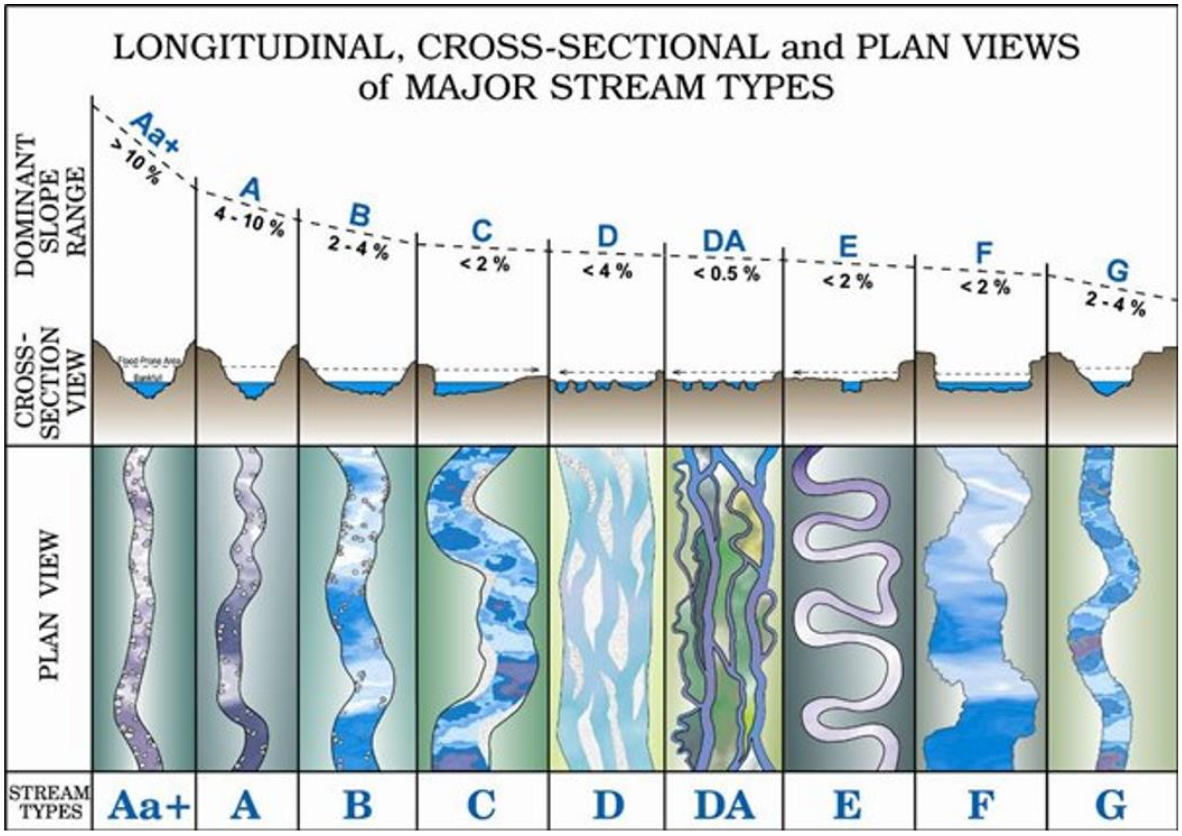

SIN	< 1.2	> 1.2	> 1.4	< 1.1	1.1-1.6	> 1.5	> 1.4	> 1.2
W/D	< 12	> 12	> 12	> 40	< 40	< 12	> 12	< 12

Figure 2-14*. Rosgen river classification of channel systems. Longitudinal, cross-section and plan view of several stream types. Modified from (The Environment Agency, 2010).*

The sinuosity of the channel is defined as the ratio between the channel length and the valley length *(Equation 2)* (Rosgen & Silvey, 1996). The channel length is measured along the thalweg of the channel, while the valley length is measured along a straight line throughout the channel (Technical Supplement, 2007).

$$Sinousity = \frac{Channel\ length}{Valley\ length} \qquad (\textbf{Equation 2})$$

2.6 Overbank Environments

2.6.1 Floodplain, channel-levee system and crevasse splay

Many rivers alter between being in state of flood or not. This dynamic interaction defines the process of alluvial architecture in the river, creating alteration of channel and levee sediments in the stratigraphic section *(Figure 2-1).* According to (Perry & Taylor, 2007), floodplains are sites

of sediment accumulation within a river. Its organic richness is developed from flooding events, where nutrients, habitats and soils are preserved (Leeder, 2011). Levee deposits are the largest and most extensive sand-prone architectural element of channel belts (Janocko, et al., 2012). In times of flooding, the water outside the channel will normally be very shallow and have low flow velocity. Fine grained sediments, transported in a suspension and deposited as overbank sediments, may built up to an elevated bank called levee *(Figure 2-15)* (Bjorlykke, 2010).

In this process, most sand is dumped on the levee areas adjacent to the channel, unless the floodwater decelerates, leading to deposition of only fine sediments (Leeder, 2011). Channel-levee deposits are commonly divided into two main facies: Mud rich and sand rich sediments. Mud rich sediments are distal to the channel, and have abundant starved ripples, which indicates limited volume of sand-size sediments. Sand rich deposits are present at high flow velocity and high deposition rate. They occur close to the channel, with parallel lamination, ripple cross-lamination or climbing ripple cross lamination (Kane, et al., 2007).

When moving away from the channel body, both sandstone thickness and sandstone proportion are decaying. When the river is in flood state, as the flow magnitude increases and the channel floor aggradates, the levee grows vertically, and the levee crest migrates in a channel-distal direction (Weschenfelder, et al., 2010). Such channel-levee geometries are formed as a result of migration of a single channel form (Sylvester, et al., 2010). Major floods may extend to the areas beyond the levees, leading to the deposition of clay and silt, as the deceleration of floodwater leads to a gradual deposition of finer sediment from the channel margin (Leeder, 2011).

Channel-levee system sediments have a special interest since they are sites of soils and organic remains preservation. If not remobilized through physical erosion, these depositions can become sources as result of post-depositional processes (Perry & Taylor, 2007). The channel-levee sediments are highly variable. Depending on climate, their characteristics can change. In humid-tropical regions, coal can be found if the overbank has developed as a raised swamp (Miall, 1992).

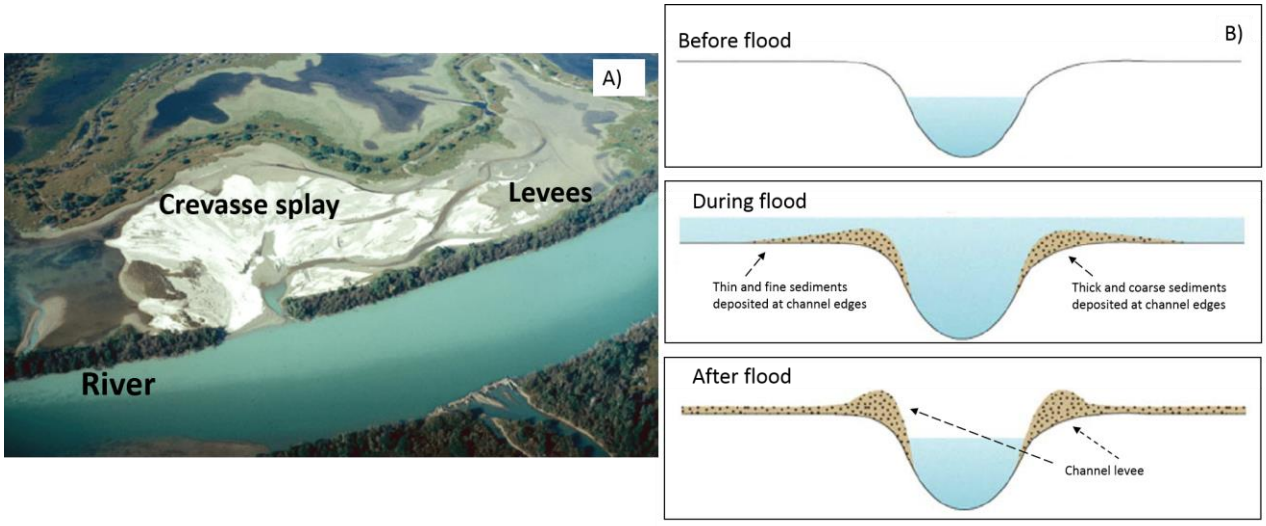

***Figure 2-15**. **a)** River system with crevasse splay and natural levees (Ellen Wohl, 2013)**b)** Illustration of the origin of channel levees, and example of levees (Rogers, 2008).*

Water flow and sediment transport on floodplains is defined by variable floodplain width and surface topography. One type of overbank deposits is the crevasse splay (*Figure 2-15)*, which normally cut through discontinuous levees in rising flow conditions, where the channel spills into the overbank environments (Bridge & Demicco, 2008). The geometry of crevasse splay deposits differ from levee deposits. They can have their own levees and mouth bars, and internal channel-bars and channel-fill deposits are common (Bridge & Demicco, 2008). It can be difficult to distinguish these from the main channel deposits. Here, groups of strata could be identified of a vertical thickness of a few meters, with lateral extent of up to hundreds of meters (Posamentier & Walker, 2006). Crevasse splay deposits tend to contain abundant plant roots and transported plant material, and are usually coarse grained and thicker than levee (Bridge & Demicco, 2008). The stratigraphic architecture of crevassed splay deposits is characterized by amalgamated turbidities near the apex, and less amalgamated distant to the splay apex (Posamentier & Walker, 2006). Internal structures may contain sandy turbidities, with grading, horizontal lamination and ripple cross-bedding (Einsele, 1992). Climbing current ripples leads to rapid sedimentation from suspension when flow cuts through the levees crevasse (Bridge & Demicco, 2008). Avulsion can be initiated by extensive enlargement of channels on crevasse splay. Erosion and enlargement of the crevasse channel is possible if the discharge-slope product and sediment transport rate of the overbank flow can exceed that of the channel flow, leading to increasing sediment transport rate from the channel to the floodplain (Posamentier & Walker, 2006).

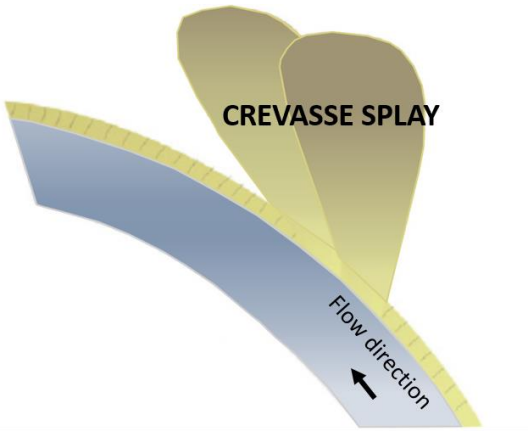

Figure 2-16. *Illustration of crevasse splay outside of a river bend. Modified from (Gulliford, et al., 2017).*

In crevasse splay deposits, overbank facies are most dominant, and sandstone is often present as sheet deposits rather than channel-fill facies. This depositional environment results in a network of cross-cutting channels, crevasse and terminal splays. Previously it was thought that all channels are active at the same time, but further studies indicate little proof of this in contemporary systems (Donselaar, et al., 2007). Random avulsions cause an active river tract to shift entirely, as the entire river tract profile shallows and a new steepest descent pathway is created elsewhere in the system. Thin-bedded crevasse-splay lenses and sheets may occur randomly in such a fluvial succession, but can also be nested in thin but laterally extensive sheets, referred to as a crevasse complex (North & Warwick, 2007). These sheets may be indicators for a future channel belt migration, as they may pave the way for an avulsion (Jones & Hajek, 2007).

2.6.2 Chute cutoffs

In periods of high flow, water may take a short-cut over the top of a point bar. This flow may become concentrated into a chute that cuts across the top of the inner bank of a meander *(Figure 2-17).* Chute channels are features of a point bar, only active during high-stage flow. They may be recognized in the deposits of a meandering river as a scour that cuts through lateral accretion surfaces (Nichols, 2009). Meander bend development could be limited if non-linear processes such as chute cutoffs and channel adjustment are following the cutoff (Van Djiik, et al., 2012). Active chutes at high discharge will potentially cut off point bars (Collinson, 1996). Single bend cutoffs occur as a meander bend migrate laterally. Bank erosion and lateral movement of the bend produces a higher amplitude bend (Van Djiik, et al., 2012). When channel geometry changes, it causes flow diversion at the outer bank. This flow diversion into chute will potentially reduce the entire flow capacity, and may lead to the formation of stable cutoff islands (Grenfell, 2012). When a chute is cut off from the main flow in period of low discharge, it becomes an oxbow lake or an abandoned meander (Collinson, 1996). When abandoned, the chute becomes filled, typically with sandy and gravel framework, migrating sand

bedforms and suspended load fines (Collinson, 1996). On chutes floor, dunes with curved crestlines are common bed forms. In times of high water velocity, sandy unit bars, point bars, and braid bars occur locally in shallow areas (Bridge & Demicco, 2008). In areas of slow velocity streams near banks, ripples may occur. Chute channels suggests a process of transition from single-thread meandering channel to braiding channel. In chute channel environment, antidunes and transverse ribs could occur in fast, shallow water (Bridge & Demicco, 2008). Depending on velocity, transported deposits of gravel and sand sediments form either gravelly sand (clast-supported gravel beds when most sands have been sorted out), lag deposits when the velocity is slower, or river beds dominated by sand (Collinson, 1996), (Einsele, 1992).

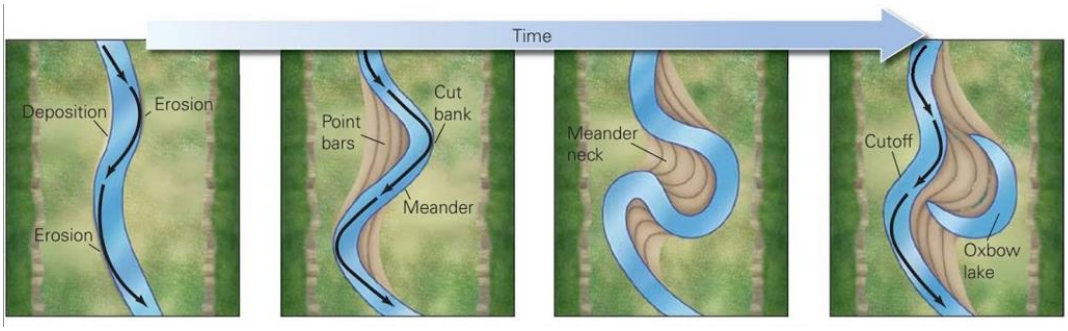

Figure 2-17. *The development of oxbow lake in a meandering river (Marshak, 2005).*

2.6.3 Channel systems and hydrocarbon prospectively

Petroleum is a collective term for naturally occurring oil and gas. These materials are principally made up of hydrocarbons, compounds of carbon and hydrogen. The hydrocarbon compounds originate from organic material that has accumulated within sedimentary rocks, and is transformed into petroleum by the processes of hydrocarbon maturation. This takes place in a series of stages, dependent upon both temperature and time (Nichols, 2009). When it comes to river systems and hydrocarbon potential, the implication for exploration is to predict sand-rich, sinuous channels locations, which can be important reservoir elements (Kane, et al., 2010). Such reservoir elements may be present as distinctive features of sandstone bodies, which can act as good hydrocarbon reservoirs if they meet critical factors, such as homogenity, degree of lateral continuity and vertical connectivity (Clark & Pickering, 1996). The study of channels is of great relevance in hydrocarbon exploration, since they both can be conduits for sediments transported to deep basins and repositories of coarse-grained sediment, and in that way represent promising hydrocarbon reservoirs. Fluvial sandstones are frequently found in mid-channel sequences in braided rivers or in point bars of meandering river systems. The lateral accretion of bars will deposit sandstone layers corresponding to the river width, but limited in thickness by depth. After deposition, later compaction reduces primary thickness at the time of deposition by 10-30% or more.

The overbank deposits of muds, on the other hand, will become tight shale. This will subsequently reduce the vertical permeability (Bjorlykke, 2010).

Fluvial deposits in river systems form labyrinth-like reservoirs with a complex geometry of interconnected fluvial channels within floodplain sequences. Such sequences have earlier been regarded as non-reservoirs. Recently, floodplain sequences in crevasse splays have become subject of more interest, as they could represent better reservoir qualities than previously identified (Hajek & Edmonds, 2014). Such assumed non-reservoir intervals in drilled wells may contain intervals of sediments deposited in the medial to distal zone of fan-shaped fluvial systems, represented by stacked crevasse splays. Laterally amalgamated thin sheets, may prove to be potential reservoirs for gas. The porosity and permeability of these reservoirs is low, but lateral amalgamation by compensational stacking can create extensive sediment bodies with a good reservoir potential (Mjos, et al., 1993). It is then of vital interest to investigate how individual crevasse splays develops into stacked crevasse complexes, and what their expression in the subsurface is, including spatial distribution, geometry, connectivity and lateral grain size distribution.

When a river deposited sequence is fining upward, the highest permeability is near the base, where coarse-grained sediments are deposited. For the possibility of HC potential, deep fluids produced within source rocks, should preferentially be entrapped within the channel-levee system of sandy bodies. According to (Gay, et al., 2005) such fluids can migrate from one paleo-channel level to another one along faults. Faults of this character typically develops at the crest of channel-levee system along sand, silt and dykes, or through vertical stacking pattern of paleo-channels. Factors like lithology (the coarse nature of deposits), vertical stacking (separation of sandstone-dominated lithologies from overlying shale-dominated lithologies) and connectivity (the presence of pathway for fluids to connect turbidity paleo-channels), control the ability of fluid migration from a sand body to another. As fluid migrate from one level to another, one migration pathway (chimney) are more concentrated when underlain by three to four stacked paleo-channels (Gay, et al., 2005).

2.6.4 Geophysical properties in channel interpretation

In a river generated fluvial-deltaic environment, channels are cut and filled with different lithology. These cut and fill controlled breaks in lithology could potentially give increasing acoustic impedance contrast. Lateral changes in lithology give rise to differential compaction (Chopra & Marfurt, 2012). The channel levee system could have a seismic appearance of high amplitude, negative phase-reflection segments, with a mounded outer shape at the sides of a channel as a single reflection. Other possibilities are several high amplitude reflections stacked upon each other, where low amplitudes can

be correlated with shales and/or mudstones, and high amplitudes could indicate sands (Andreassen, et al., 2007) (Gay, et al., 2005), (Weschenfelder, et al., 2010).

The occurence of strong negative-phase seismic reflections might be associated with the channel levees, and suggest that they are gas-bearing, most probably consisting of sandy sediments (Andreassen, et al., 2007). An identified strong and continuous reflector of the overlying strata, truncates the upper reflectors of the seismic facies, filling up these paleochannels (Weschenfelder, et al., 2010).The presence of gas or may be caused by lithological contrasts, indicated by high RMS amplitudes. Minimum-value seismic amplitude attribute map could be made to display strongest negative-amplitude values or negative-amplitude bright spots. These markers in the data could indicate the precence of gas. It could be in fan-shaped sediment lobes, in continental slope channels and in deltaic deposits, as well as in the sediments at the flanks of slide scars.

Pickering & Clark (1996) describes sites of preferential sand accumulation in channels as follows: 1) channel bends; 2) channel confluences; 3) point-bars associated with high-sinuosity lateral accretion; 4) channel benches and terraces and 5) channel thalwegs.

When waterways take new directions as response to regional tectonic activity, it results in frequent avulsion, rapid subsidence rate and high quantity of sediment supply, with high proportion of fine deposits. According to (Gay, et al., 2005), massive sands often frequently form the basal units of channel sequences. These sequences grade upwards into horizontally laminated successions of fine sands and silts, overlain by wavy, lenticular bedded silts and interbedded muds. Silts and sands formed within fluvial deposits in channel belts, which compose the paleo-channel infills, have high porosity. The paleo-channels itself may concentrate fluids migrating from the productive source rocks, and porous paleochannel deposits may act as effective drains for the fluids to migrate (Gay, et al., 2005). It may also act as a porous petroleum reservoir (Miall, 1992).

For petroleum exploration, sand-rich sinuous channels are important reservoir elements (Kane, et al., 2010). Gas in these features is interpreted to appear in high-porosity channel levees and delta deposits (Andreassen, et al., 2007).This may be identified on seismic data due to appearance of strong negative-phase seismic reflections, associated with gas presents. As a meandering river develops through the flatland with great influence on the deposition of peat and associated sediments, coal could be deposited as peat along the channel in regions without uniform sedimentation rates. Deposition in such regions is controlled by interaction of migrating depositional environments, and because peats bordering the river received nutrients and vegetation supply.

3. Barents Sea

3.1 Introduction

The Barents Sea is one of the largest continental shelf on the globe (Dorê, 1994), covering an area of approximately 1.4 million km^2 (Bryhni, et al., 2017). It is bordered by the Norwegian and Russian coasts in the south and to Svalbard and Frans Josefs land in the north, and extends to the Norwegian Sea in the west and Novaya Zemlya in the east (Bryhni, et al., 2017).

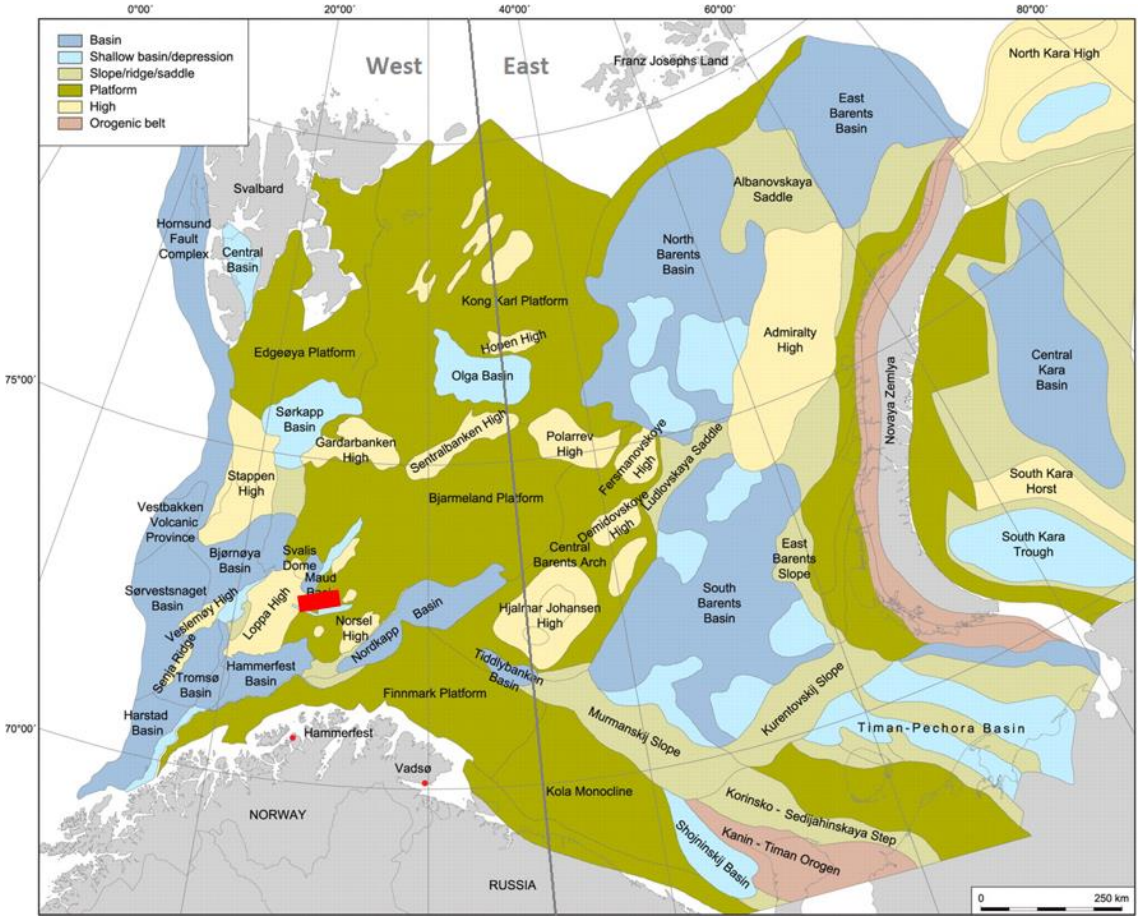

Figure 3-1. *Structural elements of the Barents Sea. Location of Study area in red rectangle. Modified from (Henriksen, et al., 2011).*

Compared to the North Sea and the Norwegian Sea, this northernmost part of the Norwegian shelf is the least explored area offshore Norway. In the 1970's, the first geophysical investigations were carried out by the NPD, and the first exploration well was drilled by Norsk Hydro in 1980. The year after, the Statoil well 7120/8-1 in the Hammerfest Basin gave the first Barents Sea discovery. This was the Askeladd gas field, today a part of the Snøhvit field (NPD, u.d.). In more recent years, new discoveries have been found. In 2011, the Skrugard oil field was discovered, later renamed to Johan Castberg, where the plan for development and operation (PDO) was delivered in 2017 (NPD, 2018). During the recent years, the level of exploration activity in the Barents Sea has been high. The Norwegian Petroleum Directorate has recently mapped the eastern part of the Barents Sea. This is an

area of about 170,000 square kilometers, larger than the Norwegian part of the North Sea. Most of the new information has been collected after the demarcation line agreement with Russia took place in 2011. The share of undiscovered resources in the Barents Sea has thus been increased from 50 to nearly 65 per cent of the total undiscovered resources on the Norwegian shelf. The resources in the new area are estimated at 1.4 billion standard cubic meters of oil equivalents, according to the (NPD, 2017).

The bathymetry of the Barents Sea is generally flat (Smelror, et al., 2009), with a water depth varying between 200-500 meters (average of 230 meters) (Bryhni, et al., 2017). It contains only a few visible features on the seafloor; shallow banks and deeper trough, formed under the last ice age (Bjarnadôttir, et al., 2013), as well as new sediments deposited on top (Smelror, et al., 2009). At a large scale, the Barents Shelf can be divided into two geological provinces; East and West (*Figure 3-1).* The structures of the eastern Barents Sea are influenced by a complex tectonic history of the Novaya Zemlya and the Timan-Pechora basin, and also by the Uralian Orogeny. The western parts have mostly been controlled by the post-Caledonian rifting phases, and by later rifting episodes (Faleide, et al., 1993).

The geological development of the Barents Sea occurs through a complex network of large-scale processes, where plate movements, changing climate and different deposit conditions took place through hundreds of millions of years. This development took place within the following tectonic main stages (Smelror, et al., 2009);

- The formation of the Timanian, Caledonian and Uralian orogenies.
- The proto-Atlantic rifting in the west.
- The opening of the Euramerican Basin in the north.
- The break-up and opening of the northern North Atlantic Ocean along the western margin of the shelf.

In addition to these major events, a series of smaller tectonic changes took place in the Barents Sea, which locally led to large variations in deposition and paleographic settings.

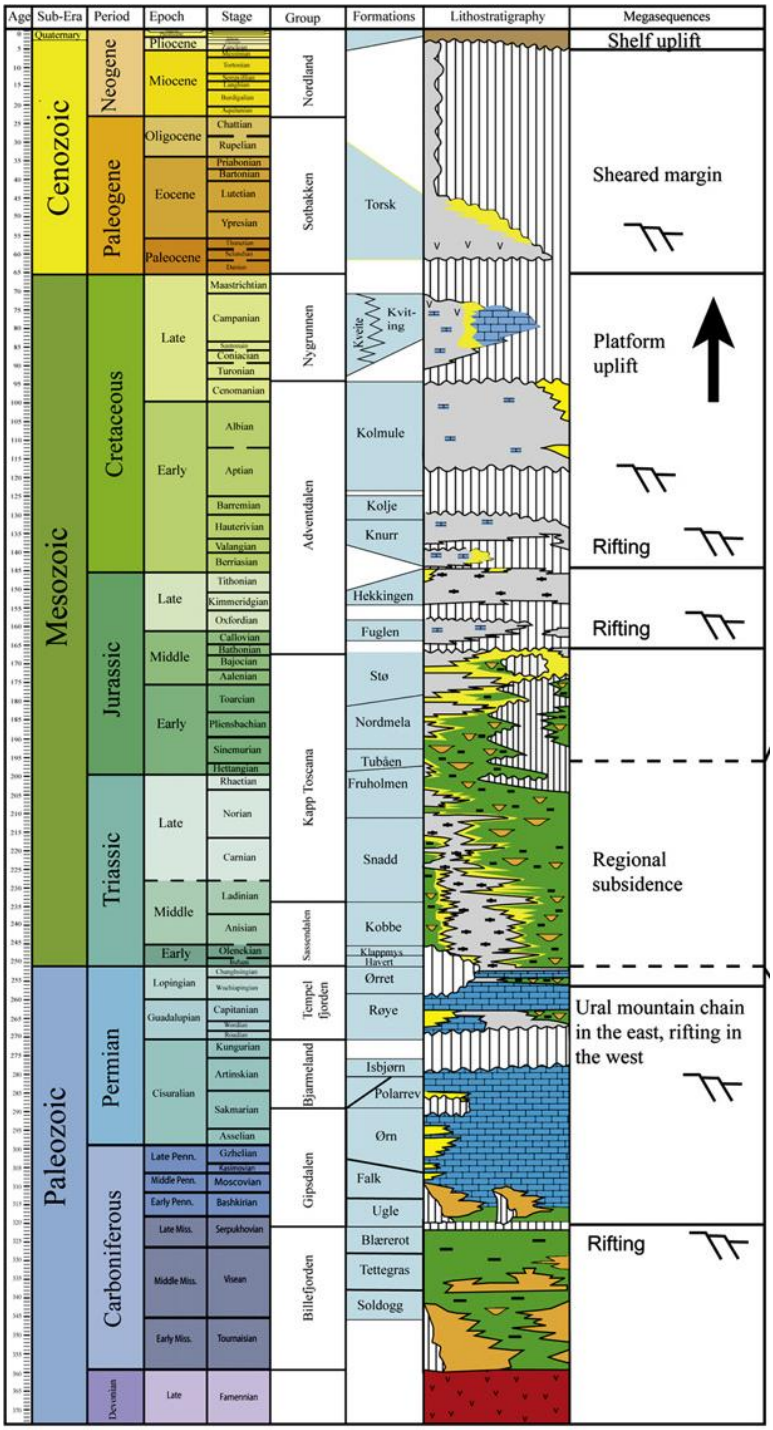

Figure 3-2. *Overview of the lithostratigraphy in the Western Barents Sea. Modified from (Glørstad-Clark, et al., 2010).*

The bedrock below the Barents Sea consists of several up to 15 kilometers deep sedimentary basins. These were formed through complex geological processes that together constitute the Barents Sea´s history. According to Faleide, et al. (2009), the western Barents Sea contains some of the world´s deepest sedimentary basins.

Smelror, et al., (2009), point out that the knowledge of the deformation history of the Earth's crust, and how its thickness varies, is essential for the understanding of the geological history of an area. In their work, a description of Moho, the horizon separating the crust from the mantle, is given. Moho has a far greater density than the crust, and therefore, gravity anomalies can be used to calculate the thickness of the crust. Crustal extension models show that the top basement correlates to the Moho geometry, such that deeper basins are underlain by thin crust (shallower Moho). This correlates more in the west than in the east. The depth of Moho is relatively constant over large parts of the Barents Sea, 32.5–35 km in the western part, and 35-37 km in the eastern part of the area, despite the fact that the Barents Sea contains deep basins. Subsequently, other mechanisms must explain the structure of the crust that is located under the major basins in the eastern Barents Sea, especially under the North and South Barents basins (Smelror, et al., 2009).

The western Barents Sea has been the area most affected by tectonic activity in Mesozoic and Cenozoic, while the eastern and northern parts have undergone less tectonic events. The various structural elements of the Barents Sea are characterized and formed under different sedimentary processes with different deposit conditions, and under tectonic influences from a varying structure of the crust. (Smelror, et al., 2009). The study area of this thesis is located in the western part of the Barents Sea *(Figure 3-1*), which will have the main focus in this section.

3.2 Tectonic history of the western Barents Sea

The geology of the Barents Sea is heavily influenced by two major continental collisions and by continental separation, events that have laid the foundation for the structural framework of the present Barents Sea (Dorê, 1994). The western part has gone through extended tectonic activity, which has led to a geology that is dominated by structural trends, moving in a few main directions. Glørstad-Clark, et al., (2010) refer to three important phases of rifting in the geological development in the west *(Figure 3-3).* The first phase occurred as early as late Devon - Carbon age, while the last two happened significantly later, in the age of late Jurassic – early Triassic, and in late Cretaceous – Paleocene times.

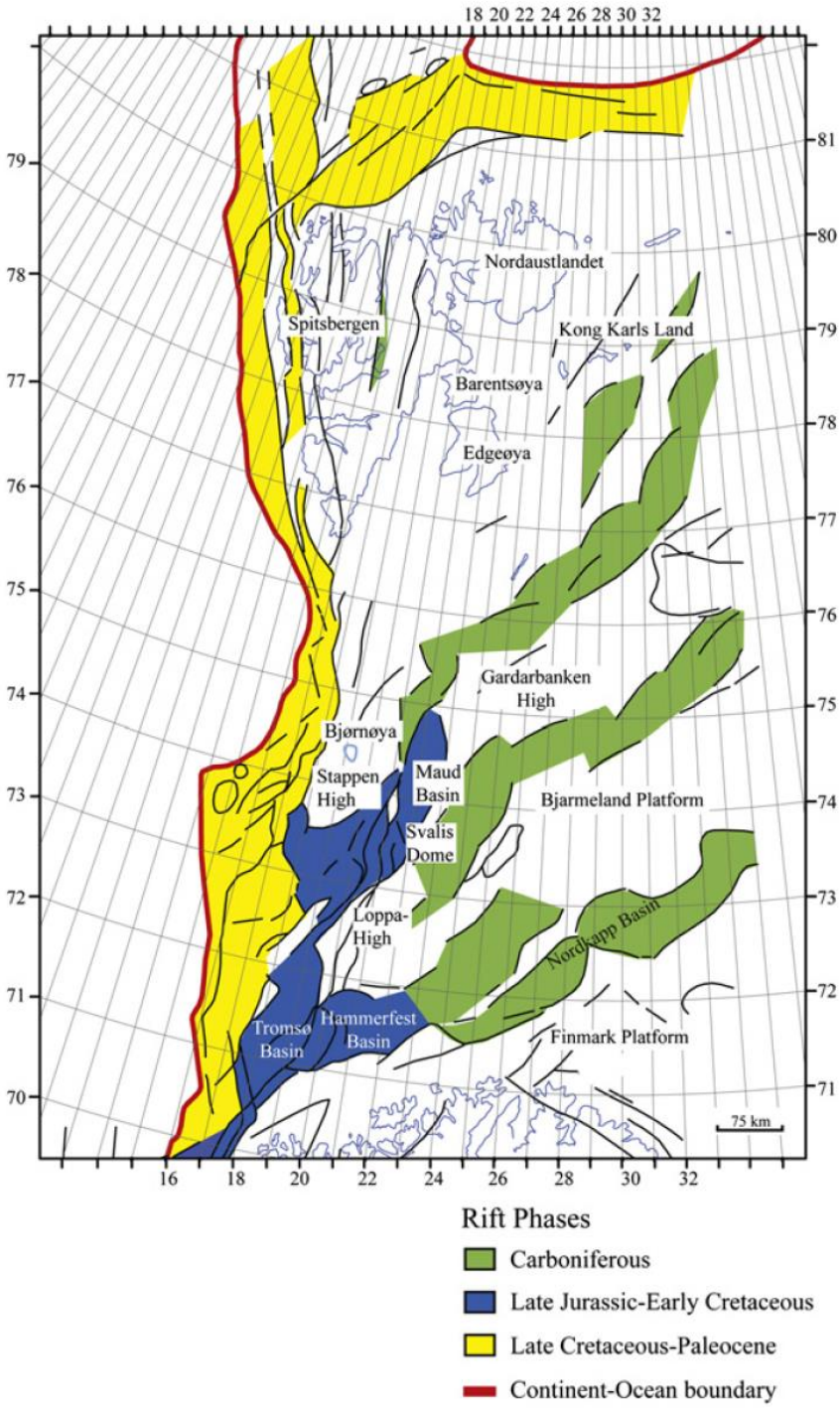

Figure 3-3. *The main structures in the Barents Sea after Glørstad-Clark, et al., (2010). The color represents the main tectonic events in the western Barents Sea.*

3.2.1 Paleozoic (541–254Ma)

The geology in the western part of the Barents Sea has been largely influenced by tectonic plate extensions and rifting in the Paleozoic age. Main events are movements westwards, with the formation of well-defined rift basins in south-west and the development of large fault systems in the north. Vital

parts of the geologic development of the Barents Sea corresponds to the Caledonian orogeny. These events took place as a response to the closing of the Iapetus Ocean, approximately 400 million years ago, which resulted in a collision of the Baltican and Laurantian plate into the Laurasia plate. (Smelror et al., 2009). The inherited structures from this orogeny affected the structural evolution of the SW Barents Sea. The Caledonian influence is observed varying between the N-S structural grain of the western Barents Sea margin and the SW-NE trends of the SW Barents Sea (Smelror et al., 2009). The Caledonian structures visible onshore, have a northeastern trend in Northern Norway, and a northwestern trend at Svalbard (Ritzmann & Faleide, 2007). After the Caledonian Orogeny, the region underwent extensive erosion in Devonian and Carboniferous, when the area was subject to exhumation, leading to accumulation of Old Red Sandstones in the western parts.

During late Devonian-early Carboniferous, a change occurred in the stress regime. The area went from being a compression regime to an extension regime with blockfaulting when the Norwegian-Greenland sea opened. The Caledonian compression was transferred into a large-scale regime of "strike-and-dip" plate movements. These movements lead to formation of folding horst- and graben structures. A 300 kilometer wide and at least 600 kilometer long rift zone in the NW direction was formed. The rift zone was a direct continuation of the northeastern Atlantic division between Greenland and Norway. These rifting phases in late Devonian – middle Carboniferous resulted in development of several continuous basins, filled with deposits of syn-rift (deposited during active rifting), separated by fault-defined hights. The rift had a fan shaped range of basins. The heights which at that time were oriented north-east, according to the corresponding rift zone, are today orientated north on the western continental shelf. The rift basins were filled with continental clastic material, carbonates and evaporates (Faleide, et al., 1984).

From the beginning of late Carboniferous, as the rifting ceased, the western Barents Sea underwent regional subsidence. This development was interrupted by a rift phase that took place in Permian to early Triassic. This episode resulted in the formation of structures with a northern trend in the western part of the rift zone. The Southern part of the Barents Sea is dominated by structural trends that go towards north-northeast. (Gudlaugsson, et al., 1998).

As the Pangea continent moved northwards in Carboniferous, the climatic conditions changed. A warmer climate together with a regional transgression led to the formation of enormous carbonate platforms, where thick successions of evaporates were locally deposited in graben structures that had developed in the southwest, like in the Tromsø and Nordkapp Basins (Faleide et al., 2008; Smelror et al., 2009).

3.2.2 Mesozoic (252 – 72Ma)

During the Mesozoic and Cenozoic, the western part of the Barents Sea has been the most active (Gabrielsen et al., 1990), and its geology has mostly been controlled by the post-Caledonian rifting phases, as well as later rifting episodes (Faleide et al., 1993). The Mesozoic succession was deposited in a shallow intercontinental sea, and shows a gradual infill of the basin trough Triassic west/northwest over time. Glørstad-Clark, et al. (2010) refers to information from interpreted seismic and core data, that shows a complex structural and stratigraphic development of the area. This has been described in many scientific articles. Main sediment source was the Urals in the southeast, the Norwegian Caledonides and the Baltic craton to the south and the North American craton to the west, with the sediments being transported to the Finnmark Platform, the Hammerfest Basin and the Nordkapp Basin (Smelror, et al., 2009)

Triassic is defined as the period between 251-200 million years ago, and the Barents Sea was covering the continental shelf of the northwestern Eurasian. It bordered to the Baltic continental in the south, the North American continent in the west, and an open sea in northwest (Smelror, et al., 2009). At this time, the supercontinent Pangea started to break up. In north-west of Europe and between Norway and Greenland, rift basins and lowland areas were formed. These rifting processes led to the creation of the Boreal Sea, which extended southwards to the mid-Norwegian shelf. (Bryhni, et al., 2013).

Triassic was a tectonic quiet period, characterized by regional subsidence and development of local heights (Faleide, et al., 1993). This tectonic setting proceeded to the middle of Jurassic (Gudlaugsson, et al., 1998). Although the western Barents Sea went through a period with low tectonic activity, the basins located in northern and southern parts, were exposed to subsidence, and formed important depocenters. The thickness of these could vary from 250 meters to 12 kilometers in the Svalbard area and up to 20-30 kilometers in the platform areas. According to Gudlaugsson, et al., (1998), the late Permian-early Triassic tectonic movements led to uplift, tilting and extensive erosion processes. Seismic profiles from east to west show clear evidence of syn-tectonic sedimentation and N-S trending structures in the western Barents Sea. Along the western Loppa High and north to the Fingerdjup Basin, faults showing this movements is observed. From Carboniferous to Permian times, eight tectonic events are reconstructed at Loppa High, where two of them could be of Triassic age (Faleide, et al., 1993).

This paleogeographical setting remained stable trough early- and mid-Triassic, while sediments gradually filled the shelf areas (Riis, et al., 2008). According to (Faleide, et al., 1984), the geology in the southwestern part of the Barents Sea was formed under influence of events that occurred both in the Arctic and in the North Atlantic areas. As a result of subsidence after extensive rifting in the Jurassic and Cretaceous ages, there were formed a number of sedimentary basins from Rockall and

north, in the North Atlantic Ocean (The Faroe and the Møre-Vøring Basins). The area that is called the De Geer Zone, has relations to both the North-Atlantic and the artic areas. At first, an area with canted structures was developed, linking the Arctic and North-Atlantic rift systems from middle Jurassic to early Cretaceous ages. Later, the area went through a phase with a regional setting, with fracturing caused by stress in late Cretaceous to Paleozen ages. Eventually, a phase with combined setting with fracturing and rifting took place, resulting in the opening of the Norwegian-Greenland sea. The northern Atlantic Ocean and the Artic areas are connected through transition zones that were developed during this separation phase in late Mesozoic/Cenozoic age (Faleide, et al., 1984).

In Late Triassic-Early Jurassic, substantial areas of the Barents Sea were uplifted and eroded, leading to a change of depositional environment in early Toarcian from flood plain to westward prograding coastal settings. During late Toarcian, the western basins depositional environments had a shallow marine setting. The Barents Sea regression reached its maximum in the Middle Jurassic, and large parts of the shelf was exposed to erosion. This led to a big depositional gap in large areas at the western Barents Sea. From regression maximum in Middle Jurassic, the sea level changed to a transgressional maximum. In the Loppa and Stappen Highs, erosion still went on at as their uplift continued because of the Cimmerian movements (Smelror, et al., 2009) .

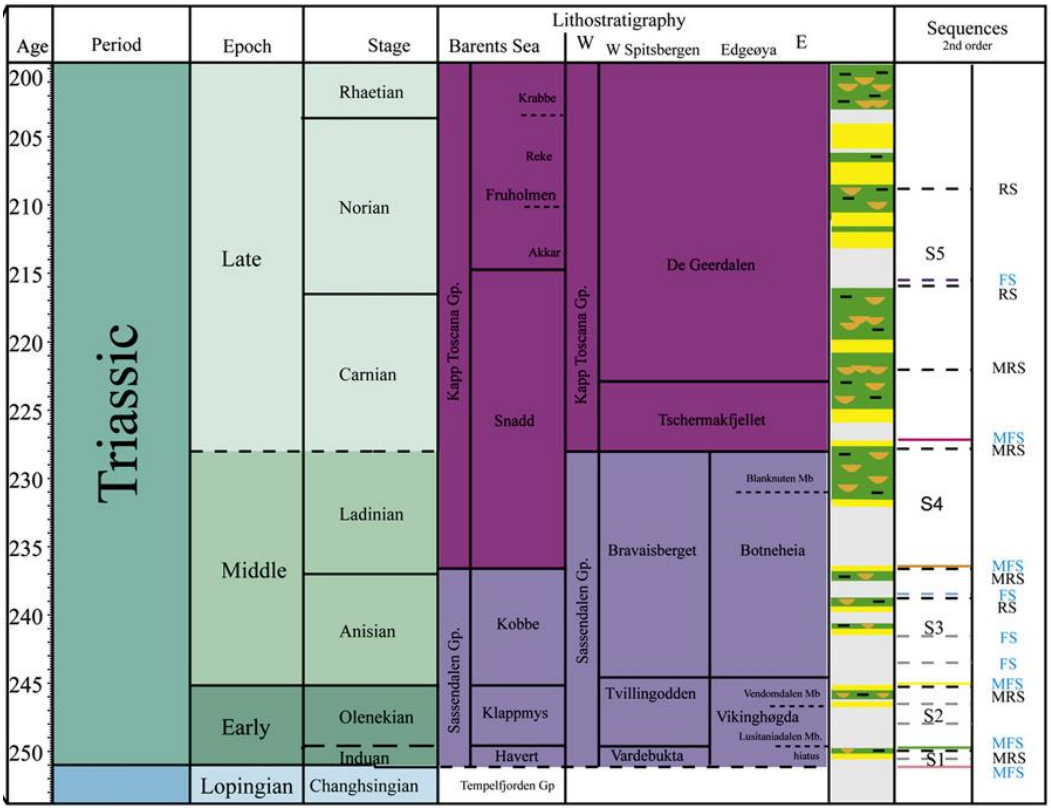

Figure 3-4. *Schematic diagram of the Triassic second-order sequences. Modified from (Glørstad-Clark, et al., 2010).*

3.2.3 Cenozoic (66Ma – present)

In late Paleocene time, the Norwegian-Greenland Sea expanded. A sheared western Barents Sea margin was developing. This margin went through both transtentional and transpressional deformation in Eocene, causing faulting and uplifting in the southern Sørvestnaget Basin. As a result of tectonic and magmatic activity in the Vestbakken Volcanic Province, the northern part experienced extensional faulting (Faleide et al., 1993). In Oligocene, the Eocene faulting activity at Vestbakken Volcanic Province was reactivated, caused by a change in the relative plate motion. Later in Oligocene, the margin became tectonically quiet. The later sedimentary deposits at the western margin and bordering areas are therefore mostly of glacial origin (Faleide, et al., 1993).

In Pliocene, large ice sheets covered major parts the Northern Hemisphere. Climatic variations led to several phases of glaciations and deglaciations, and the uplifted Barents Sea shelf went through extensive glacial erosion. Several and heavy phases of erosion in this area led to regional hiatus in the stratigraphic records, represented by URU, the Upper Regional Unconformity in most of the Barents shelf. This extensive erosion varies between estimated removal of 2–3 kilometers of overlying beds in the Svalbard area, and 1 to 1.5 kilometers in Hammerfest basin and Loppa high (Smelror et al., 2009). These huge amounts of sediments were transported by glaciers towards the western margin, and led to sediment accumulations of up to 4 km in Bjørnøya and Storfjorden fan (Smelror, et al., 2009).

3.3 Stratigraphy and depositional environments in western Barents Sea

3.3.1 Introduction

Different depositional environment can be distinguished and recognized in the seismic data, in cores and in well logs. By studying changes within the data, discrete variations can be mapped in order to fully understand the geologic and environmental development. Different patterns can be recognized to represent different seismic facies. The depositional environment of the Triassic succession in the Western Barents Sea is recognized to vary within a wide range of settings, from offshore and shallow marine through shelf and shallow marine to paralic and fluvial environment (Klausen, et al., 2015). The periods of marine influence are indicated by a maximum flooding surface, where offshore marine deposits unconformably overlay shallow and non-marine material. These surfaces are used to divide the formation into stratigraphic levels and subsequently into a sequence stratigraphic hierarchy, which will be related to in the discussion of this thesis. Klausen, et al., (2015) divides the depositional environment into five distinct seismic facies, F1 to F5 *(Figure 3-5*):

F1. Slope and basin

The seismic reflectors are characterized by a basinwards dip, with clinoform configuration which characterize the overall depositional environment. The clinoforms typically have sigmoidal to oblique form with a tangential bottomset, where the height of the clinoforms can go from 100 – 500 meters. This height represents the water depth from the shelf to the basin (disregarding the compaction). The clinoforms are representing the offshore marine shelf edge and slope, which is separating the deep marine from the platform-and-shelf shallow marine environment. The prodelta and the shelf is often dominated by mud (Klausen, et al., 2015).

F2. Shelf

This facies is located closer to land and/or higher up in the stratigraphic level relative to clinoforms. The seismic reflectors are characterized as continuous, parallel and with high-amplitudes. This seismic package is often observed on top of marine flooding surfaces, with a gradual transition to more marginal marine settings. The lateral extent of this facies can be several kilometers wide, with a thickness range from 20 to 100 milliseconds. This facies is represented to correspond with an open marine shelf or a prodelta depositional environment.

F3. Marginal marine and shoreface

The seismic facies is characterized by parallel, discontinuous reflectors, consisting of alternating high- and low amplitudes. The thickness of this unit varies from 20 to 40 milliseconds, with a lateral extent from 1 to 10 kilometers in a dip direction, and hundreds of kilometers in the depositional strike direction. The high amplitudes observed in the facies are arranged in sets up to 10 kilometers wide, and appear as elongated and straight in a plain view. In well logs, the facies is characterized by a coarsening upwards and shallower trend, and represented by a decrease in gamma ray values. This facies represent a marginal marine depositional environment.

F4. Coastal plain

This facies is dominated by discontinues, irregular and often weak amplitude reflectors. The thickness of this facies varies between approximately 30 and 450 meters, with a varying lateral extent depending on regression or not. The facies is often found conformable with a gradational relation to marginal marine facies in lower stratigraphic levels, and bounded by a sharp, unconformable relation to marine shelf facies. This facies is represented as coastal plain dominated by silt and mud. The irregular and discontinuous appearance of the seismic reflectors, is explained by variations of heterolithic depositions. Such depositions could be fluvial bodies, coal and crevasse splays, that are not seismically resolvable, but still contribute to this expression.

F5. Channel sandstone bodies

This facies is represented by strong, discontinuous seismic reflectors, with low and high amplitudes. In plan view, these features consist of straight to sinuous shapes. The width of this features is varying from tens of meters to tens of kilometers, and the length can be several kilometers. The thickness of this facies varies in the range of seismic tuning. This facies represent channel sandstone bodies, and is observed encased in the coastal plain. The channel grain size is varying from medium to fine sand, often shown with a fining upwards trend. They are often recognized in the seismic section by an erosive base.

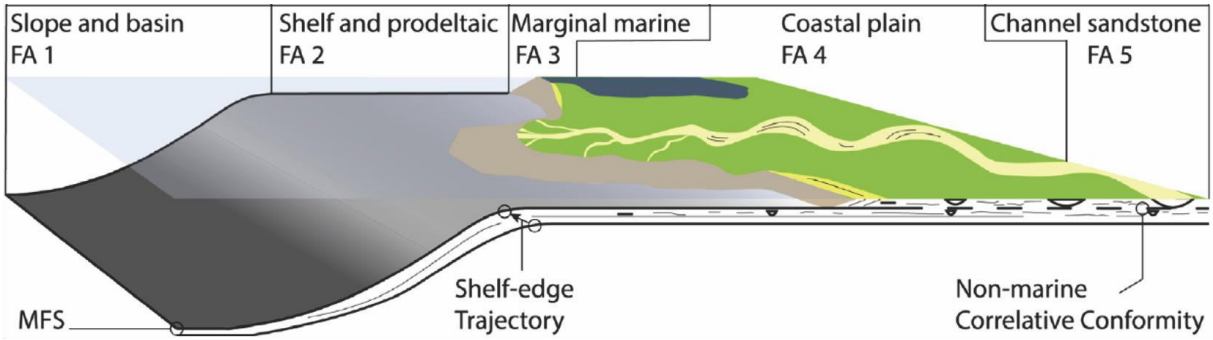

Figure 3-5. *The different marine and coastal depositional environments found within the Snadd Formation (Klausen, et al., 2015).*

3.3.2 Paleozoic statigraphy and depositional environments

The stratigraphy in the western Barents Sea range from Late Paleozoic to Quaternary, and the basement was formed under the origin of the Caledonian orogeny *(Figure 3-2)* (Gudlaugsson, et al., 1998; Glørstad-Clark, et al., 2010). During Late Paleozoic, crustal extension dominated in most parts of the Barents Sea, which created massive rifting structures. Alluvial fans of a NE-SW trend represented major infill in the rifted basins in Late Devonian to Early Carboniferous, depositing large amounts of continental clastics with a coarsening upwards trend both in rifts and on floodplains (Faleide, et al., 1984). During late Carboniferous throughout Early Permian, an extensive carbonate platform was developed, together with evaporitic deposits in local basins (Worsley, 2008; Glørstad-Clark, et al., 2010). In Permian, there was a shift in the oceanic climate from shallow warm waters to temperate. This resulted in a change in the biogenic composition to cool water carbonates, represented

by the Bjarmeland Group. In Late Permian, the water temperature decreased, changing the deposition regime to silica-rich fine clastics, represented by the Tempelfjorden Group (Worsley, 2008).

3.3.3 Mesozoic statigraphy and depositional environments

During the transition from Late Permian to Early Triassic, a change from silica-rich shale to non-siliceous shales marks a significant shift. This non-siliceous shale stratas are represented by the Sassendalen Group, which comprises the Havert and Kobbe Formations. Sassendalen Group ranges between less than 100 meters at pre-existing highs to more than 1500 m at the southwestern continental shelf, due to the precence of a significant hiatus on highs and platforms especially, from the latest Permian (Worsley, 2008). The deposition during Triassic is heavily influenced by sediments eroded and transported from the Baltic Shield and later the Uralian Orogeny, defining a northwesterly prograding coastline (Worsley, 2008; Glørstad-Clark et al., 2010).

The article "Triassic seismic sequence stratigraphy and paleogeography of the western Barents Sea area" (Glørstad-Clark, et al., 2010) focuses on the tectonic development of this area up to late Permian - early Triassic age, and tries to get an understanding of the big scale changes in the depocenters in the Triassic *(Figure 3-6)* . Furthermore, they discuss the controlling factors for the development of this succession, and how the geological settings in the different areas contributed to this development. The article tries to put their area into the same stratigraphic framework and paleographic context as the area further east. Glørstad-Clark, et al., (2010) investigate the complex interactions between tectonic subsidence, reactivation of old fault and sediment inputs, which affects the basin infill-history of the whole Norwegian Barents Sea. Further, the development of available sediment volumes over time is pointed out as a controlling mechanism for basin formation in the western Barents Sea. One critical factor, is to constantly check the coastline at any time, to understand the maximum spreading and the potential for the development of reservoir rocks (Glørstad-Clark, et al., 2010). This work refers to information from interpreted seismic and core data, that shows a complex structural and stratigraphic development of the area. This has been described in many scientific articles. According to Glørstad-Clark, et al. (2010) the western Barents Sea can be divided into three main dominant areas:

- An overall platform area north of 74 degrees.
- A regional pool province south of 74 degrees and east of the Paleo-Loppa High, with several local basins.
- A continental shelf west of the Paleo-Loppa High and south of Stappen High, characterized with thick Mesozoic and Cenozoic succesions in deep basins, with a thick Cenozoic, passive marine sedimentary wedge, which has widespread in the North Atlantic.

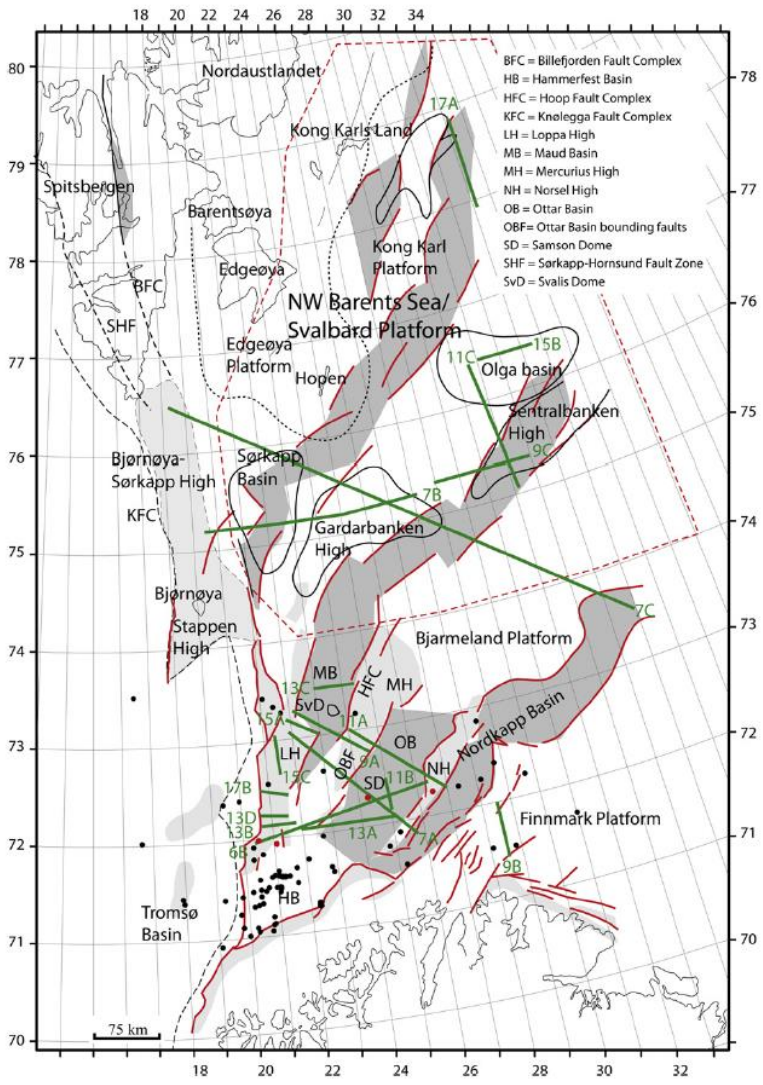

Figure 3-6*. Western Barents Sea structural elements from late Paleozoic and placements of seismic reference examples in (Glørstad-Clark, et al., 2010).*

3.4 Sedimentary infill in Triassic

A northwestern prograding system that developed during Ladinian generated deltaic and floodplain environments with widely deposited fine grained clastics at the southwestern Barents Shelf. Through Carnian, the subsidence and sedimentation continued from the Baltic Shield, resulting in a thick and widespread non-marine sedimentary package, represented by the Storfjorden Group and the Snadd Formation (Worsley, 2008; Glørstad-Clark, et al., 2010; Klausen, et al., 2015) . Time-thickness maps and maximum progradation of interpreted sequences show a progressive infill of the Barents Sea from early Triassic to late Triassic (Glørstad-Clark, et al., 2010). There is an increase in thickness in lower Triassic sequences when moving eastward, but in the middle Triassic to late Triassic, the sequences increase in thickness towards west and northwest. The deposits in Triassic were affected by both

paleo-topography, rift formations and uplift in late Paleozoic era, especially related to the latest extension event in Permian times. (Glørstad-Clark, et al., 2010)

This paleo-topographic relief was filled over time, with sediments from lower Ladinian, which filled the potential of the paleo-Loppa High. Here, the deposits in Bjørnøya-Sørkapp High was onlapped, and later developed into a depocenter of upper Triassic sediments (Glørstad-Clark, et al., 2010) Several areas with Triassic sediment sources are found in the western part of the Barents Sea, but the main source is located southeast and east in the Barents Sea, probably related to the Ural mountain range. Nevertheless, local source areas cannot be ruled out, and the island group Novaya Zemala located in the east could, according to Glørstad-Clart, et al (2010), have played a more significant role as a source in the mid and late Triassic.

As a concequence, the largest basins in the east must have been infilled in advance by one big progradation in the Barents Sea in late Induan age. Glørstad-Clark, et al (2010), have not found any evidence of a northastern sediment source from Triassic in the northwestern Barents Sea, but supports Riis, et. al (2008)'s view, that a large scale progradation from southeast and east took place, with developing of a continuous shelf and platform area from the sediment source in south and southeast, and entirely up to the Svalbard area.

Throughout the Triassic period several source areas existed. From the Fennoscandian shield in the south, to the main sediment source area in the southwest, in addition to local source areas related to uplift of paleo-Loppa High area, especially in the early to mid-Triassic. The Greenland area also represented an important area of source sediments for the Svalbard area in early to late Triassic, and may have represented a big source area of upper Triassic succession at the Bjørnøya-Sørkapp High and paleo-Loppa High (Glørstad-Clark, et al., 2010).

The northwestern Barents Sea was located distant from the main deposition source, and was not developed until the basins further south were filled. On the seismic, clinoforms from the south and east that originate from Ladinian time can be obserevd. The basins east of Bjørnøya-Sørkapp High was filled up from east during late Triassic, and possibly also from the west. There was a sediment distribution, controlled by Paleo-Loppa High until early Ladinian age, with a big uplift event in late Permian that lead to several local source systems spreading from west to east. In late Triassic, the Paleo-Loppa high area had the thickest deposits, due to the development of the North Atlantic system to the west. Clinoform geometries were formed west of Loppa High, and towards Bjørnøya Basin. Multiple clinoform units, which spread from west to east, were identified in Paleo-Loppa High in the upper Triassic, which represented a source area to the west.

In the work of Glørstad-Clark, et al. (2010), seismic facies were used to reconstruct paleogeography, and to analyze the lithostratigraphic distribution in Triassic. Clinoform geometries and marine progragation of deltas and shelf areas (*Figure 3-7)*, are key factors to understand the presence of source and reservoir rocks. In this study, seismic clinoform geometries were analyzed to be able to map out the reservoir- and source rock distribution in the key area. An important aspect of this work, was to focus on the shoreline's position relative to the observed breakup on the seismic offlap in the data, which varied across the area, migrating along platforms, as a response to changes in the sea level.

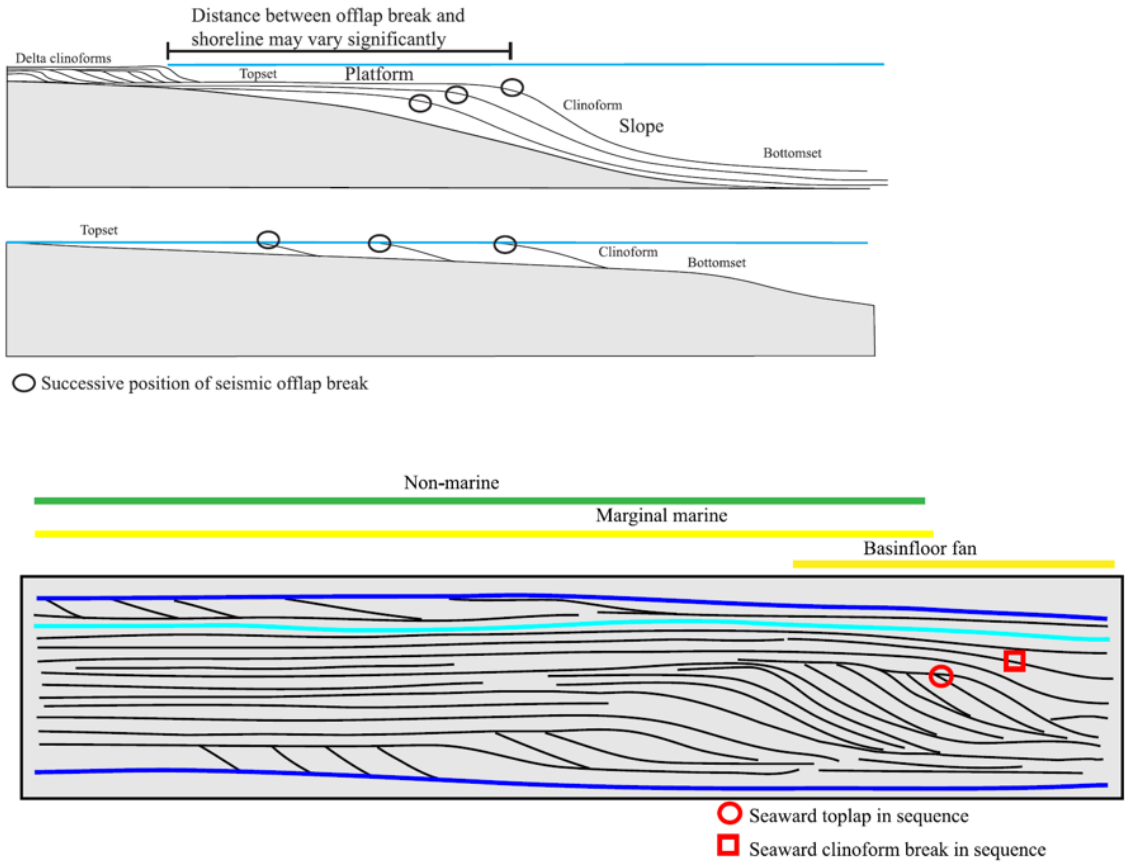

Figure 3-7. *A) Diagram showing different scale prograding delta and shelf clinoforms* (Glørstad-Clark, et al., 2010). *B) Section illustrating the prediction of depositional environments from seismic facies analysis used to reconstruct paleogeography. In this basin setting there is an overlap in potential reservoir facies within each second-order sequence due to the rapid progradation and retrogradation of continental and marginal marine facies* (Glørstad-Clark, et al., 2010).

In general, the resolution of 2D seismic will not be good enough to map small-scale delta clinoforms on the platform, or make it possible to show more detailed reservoir geometries. Glørstad-Clark, et al. (2010), however, concludes carefully, that the Triassic succession in the western Barents Sea, can be divided into five second-order sequences, controlled by regional to global tectonic events, named S1 to S5 *(Figure 3-2).*

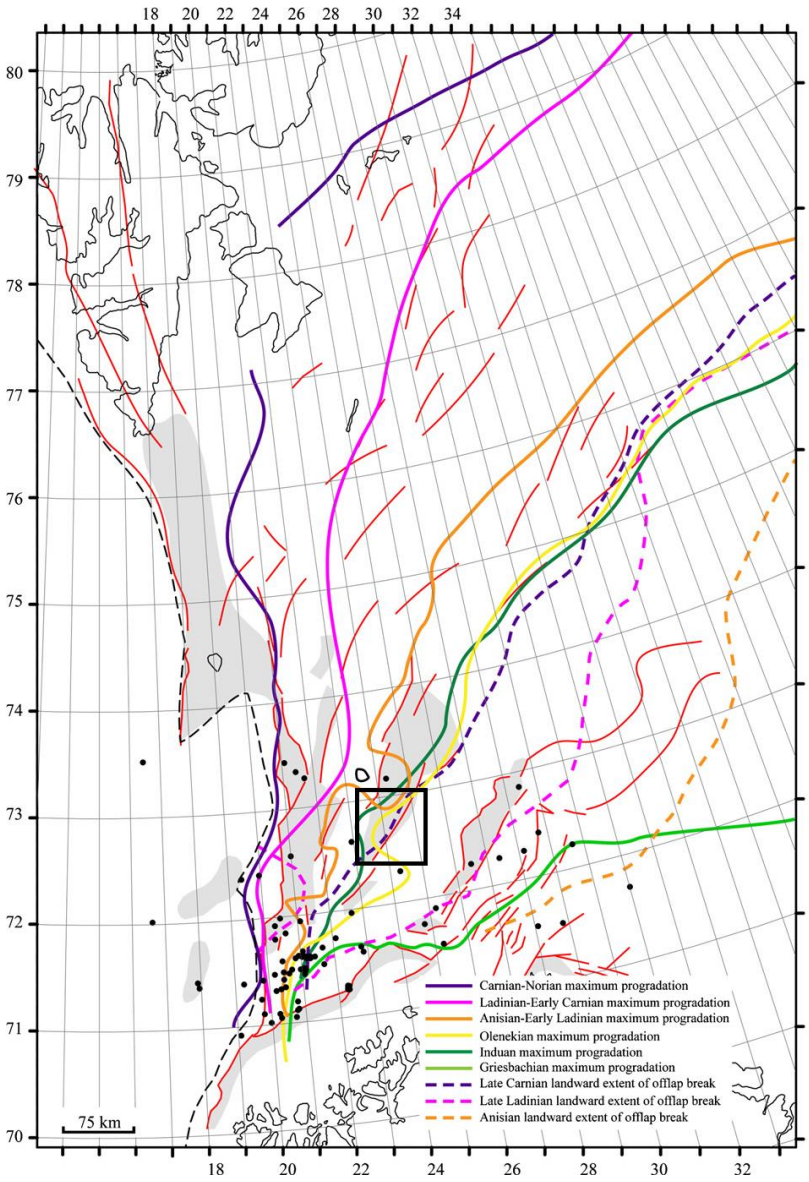

***Figure 3-8**. Gradual infill of the Barents Sea through time in the Triassic, modified from Glørstad-Clark, et al., (2010), with area of interest. Solid lines: Maximum regressive surfaces for sequence S1 to S5. Dashed lines: Landward extent of clinoform geometries within each sequence.*

Sequence S1-Induan sequence

This unit is in many areas correlated to the Havert formation by the NPD. The top of the S1 is marked with strong and continuous seismic amplitude, and can probably represent a MFS (maximum flooding surface). The surface represents an angular unconformity in the paleo-Loppa High area, and the upper boundary of this sequence is one of the most prominent surfaces in the Norwegian Barents Sea, characterized with downlap stratal geometries close to source areas and onlap in the basin close to highs. The lower limit of the sequence is difficult to map because of the late Permian-Triassic unconformity, represented by significant Upper Permian facies variations with carbonates on the Finnmark Platform, clastics in the Hammerfest Basin and spiculites in the Nordkapp Basin and

Bjarmeland Platform. The main depocenter in the Early Triassic is the Bjarmeland Platform, with depositional thinning to the west towards the ancestral Loppa and Stappen highs, but also north in the NW Barents Sea (Glørstad-Clark, et al., 2010).

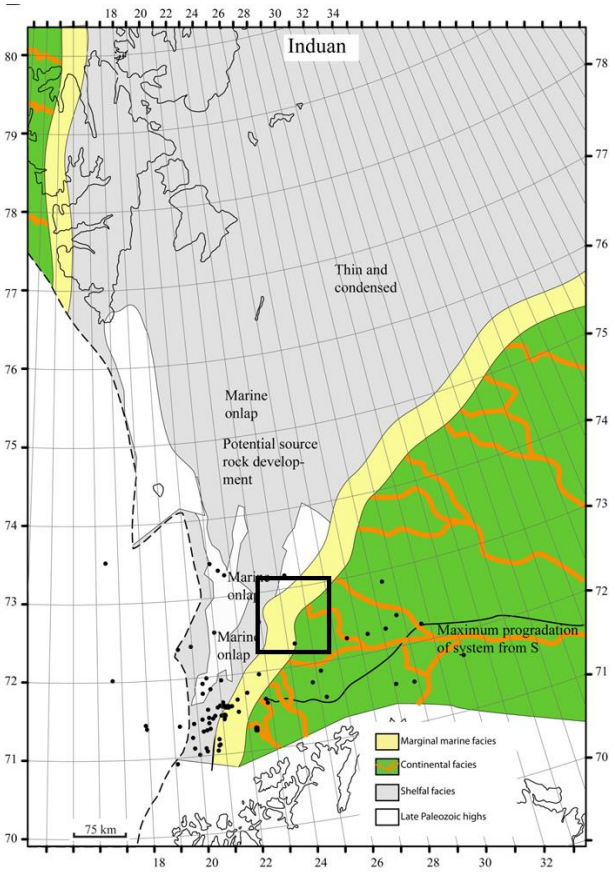

Figure 3-9. *Paleographic reconstruction of the maximum progradation in Induan. Study area in black square. Modified from (Glørstad-Clark, et al., 2010)*

Sequence S2-Olenkian sequence

The sequence is bounded (both upper and lower limit) by strong, continuous seismic amplitudes throughout the study area. It is interpreted to represent a MFS, where a significant increase in sea level marks the border between the Induan (Havert Formation, S1) and Olenkekian (Klappmys S2) times. The sequence is clearly divided into two events. In the lower part of the sequence there is observed clear north-vest orientated clinoforms that may indicate marginal progradation of marine sediments from the south-east. The upper part of the sequence consists of clear, relatively continuous, parallel reflections, which may indicate marine deposits. The seismic facies on the Bjarmeland Platform is generally parallel, with relatively weak, discontinuous amplitude. Strong continuous amplitudes are observed in areas where the sequence thins out and onlaps the underlying units towards the paleo-Loppa High and NW Barents Sea. Thickest sequence development is observed on the Bjarmeland Platform, as the underlying sequence S1, but S2 is thicker developed in the Hammerfest Basin. The sequence can be correlated to the Klappmys Formation in most wells (Glørstad-Clark, et al., 2010)

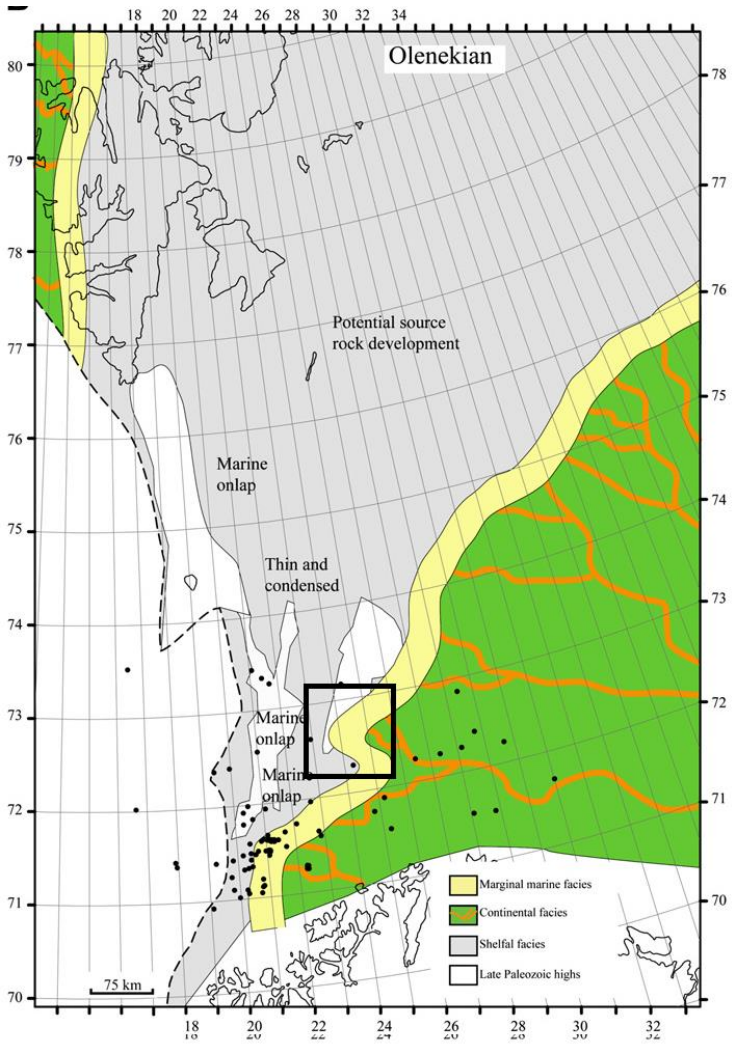

Figure 3-10. *Paleographic reconstruction of the maximum progradation in Olenkian. Study area in black square. Modified from (Glørstad-Clark, et al., 2010)*

Sequence S3-Anisian - early Ladinian sequence

The top and bottom of the sequence is marked with strong, continuous amplitudes that are interpreted to represent MFS. This sequence has a rather constant thickness throughout the study area of (Glørstad-Clark, et al., 2010). A main part of this sequence, from the lower limit to a little past halfway through, is shown as continuous, parallel and clear reflectors that might indicate a quiet depositional environment, probably marine. The upper section of the sequence consists of discontinuous low seismic amplitude reflectors, with spots of high amplitudes. These high amplitudes is later interpreted to be fluvial channels, which builds out from the south-east and suggest a sea level drop. This surface shows downlap geometries closer to the paleo-Loppa High, on top of the high in the south, towards the Svalis Dome and north of 74 degrees N. The sequence has very strong internal

amplitude surfaces developed, subdividing this sequence into four third-order sequences. The internal surfaces are best developed to the west and northwest, particularly around the paleo-Loppa High and the Maud Basin, where it displays downlap stratal patterns. In the Hammerfest Basin and on the Bjarmeland Platform, they are only correlative conformities. The sequence thickens from the Bjarmeland Platform and north of 74 degrees N, accompanied by a change from parallel seismic facies to the development of clinoform geometries before it rapidly thins in the NW Barents Sea. This sequence is correlated to Kobbe- and Steinskobbbe formations in several wells (Glørstad-Clark, et al., 2010)

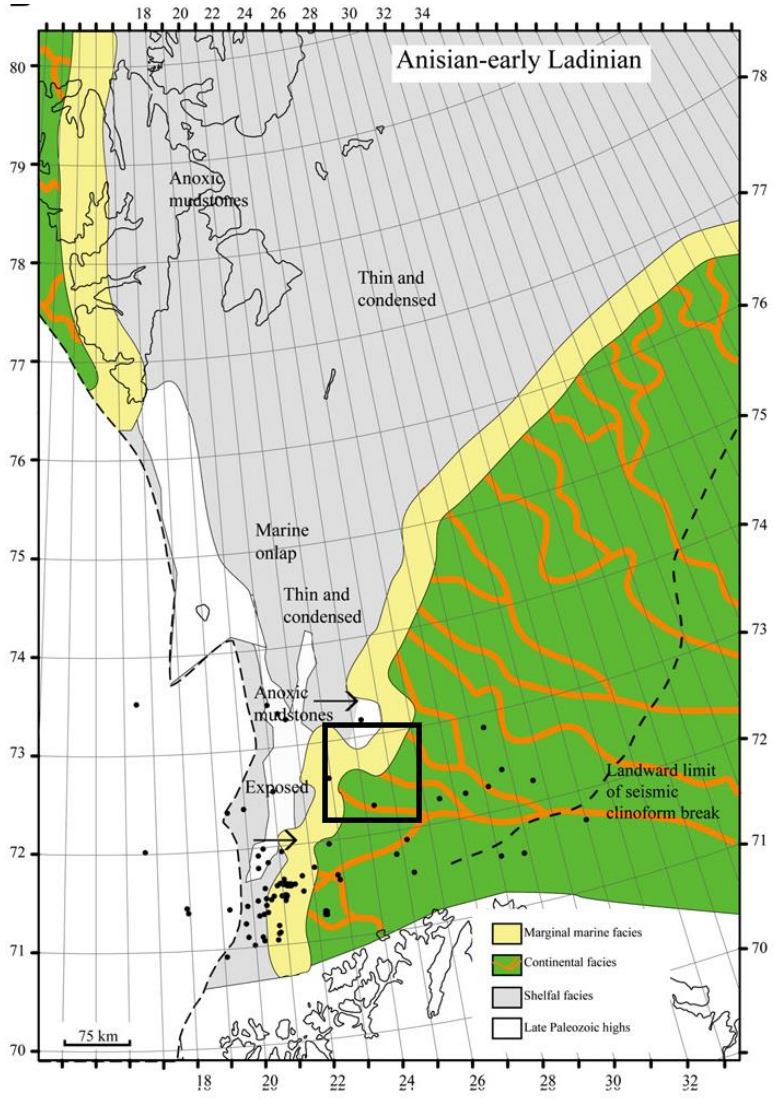

***Figure 3-11**. Paleographic reconstruction of the maximum progradation in Anisian-early Ladinian. Study area in black square. Modified from (Glørstad-Clark, et al., 2010)*

Sequence S4-Ladinian-early Carnian sequence

Sequence S4 has top and base with strong amplitudes of significant regional extent, best identified near the Loppa High. It correlates with the lower part of the Snadd Formation in most wells. The basal surface displays downlap stratal patterns, and looses character to the south, southeast and east, where it is a correlative conformity (Glørstad-Clark, et al., 2010). It is bounded at the base and top by maximum flooding surfaces. An internal maximum regressive surface is mapped out at the Ladinian/Carnian boundary, which is interpreted by Glørstad Clark et. al (2010) to represent a change in seismic facies on the Bjarmeland Platform, and clinoform geometries further west into the basin above and west of paleo-Loppa High.

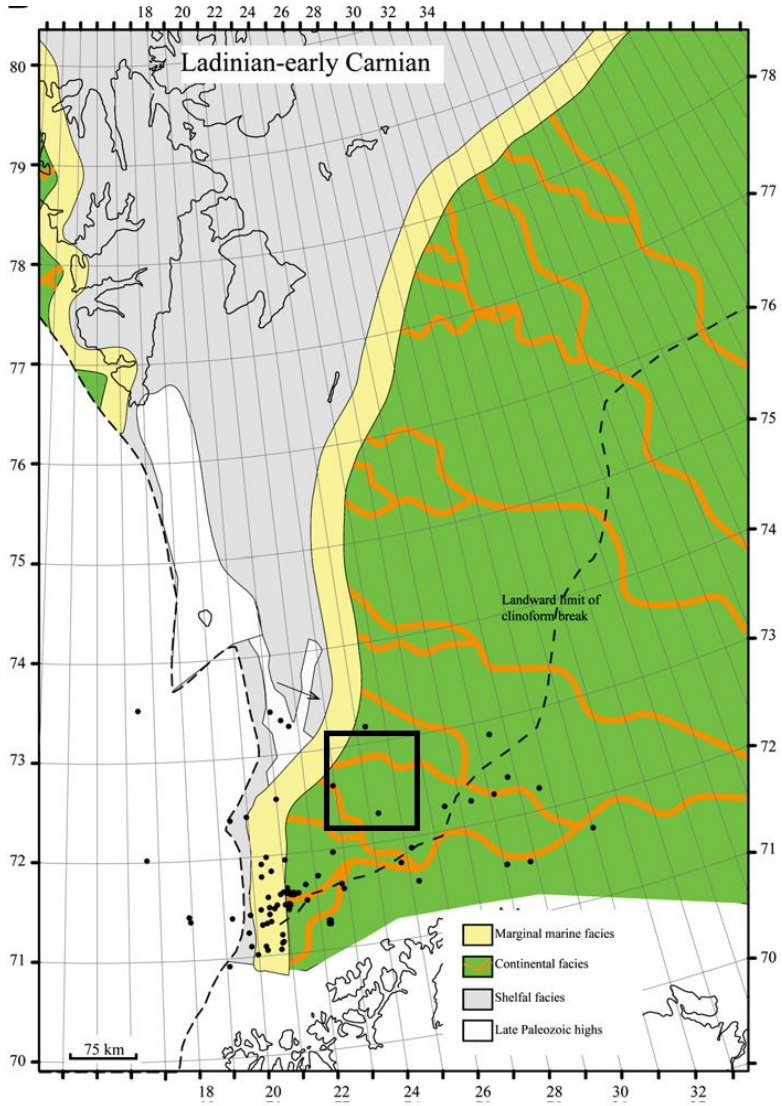

Figure 3-12. *Paleographic reconstruction of the maximum progradation in Ladian-early Carnian.. Study area in black square. Modified from (Glørstad-Clark, et al., 2010)*

S4 shows an easterly thinning to the west, close to and west of paleo-Loppa High, where it shows development of local depocenters. According to Glørstad Clark et. al (2010), the lower part of the sequence onlaps and partly blankets the eastern flank of the paleo-Loppa High, and it shows parallel to transparent and reflection free seismic patterns in the eastern part of their study area. Towards west and northwest, S4 is represented by clinoform geometries. The sequence shows parallel, discontinuous high amplitude seismic reflections higher in the sequence east of the paleo-Loppa High area and south of 75 degrees N. A system prograding west to east is observed west of the Svalis Dome, and a similar system is found further south slightly west of the paleo-Loppa High prograding from the west to the east (Glørstad-Clark, et al., 2010) . The change in seismic facies from low-angle clinoform geometries to parallel high amplitude seismic reflectors correlates to the maximum regressive development within this sequence, and is interpreted to represent a significant drop in relative sea-level. Basinward, this transition correlates to clinoforms with frequent toplap geometries, supporting the interpretation of a fall in relative sea-level (Glørstad-Clark, et al., 2010).

A transgression marks the onset of this sequence and pushed the shoreline significantly further towards the southeast. Glørstad Clark, et al., (2010) interpret this change in depocenters to be caused by continued infill of the Norwegian Barents Sea towards the west and northwest. The paleo-Loppa High appears to have started developing into a basin particularly during deposition of the upper part of the sequence. The thinning of this sequence to the east is interpreted to express slower generation of accommodation space on the Bjarmeland Platform allowing sediments to bypass this area and be deposited basinward, which means that the sediments was transported across this area from east and accumulated in the basins westwards. The upper part of the sequence shows a significant level of local high amplitudes on the seismic interpreted to be channel systems. In general, the seismic facies indicate that the upper part of this sequence is dominated by continental deposits, where a high number of channel systems can be mapped out (Glørstad Clark et. al (2010). The lower part of the sequence is interpreted to represent mainly distal shelfal deposits, also confirmed by well logs in well 7324/10-1.

According to (Glørstad-Clark, et al., 2010), S4 is the first sequence that shows significant thickening behind the paleo-Loppa High. At this time, the paleo-Loppa High is no longer a pronounced structural feature, and accommodation space is generally filled in east of this area.

Sequence S5-Upper Triassic

The lower and the upper limit of this sequence is represented by strong and continuous seismic amplitudes, where large parts of the upper limit has been eroded by the Base Cretaceous Unconformity or the Upper Regional Unconformity (URU). The lower limit represents MFS, based on extent and the

observed stratal patterns (Glørstad-Clark, et al., 2010). The sequence consists of several seismic facies, which is relatively parallel to several channel-like features observed in the seismic survey. The sequence shows a distinct thickness to the west and does not correlate well to the lithostratigraphy. S5 is linked to the upper part of the Snadd formation and the entire Fruholmen formation in several wells. The lithostratigraphic border between the Snadd and the Fruholmen formations is not obvious on 2D seismic data as observed in this study (Glørstad-Clark, et al., 2010).

According to Glørstad-Clark, et al. (2010), these sequences show a gradual infill from several different sediment sources, but with a main provenance area in the east and southeast. The deep and wide East-Barents Sea basin was filled in late Permian to early Triassic, and due to severe progradation, this also reached the western Barents Sea. These sequences show a progressive infill of depocenters throughout time and important infill in structures, which were formed by tectonic events in Permian. Limited number of seismic clinoforms are observed within this sequence east of the paleo-Loppa High, but seismic facies indicate very strong local reflection packages. The facies occur mainly as parallel with some channel-like features, thinning to the south and east. In sequence S5, no progradational geometries are observed on the Bjarmeland Platform. Available accommodation space was filled on the Bjarmeland Platform and the area was mainly bypassed. Sediments were transported to the west (paleo- Loppa High), north and north-west in the previously underfilled NW Barents Sea. S5 represents the change of focus of main deposition from the Bjarmeland Platform to occur above the paleo-Loppa High. S5 is the first sequence exhibiting clinoforms prograding from west to east on top of the paleo-Loppa High within the upper part of the sequence (Glørstad-Clark, et al., 2010).

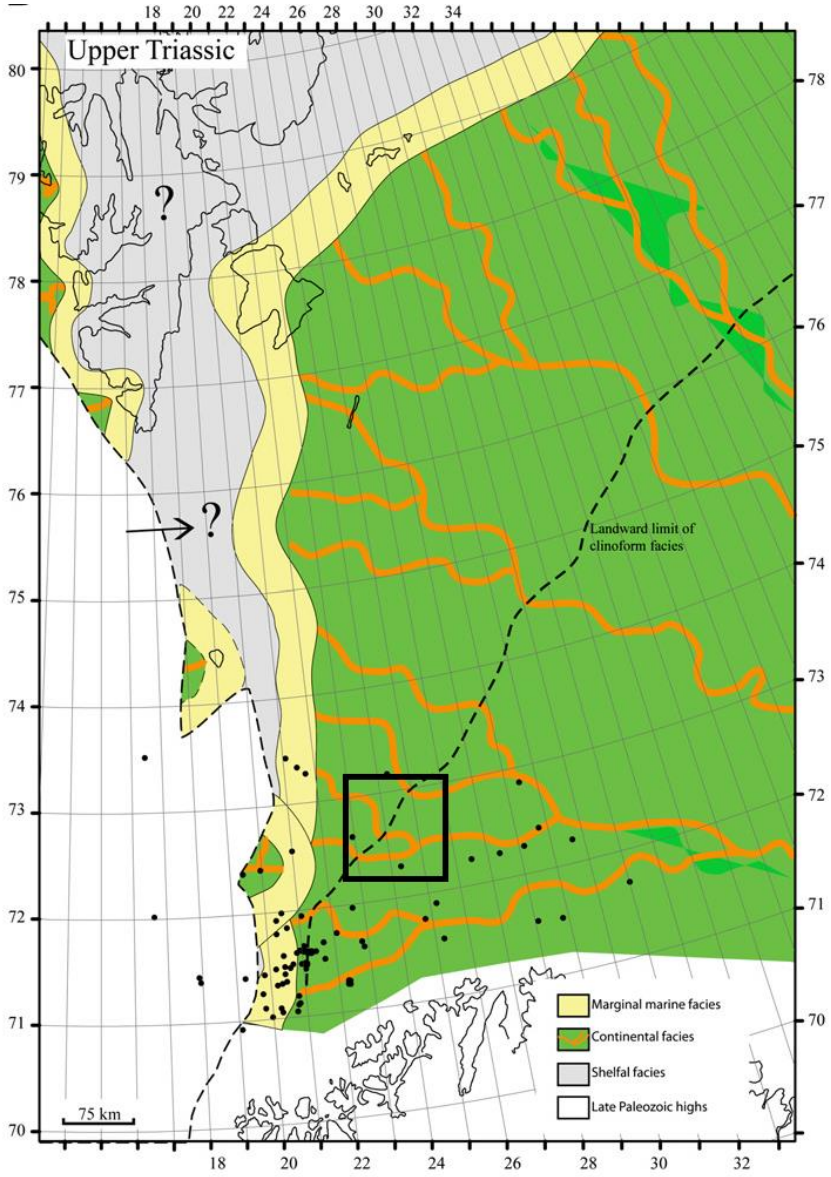

***Figure 3-13**. Paleographic reconstruction of the maximum progradation in Upper Triassic.. Study area in black square. Modified from (Glørstad-Clark, et al., 2010)*

Recent revisions on the Snadd Formation

The work by Glørstad-Clark et al., (2010) presents the Middle to Late Triassic succession, the Snadd Formation, as two second-order units, S4 and S5. Later work by Klausen et al., (2015) presents a refined sequence stratigraphic framework for the Snadd Formation. This sequence is interpreted to be separated into two second-order that internally borders differently than S4 and S5 in (Glørstad-Clark, et al., 2010). Stratigraphically, the second-order boundary in this study is located higher compared to Glørstad-Clark et al., (2010), which have located the boundary in the change from marine to coastal

settings. Furthermore, Klausen et al., (2015) introduce six third-order subunits, where the top S4 Sequence S4-Ladinian-early Carnian sequence in Glørstad Clark corresponds with the 3rd order sequence L1 (top Ladinian in (Klausen, et al., 2015). L1 is described as a Ladinian prograding sequence, followed by the Early Carnian unit C1. C1 is described as a sequence with progressively larger channel bodies than L1, with well-defined channel sandstones within floodplain facies. The Top Ladinian boundary between S4 and S5 in (Glørstad-Clark, et al., 2010) is interpreted to correspond with global sea-level changes in response to changes in the configuration of the lithospheric plates (Klausen, et al., 2015).

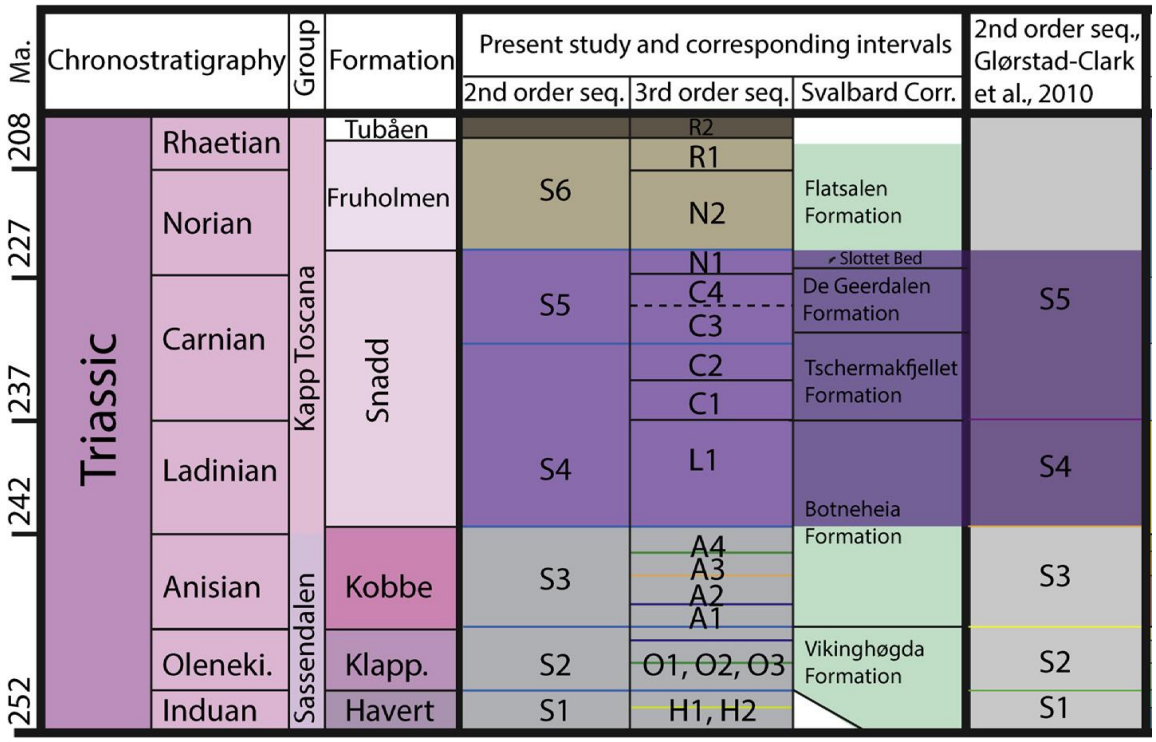

Figure 3-14*. Comparison of Triassic sequence subdivisions, including third order sequences of the Snadd Formation, with supplementary data from Glørstad-Clark et al. (2010). Modified from (Klausen, et al., 2015)*

4. Data and methods

4.1 Seismic cube

The seismic survey used in this thesis is based on a 3D survey called WIN12003, finished 09.08 2012. It is provided by Wintershall Norge As on behalf on the later relinquished license 611, and acquired from Polarcus AS (NPD, 2012). The survey covers an area for approximately 1500km^2 in the northern Loppa High, in the Southwestern Barents Sea. Further survey details is presented in *Table 4.1*.

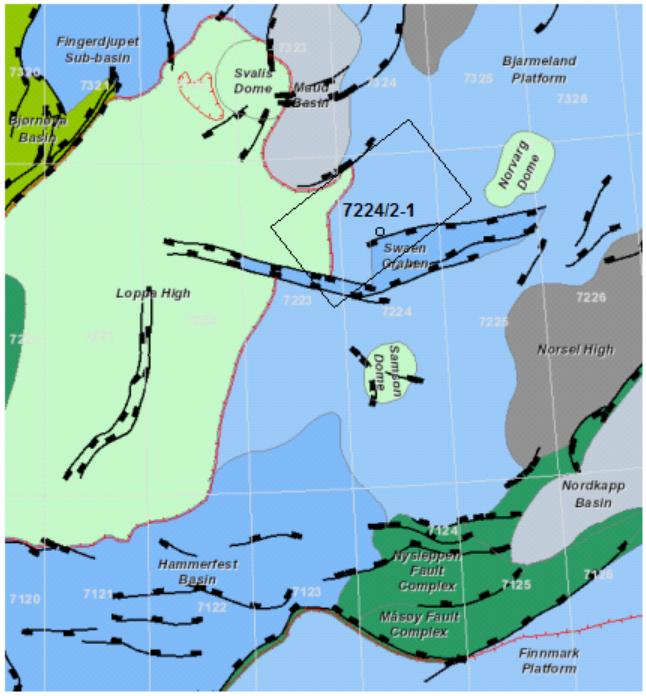

Figure 4-1. *Location of the seismic cube WIN12003 in the SW Barents Sea (black rectangle). Modified from NPD factmaps (NPD, u.d.).*

```
@@@
@@@ Output File: WIN12003-PSTM-FINAL.MIG_FIN.POST_STACK.3D.JS-013520.segy
@@@
---------- Text Header ----------
C01 CLIENT      : WINTERSHALL NORGE ASA
C02 AREA        : KVALROSS 3D PL611 BARENTS SEA
C03 CREATED     : MAY 2013
C04
C05 DATA TYPE   : FINAL MIGRATED STACK
C06 ACQUISITION PARAMETERS:
```

Term	Description
ID	WIN12003-PSTM-FINAL NPD ID: 7615
Energy source	Bolt LLX-LLX
Volume pressure	3480 CU.IN 2000 PSI
Recorded	SEGY-D 8058
Format	SEGY
Sample Code	Floating Point 32bit
Source	Airgun Arrays 18.75 m flip-flop
Separation	50 m Lateral Separation
Shot Point Interval	18.75 m
Traces Sorted	CDP
Gun depth	6 m
Cable depth	8 m
Cable lenght	6000 m
Number of Inlines	2744
Number of Crosslines	5817
Inline Interval	12.50 m
Crossline Interval	12.47 m
Sample Interval	4 ms
HI filter	200HZ 370DB
LO filter	2HZ
Datum	ED50
Projection	UTM zone 34N
Central Meridian	21 degree east

Table 1. *Acquisition documentation from original final mig* SEGY header of WIN12003

The data set is processed to zero-phase reversed polarity (SEG standard polarity). This implies that a central negative amplitude (trough) will correspond to an increase in acoustic impedance, while a central positive amplitude (peak) correspond to a decrease in acoustic impedance *(Figure 4-2).*

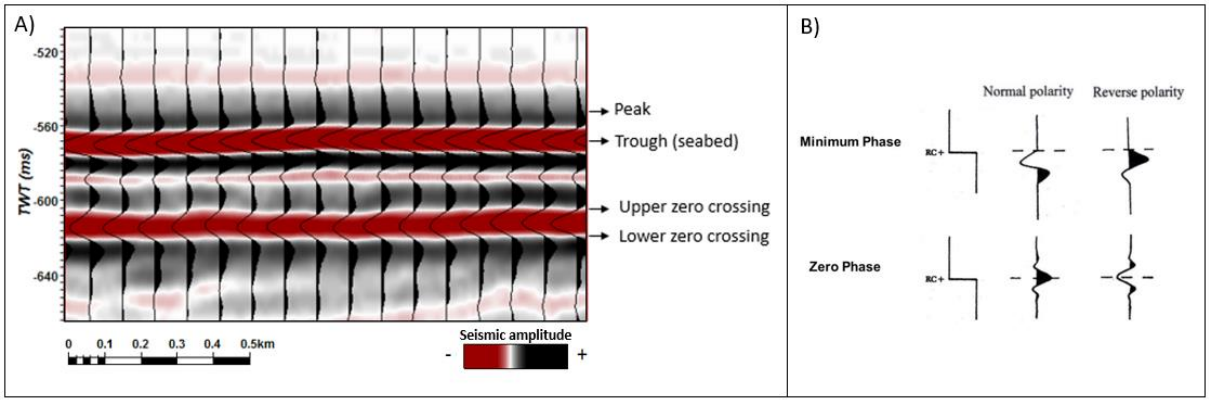

Figure 4-2. A) *Random line through the seismic cube WIN12003. Seabed is represented by negative amplitude (trough), indicating an increase in AI.* ***B)*** *SEG (Society of Exploration) standard of Sheriff (2006). Modified from (Nainggolan, 2014)*

A frequency spectrum analysis extracted from the interesting part of the seismic *(Figure 4-3)*, shows that the dominant frequency in the data set is between 18 and 22 Hz. The bandwidth of the wavelet lies between approximately 5 Hz as a lover boundary and 65 Hz as an upper boundary *(Figure 4-3).* The spectrum analysis is taken from a seismic line crossing the seismic in a SW-NE direction, with an interval from the seabed and throughout the Snadd formation.

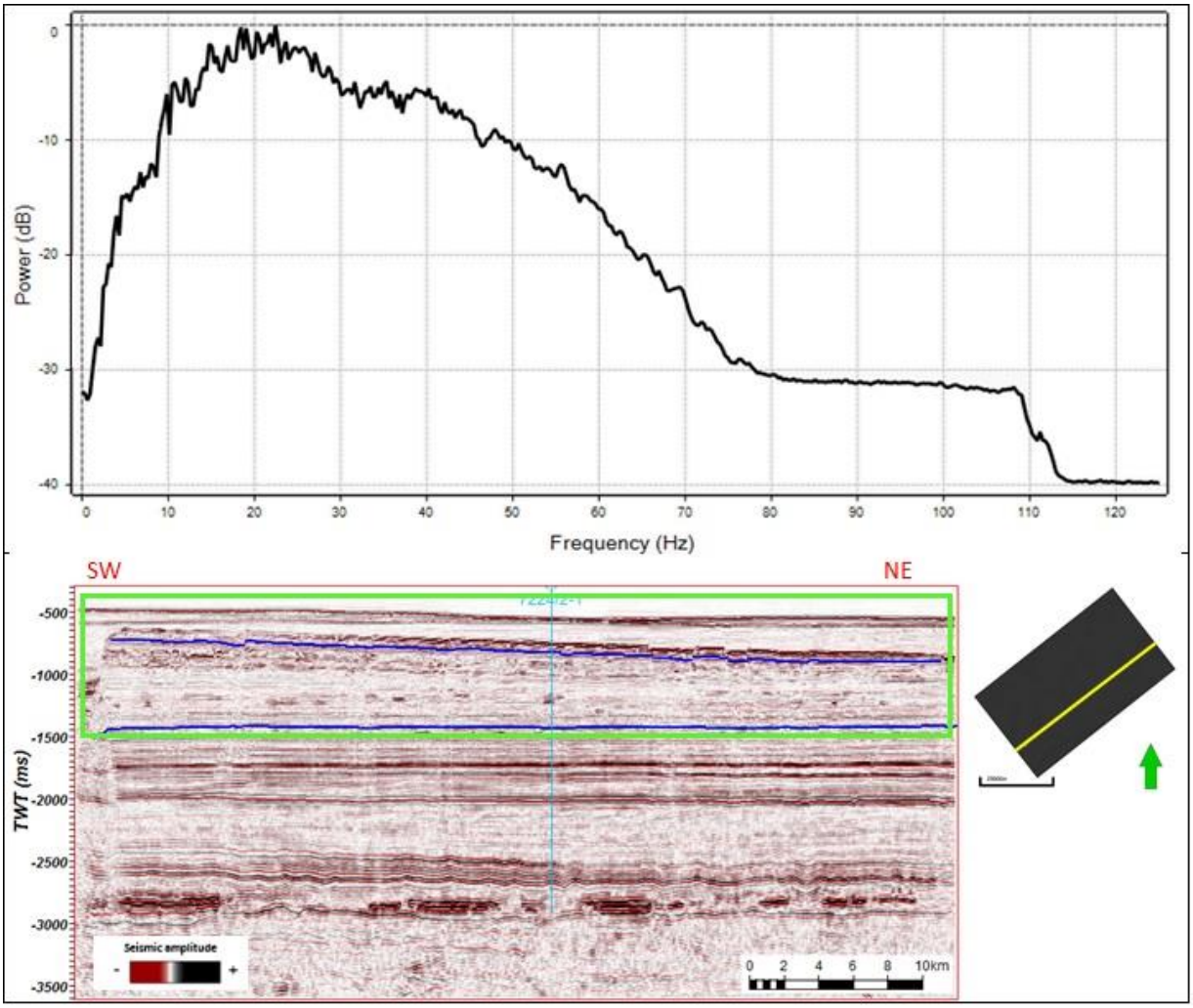

Figure 4-3. *Frequency spectrum from seabed and throughout the Snadd formation from inline 2500. Green rectangle indicates where the spectrum analyses is taken from.*

4.1.1 Vertical resolution

By calculating the vertical resolution, the minimum vertical distance between two layers (reflectors), needed to see the reflection in the seismic section, is found. It also determines how small an object or a feature can be in order to be observed in the data (Kearey, et al., 2002; Lin, 2012) Vertical resolution is calculated to be ¼ of a wavelength, λ, which is defined as:

$$\lambda = \frac{v}{f} \qquad \textbf{(Equation 3)}$$

Where v = velocity (m/s) and f = frequency (Hz). If a stratigraphic layer or an object in the data has a thickness that is less than the calculated resolution, the top and bottom reflector most likely will merge

into one waveform, causing destructive interference (Bilat, 2005). While the seismic velocity increases with depth, the frequency decreases. This makes the vertical resolution poorer with depth.

The vertical resolution in the Snadd formation is calculated to 29 m *(Table 4-2).* Vertical resolution was found by multiply the wavelength *(Equation 3*) by ¼. The dominant frequency was found to be approximately 19 Hz, by using the frequency spectrum *(Figure 4-3).* Seismic velocity was found to be approximately 2200 m/s by using the velocity table from the VSP from well 7224/2-1 *(Figure 5-11 and Figure 5-16, average velocity).*

4.1.2 Horizontal resolution

Horizontal resolution is defined as the ability to distinguish between two reflectors displaced horizontally with respect to each other, and it determines the size a feature needs to have to be detectable (Kearey, et al., 2002) Seismic waves travel as wavefronts, not as rays. The reflection is therefore not generated from a small point on a reflector but from a circular zone instead. This circular area of the subsurface that reflects the seismic wave, is called the Fresnel zone. The Fresnel zone of the first wavefront is dependent on the arrival of the following wavefront, which arrives 1/4 of the wavelength behind. The reflection from the second wavefront will interfere destructively with the reflection from the first. The horizontal resolution on unmigrated data is defined by the width (diameter) of the first Fresnel zone.

$$rf = \frac{v}{2}\sqrt{\frac{t}{f}}$$ ***Equation 4***

Where *rf* is the Fresnel zone diameter(m), *f* is frequency (Hz), *t* is two-way time (s) and *v* is velocity (m/s) (Kearey, et al., 2002).

In the processing of seismic data, a technique called migration will reduce the size of the Fresnel zone, improving the horizontal resolution. During migration of 3D data, diffractions are collapsed back to their point of origin. This process reduces the radius of the Fresnel zone and increases the horizontal resolution. In theory, with perfect migration of the data, the extent of the Fresnel zone will be around, and ¼ λ, and the Fresnel zone is reduced to a small circle (Kearey, et al., 2002).The horizontal resolution is calculated to be 28.95 m, listed in *Table 4.2.*

Formation	Seismic velocity (m/s)	Dominant Frequency (Hz)	Wavelength	Vertical Resolution (m)	Horizontal Resolution (m)
Snadd	2200	19	115.78	28.95	28.95

Table 4-2. *Vertical and horizontal resolution calculated within Snadd formation, using dominant frequency and velocity.*

In order to have a more efficient and responsive software, the seismic cube was both cropped in smaller volumes and realized. By realizing the seismic cube from 32 bit to 8 bit, the memory loading speed increases. The cropping and the realizing of the seismic volume made it easier and faster to interpret the data, and saved time while testing different settings and methods.

4.2 Well data

The lithostratigraphy within the seismic area is interpreted and tied to the seismic using the exploration well 7224/2-1, located within the seismic area at position 72° 46' 25.93" N and 24° 23' 56.17" E, between the Loppa High and the Norvarg discovery 7225/3-1. According to the NPD, the well objective was to test the Kvalross prospect within clinoform facies of the Early Triassic Klappmyss Formation (NPD, 2017). Based on regional mapping, field analogues on Edgeøya, Svalbard and on geophysical analyses, these strata were believed to include sandstones. The well result showed no Klappmyss reservoir sandstones. Second target for the well was the Upper Triassic channel sandstones of the Kvaltann prospect. Good reservoir sandstones were penetrated as predicted, but the trap seemed to have failed. The well is classified as dry. The information of the different formations, depths, depositional environment and released well logs is gathered from NPD, along with released well data. The penetrated formations trough the well, are sown in *Figure 4-4*.

Groups	Formation	Top Depth (m)
Nordland GP	Undifferentiated	439
Advendalen GR	Undifferentiated	456
	Hekkingen FM	657
	Fuglen FM	669
Kapp Toscana GP	Stø FM	682
	Nordmela FM	703
	Fruholmen FM	703
	Snadd FM	783
Sassendalen GP	Kobbe FM	1720
	Klappmys FM	2257
	Havert FM	2735

Figure 4-4. *Well formation tops within the survey WIN12003 of well 7224/2-1 modified from (NPD, 2017).*

4.2.1 Well logs

When drilling wells, information from the borehole is collected by different logging tools in, or after drilling operations. This data is called MWD (measured while drilling or WL (wireline) data). A well log is defined as a continuous recording of a geophysical parameter along a borehole (Rider & Kennedy, 2011). Some of the most important well logs are the gamma ray log, sonic, density, neutron porosity and the resistivity log. In this study, mapping and describing Triassic channel systems, the use of gamma ray, sonic, density and neutron logs was supportive for the interpretation. The gamma ray log curve from the well was used to further interpret the deposition environment, where high content of radioactivity in the sediments give high API values on the logs (*Figure 5-2*). This may indicate a high organic rich shale content, which can represent a marine low energy environment, where fine shale particles is deposited, in accordance with the Hjulstrøms diagram (*Figure 2-5)*. Opposite, lower API values in the log indicate lower radioactivity, hence more sandy sediments, which can represent a more continental environment.

The gamma ray log

This log measures the natural gamma radioactivity from uranium, thorium and potassium in a formation, where the output is the total count rate of these. The GR does not distinguish between the individual elements (Rider & Kennedy, 2011). Metamorphic, igneous and sedimentary rocks contain traces of gamma-emitting elements. When it comes to sedimentary rocks, shale exhibit the highest radioactivity. Because of this, the gamma log is often called the “shale log”, even though it is not equivalent to the amount of shale content. (Rider & Kennedy, 2011). The gamma ray is commonly used for correlation of different strata, like picking well tops while drilling. It is also helpful in

identifying lithology, stratigraphic surfaces, facies and sequences. The unit for the GR log is the API, defined as 1/200 of the difference between two reference units. An average shale usually represents 100 API units, while sandstones and carbonates normally have low API (10-40 API) compared to shales (Rider & Kennedy, 2011).

The gamma ray is considered as the most useful logging tool in sequence stratigraphic analysis, as it can be used to assess the relative proportions of sand and mud within a succession Nichols (2009). In general, muddy sediments indicate deeper marine deposition than sandy successions. Lower energy in deeper marine environment causes smaller grains to be deposited, contra shallower marine environment with more energy and capacity to accumulate coarser grains (*Figure 2-5)* (Nichols, 2009). A trend with decreasing values upwards on a gamma-ray log can indicate increase in sand content and be interpreted as a shallowing-up succession. An increase in the reading indicates a higher mud content. This can be used as evidence for a flooding surface (Nichols, 2009). Trends in sand and mud content on gamma logs within flooding surfaces can be used to identify patterns which can be recognized as either progradation, retrogradation or aggradation through the succession. The gamma ray log can also be used to distinguish between sand-filled channel successions and mud-rich floodplain. River channels are characterized by sharp increases in sand content (low gamma log value) at the base followed by a trend with increasing gamma log values, meaning more mud-rich material. The GR can also be important to help identify fluvial facies which can be indicators of sequence boundaries. Maximum flooding surfaces may also be picked up on more sophisticated gamma logs, the spectral gamma logs, which could read a characteristic increase in the potassium content indicating a concentration of glauconite (Nichols, 2009).

The density log

Density logs reads the bulk density of formations, including the density of the rock and potential fluids enclosed in the pores. By emitting gamma radiation into the formation, the density log measures the induced radiation. The attenuation and re-emitting of gamma rays is a function of the electron density (electrons/cm3) of the formation, which is closely related to density, measured by g/cm3. (Rider & Kennedy, 2011). The density log can calculate the hydrocarbon volume and density. It can also model seismic response by calculating acoustic impedance (density multiplied with sonic log). When combined with the neutron log, it is a good indicator of general lithology (Rider & Kennedy, 2011).

The neutron log

This log measures how a formation reacts to neutron bombardment. A source emits high energy neutrons into the formation, and a receiver measures the numbers of low energy neutrons that are re-emitted back. Since emitted neutrons strongly respond on hydrogen in the formation, the returning amount of neutrons strongly depend on the hydrogen content. In high porosity rocks, the neutrons are

slowed quickly down and absorbed. This causes the count rate to be low. In low porosity rocks, the emitted neutrons travel further, making the count rate higher (Rider & Kennedy, 2011).

Hydrogen appears in all formation fluids (water, oil and gas), but not in all minerals. Because of this, the response from the neutron log could be correlated with porosity (Rider & Kennedy, 2011).
The neutron log output scale is given in neutron porosity units. This is an indication of the Hydrogen Index for the formation, and is given as percentage or fraction. Typical values for sandstones is between 0 - 30 %, and for shales, values between 25 – 75 % is normal. The neutron log is often plotted with the highest values to the left and lowest to the right (Rider & Kennedy, 2011)

The sonic log

The sonic measures the formation's capacity to transmit sound waves by measuring the time it takes for a sound wave to travel a known distance within the formation. The sonic logging tool consists of one or two transmitters and several receivers where the distance between them is known. (Rider & Kennedy, 2011). The sonic log measures the velocity, but it is frequently expressed as slowness, with unit μs/ft. Typical values for formations in the subsurface range from 50-150 μs/ft, corresponding to velocity of 6000-2000 m/s. The main use of sonic log is seismic investigations by contribute to depth conversions, velocity modelling and performing well-to-seismic tie. By combining the sonic log with the density log, an acoustic impedance log can be established, which can be used to create a synthetic seismogram. (Rider & Kennedy, 2011)

4.3 Methods

The methods taken into use, were intended to improve the interpretation and imaging of channel systems observed in the dataset. The software Petrel E&P 2016, CorelDrawX6 and GeoTeric 2017 have been used for mapping, visualization and description of relevant channels observed within the study area.

4.3.1 Petrel

The Petrel software is a platform developed and owned by Schlumberger. The application gives the users the ability to interpret 2D and 3D seismic data, correlate well data, produce different maps, build reservoir models, visualize reservoir simulations, and estimate volumes. The software makes it possible to develop strategies to maximize the reservoir utilization, and it is a common used tool for the industry in terms of integrating different disciplines, including extensive use of well and seismic data. Petrel uses negative Two-way Travel time (TWT) for the Y-axis, the figures of well and seismic sections will therefore have a negative TWT value, while in the text, the travel time will be positive.

4.3.2 GeoTeric

GeoTeric is a 3D seismic analysis software tool that includes different technologies for data conditioning. Using noise reduction, color blending and geobody delineation functionality, details in the seismic data can be revealed, giving a better understanding of the subsurface geology in a certain area. GeoTeric is a useful tool in reservoir development and in exploration. Relevant for this work, is the ability to offer better imaging of channels, and relate them to river systems.

4.3.3 Seismic interpretation

Horizon interpretation

In the interpretation process, both inline, crossline and random line have been taken into use. For horizons with particular strong reflections, the 2D auto tracking function has been used, with an applied confidence grade at 30 %. Some areas are represented by discontinuous reflectors, caused by faults or acoustic masking. Here, the manual draw has been used to prevent misinterpretation, together with the manual paintbrush tool. During the interpretation process, a grid has been generated in the 2D-window. At the seabed, which includes a continuous negative reflector *(Figure 4-2*), the 3D track has been used to generate the map. However, this auto-tracking tool tracks the entire surface with the interpreted gridlines as a reference. During this process, the track comes from an arbitrary direction, without any concern regarding structural features. Based on the interpreted horizons, several surfaces have been generated.

Attributes

A seismic attribute map is a visualization method that can highlight geological shapes, structures, amplitude anomalies or other features of interest (Holdaway, 2016). A seismic attribute is defined to be one quantitative measure inherent in the seismic data. It could be a special characteristic feature in the amplitude, frequency or in the phase content of the reflection data. In the interpretation process, detection of stratigraphic and structural information in the data, based on seismic attributes and spectral decomposition, is a fundamental workflow, giving the opportunity to further understand subsurface features and reservoir characteristics (Ashutosh, et al., 2013).

Volume attributes

The variance attribute (frequently called edge method)

This method estimates the local variation between different traces, so that areas with major trace changes are highlighted (Schlumberger, 2010). This technique is good for isolating edges and

visualize faults, but also to reveal deposits, like channel accumulations. The variance attribute method gives a volume attribute generated on the entire cube or in interesting cropped areas.

The chaos attribute

The chaotic signal pattern contained within the seismic data can be considered as a measure of the lack of organization in the dip and azimuth method. In other words, the chaos attribute maps out the "chaoticness", or the degree and extent of chaos in the local seismic signal. Chaos mapping is often considered to be a useful tool when identifying channel infill, gas chimneys and diapers (Schlumberger, 2010).

The envelope attribute (reflection strength)

The trace envelope is a physical attribute, also called the instantaneous amplitude. It varies approximately between null and the absolute of the maximum amplitude of the trace. Reflection strength is the amplitude of the envelope, and represents the instantaneous energy of the signal. The reflection strength (magnitude) is proportional to the reflection coefficient, and represents mainly the acoustic impedance contrast, hence reflectivity. The trace envelope may represent the individual interface contrast or, more common, the combined response of several interfaces, depending on the seismic bandwidth (Taner, 2003). Discontinuities, faults, changes in deposition and sequence boundaries are features that physically represent changes in the acoustic impedance. By making envelope cubes from the seismic data, this information can be revealed in more detail. Some of the seismic amplitudes get clearer, allowing morphological structures with acoustic impedance contrast to the surrounding sediments to become more visible. Because the acoustic impedance contrast between water and hydrocarbons causes reflection events, envelope attribute maps can also be regarded as hydrocarbon indicators. In hydrocarbon accumulations, high amplitude reflections, often named bright spots, can be identified. The trace envelope is also useful to identify changes in lithology or porosity, and in thin-bed tuning (Chopra & Marfurt, 2005).

Fault expression (SO semblance)

A preferred way to further incorporate edge information into a blend, is to do an opacity blend with an edge attribute (Frick, 2015). This method limits the individual channels much clearer.

Frequency decomposition and RGB blending

When using frequency decomposition, three frequencies are selected to decompose the data and produce volumes that show the magnitude response at these frequencies. In the channel detection in this study, frequencies of 19, 32 and 45 Hz are used, assigned to red, green and blue colors respectively. Three individual conditioned volumes are normalized and assigned to these colors. Selecting low frequency in the red channel, mid frequency in the green channel and high frequency in

the blue channel gives high resolution color visualization of the three volumes, and the strength of their response relative to each other. The resulting composite RGB image shows variation in color and intensity that correlates with the change in magnitude response at the different frequencies. A white, brightening color indicates a high response from all three frequencies, while black/dark colors indicate low response from all three frequencies. The other colors (red, green, blue) indicate which frequency that has a relatively higher response than the others (Frick, 2014).This has the ability to show variations in lithology, bed thickness and pore fill with high visual contrast. In mapping of river channels, RGB blending method could give good results, as it has the potential to give increased stratigraphic information. (Schmidt, et al., 2013) (McArdle, et al., 2010). Generally, high frequency response indicates predominantly thin layers, while the lower response indicates a more massive structure (Naseer, et al., 2014).

Opacity blend

In this method, the structural and stratigraphic attributes are blended together. By setting their opacity to allow information from both volumes being displayed as one, a better understanding of the geological interplay between identified structures and stratigraphic bodies is achieved. In opacity blend the user can overlay attribute volumes together, or overlay attribute volumes with color blends. Each attribute has its own color map and opacity set separately. The opacity of one layer will affect the visualization of the subsequent layers, since the volumes are overlaid one on top of the other.

Fault expression (SO semblance)

A preferred way to further incorporate edge information into a blend, is to generate a structurally oriented SO semblance edge attribute, in order to highlight channel edges.

Surface attributes

The isochron time-thickness attribute

This attribute was used to calculate the time thickness between two seismic horizons in two-way travel time. Making thickness maps is essential in order to describe the thickness of a sediment package in an area.

Extract value attribute

This attribute gives the opportunity to extract a generated attribute volume on interpreted horizons, to give a better visualization of internal morphology and geological properties along stratigraphic surfaces in the seismic data set.

5. Results and interpretation

5.1 Main focus

This chapter is based on horizon and channel system interpretation from the 3D seismic dataset WIN12003 (*Figure 1-1*). The main focus has been to interpret channel systems in terms of channel accumulation, distribution and migration. For this purpose, vertical and horizontal time slices have been taken into use, together with volume and surface attributes. Some formation tops have been interpreted and correlated with the exploration well 7224/2-1 to interpret the stratigraphy in the area. Several channel depositional elements have been observed in this dataset. Most of the channels identified and interpreted in this thesis, are located in the Snadd formation and in the upper Kobbe formation from Triassic age. Stratigraphy has been interpreted with use of seismic cross sections, seismic facies, together with well log curves and lithology descriptions from the composite log. Further, the Triassic formation is subdivided following the division given by Glørstad-Clark, et al., (2010) east of the Loppa High. Depositional environment interpretations have been carried out on the basis of seismic attributes and the interpreted cross-sectional seismic facies, together with the GR log from well 7224/2-1. Since this well was dry, no cores were taken. This could have provided important information through core phots and core measurements.

5.2 Interpretation of the stratigraphy within the area

The data is interpreted to show an almost complete Triassic succession between late Permian and lower/middle Jurassic mega sequence (Stø formation) *(Figure 5-1).* The bordering horizon between Triassic and Jurassic is shown by a bright and extensive reflection, indicating a significant shift in depositional and erosional conditions *(Figure 5-1*). The weak, discontinuous seismic reflections between the late Permian and Triassic *(Figure 5-1)* makes it difficult to recognize the exact boundary between these ages. The focus in this thesis will be channels identified within the Triassic succession. Furthermore, the Triassic succession is subdivided and analyzed, to see if there are some higher-order sequence boundaries, indicating changes in the depositional environment through Triassic. According to Glørstad-Clark, et al., (2010), "*Each boundary represents a maximum flooding surface, MFS, characterized by strong, continuous seismic reflectors.*" Five sub sequences, S1 to S5, are identified in this work *(Figure 5-1*).

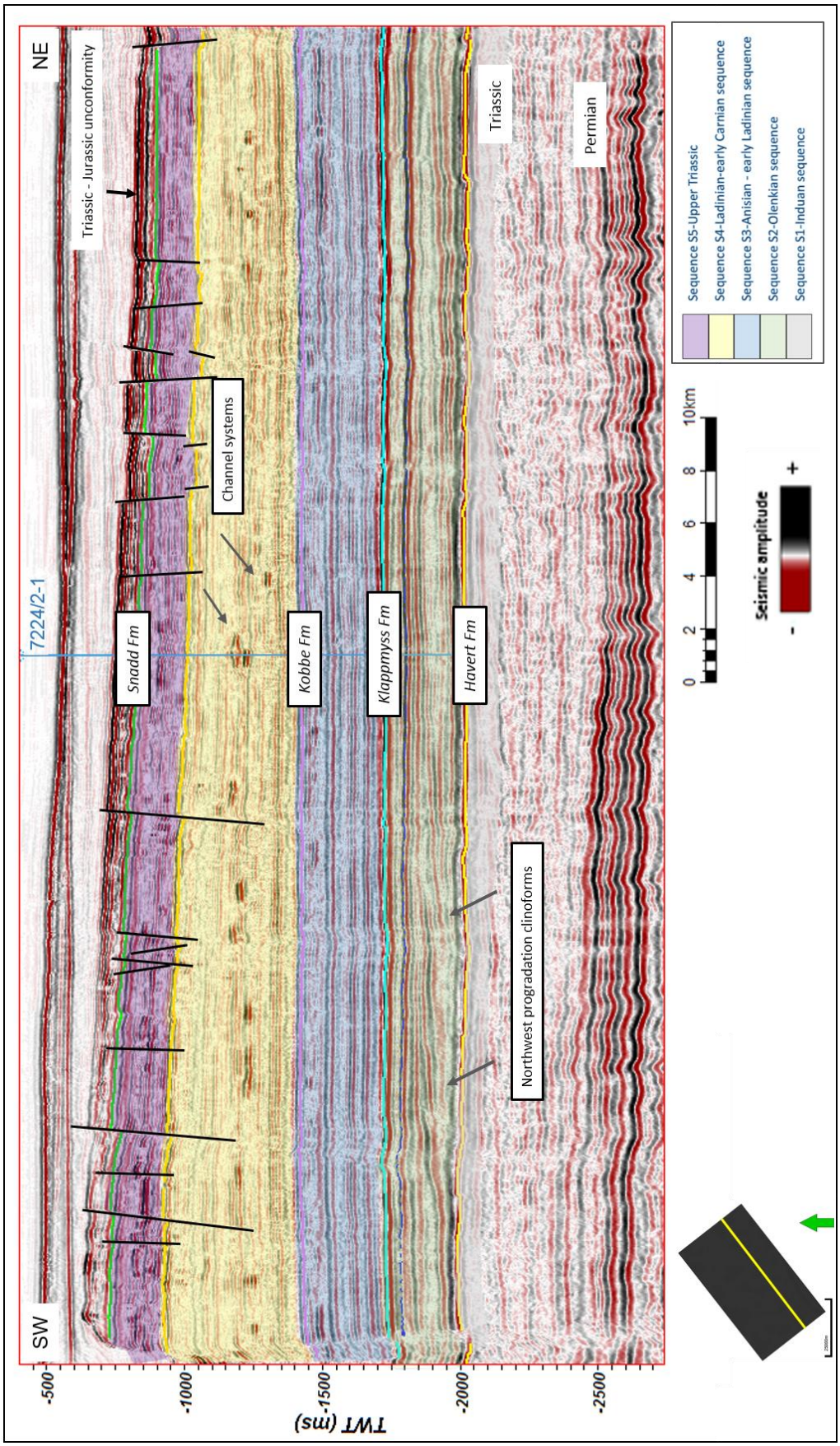

Figure 5-1. *Vertical section of inline 2500 in cube WIN12003, with an overview of different sub-sequences in observed in the dataset.*

The sequences are interpreted in the seismic section and correlated to the formation tops in well 7224/2-1. These Triassic sequences are presented in chapter 3.4, where they are linked to different formation tops. The gamma ray log curve from the well was used to further interpret the deposition environment, where high content of radioactivity in the sediments give high API values on the logs *(Figure 5-2).* This may indicate a high organic rich shale content, which can represent a marine low energy environment, where fine shale particles is deposited, in accordance with the Hjulstrøms diagram *(Figure 2-5)*. Opposite, lower API values in the log indicate lower radioactivity, hence more sandy sediments, which can represent a more continental environment.

It was also relevant to investigate if the sequences were deposited in a transgressive environment with a retrogressive coastline, a regressive setting with a prograding shoreline or a stable environment with an aggrading shoreline.

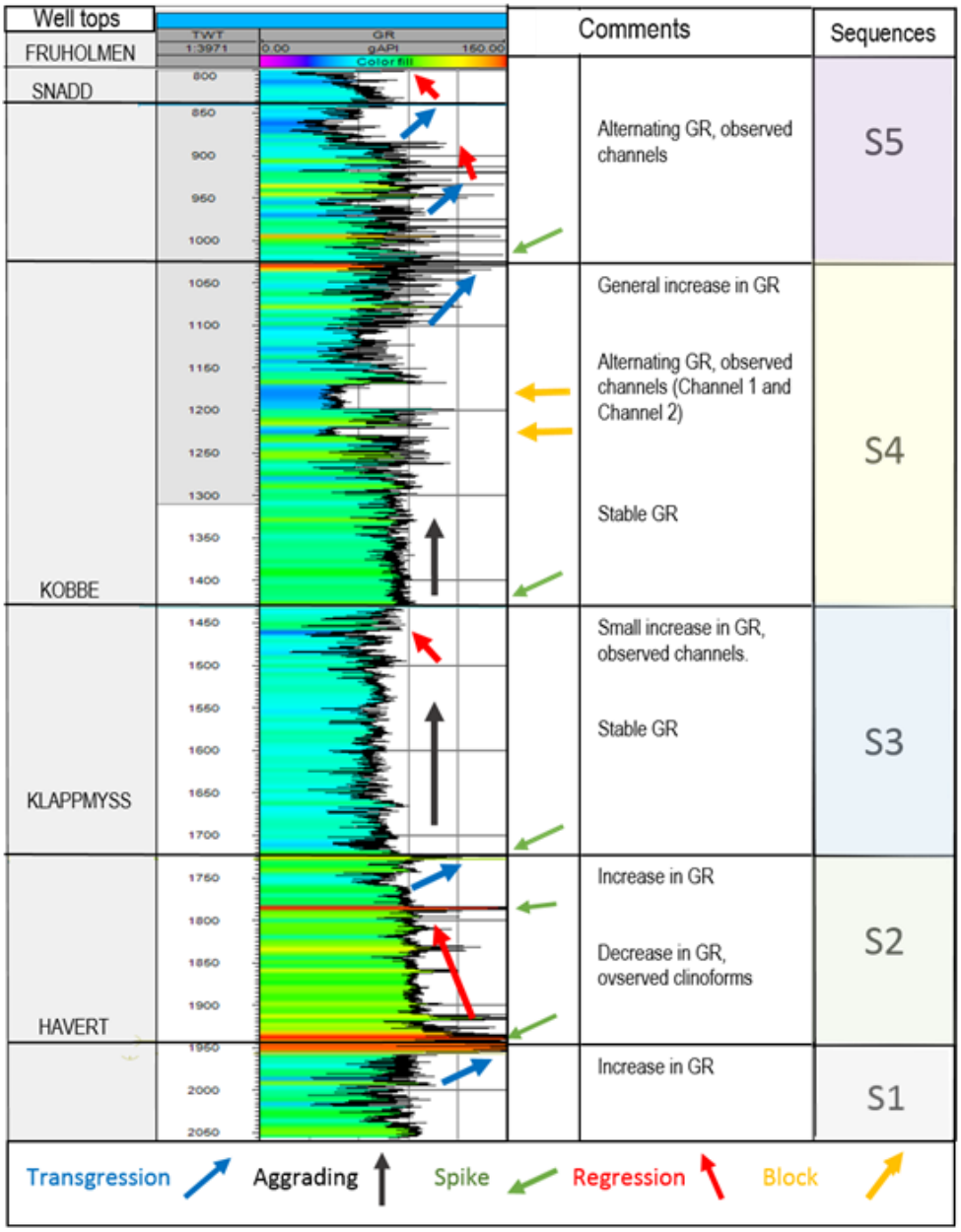

Figure 5-2. *Gamma ray log from well 7224/2- 1. Red, black and blue arrows represent different interpreted depositional environments.*

Sequence S1

According to Glørstad-Clark, et al (2010), Top S1 is correlated to Top Havert formation, and represents a maximum flooding surface. This boundary was found in well 7224/2-1, and represents a strong, continuous seismic amplitude in the seismic section *(Figure 5-1).* The gamma ray log showed a sudden shift from lower to high API values at the top of the sequence (Top Havert), (*Figure 5-2).* The lower limit of the sequence was relative difficult to map, because of the late Permian-Triassic unconformity, and because well 7224/2-1 ends right below the top Havert Formation. This sequence

was therefore difficult to correlate deeper in the seismic dataset, and gets limited attention in this work.

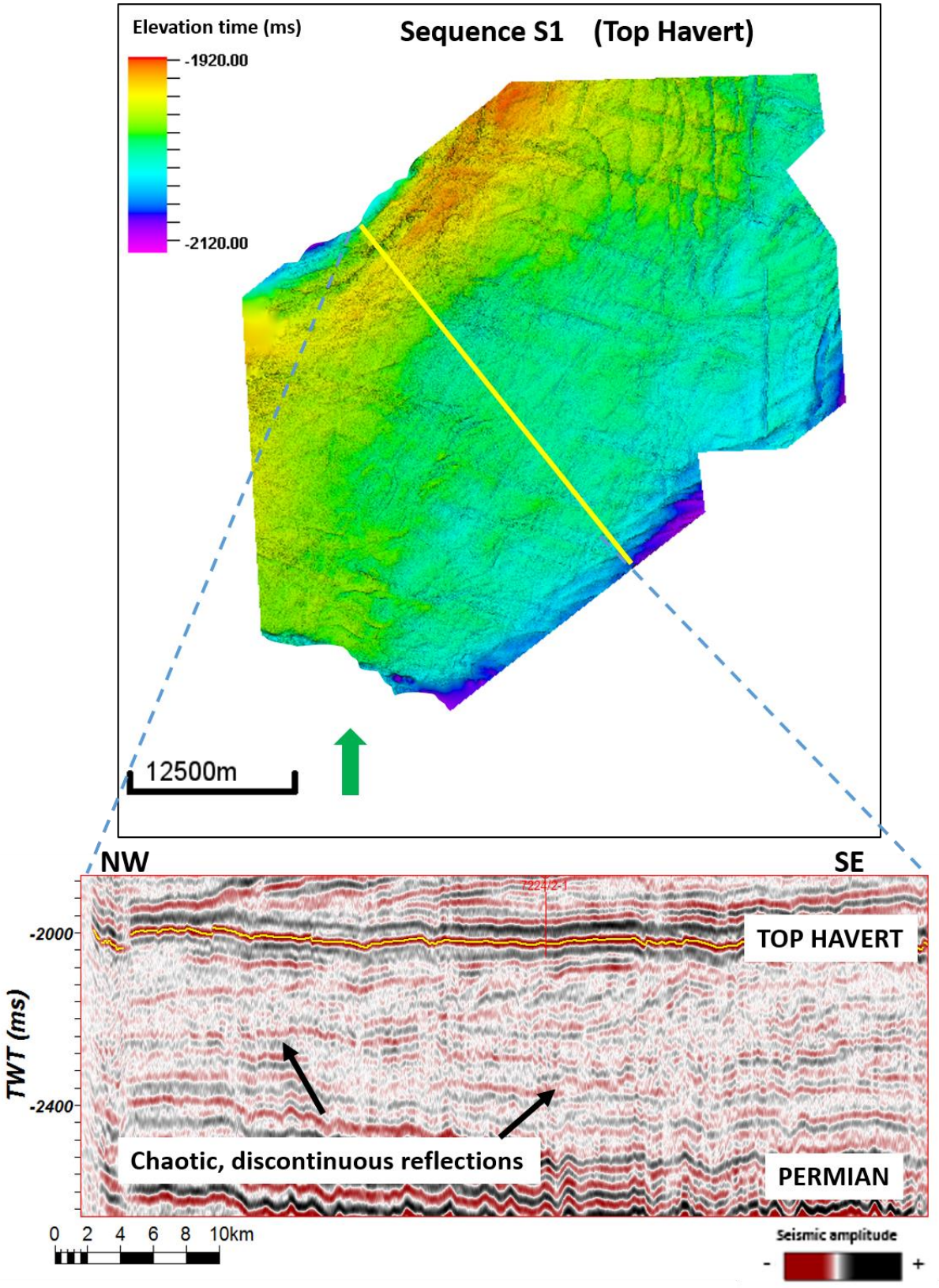

Figure 5-3. *Time-structure map of Top Havert (S1) together with seismic section of random line inn WIN12003. Black arrows show chaotic, discontinuous reflections separating Permian and Triassic.*

Interpretation

High API values at the Top of Havert formation implies high content of radioactive materials as silt and shale. Together with continuous seismic reflectors, this may indicate marine sediments. The significant shift in API values at the top for the sequence can be interpreted to represent a transgression. The lowermost part of the sequence was difficult to interpret, due to absence of associated reflectors, and has probably gone through structural or stratigraphically changes in, or after deposition. This corresponds to Glørstad-Clark et al., (2010), where the S1 lower boundary is difficult to map regionally. This is due to the identified strong variation in the upper Permian facies. These facies vary from carbonates in the Finnmark Platform, clastics in the Hammerfest basin and spiculites in the Nordkapp Basin and the Bjarmeland Platform (Glørstad-Clark, et al., 2010) (*Figure 3-8)*.

Sequence S2

The sequence is bounded by top S1 in the lower part and by a strong, continuous seismic amplitude reflection, correlated to Top Klappmyss in the upper part *(Figure 5-4)*, representing a maximum flooding surface (Glørstad-Clark, et al., 2010). In the gamma ray log, a spike represents the upper limit, see *Figure 5-2.*

The seismic investigation of the lower unit has showed a consistent sedimentary unit with continuous, high amplitude reflectors, showing a dipping structure against northeast *(Figure 5-4)*, and a general decrease in gamma ray values *(Figure 5-2).* The upper half of the sequence consists of parallel, continuous and high amplitude reflections, with a general increase in gamma ray values *(Figure 5-2).*

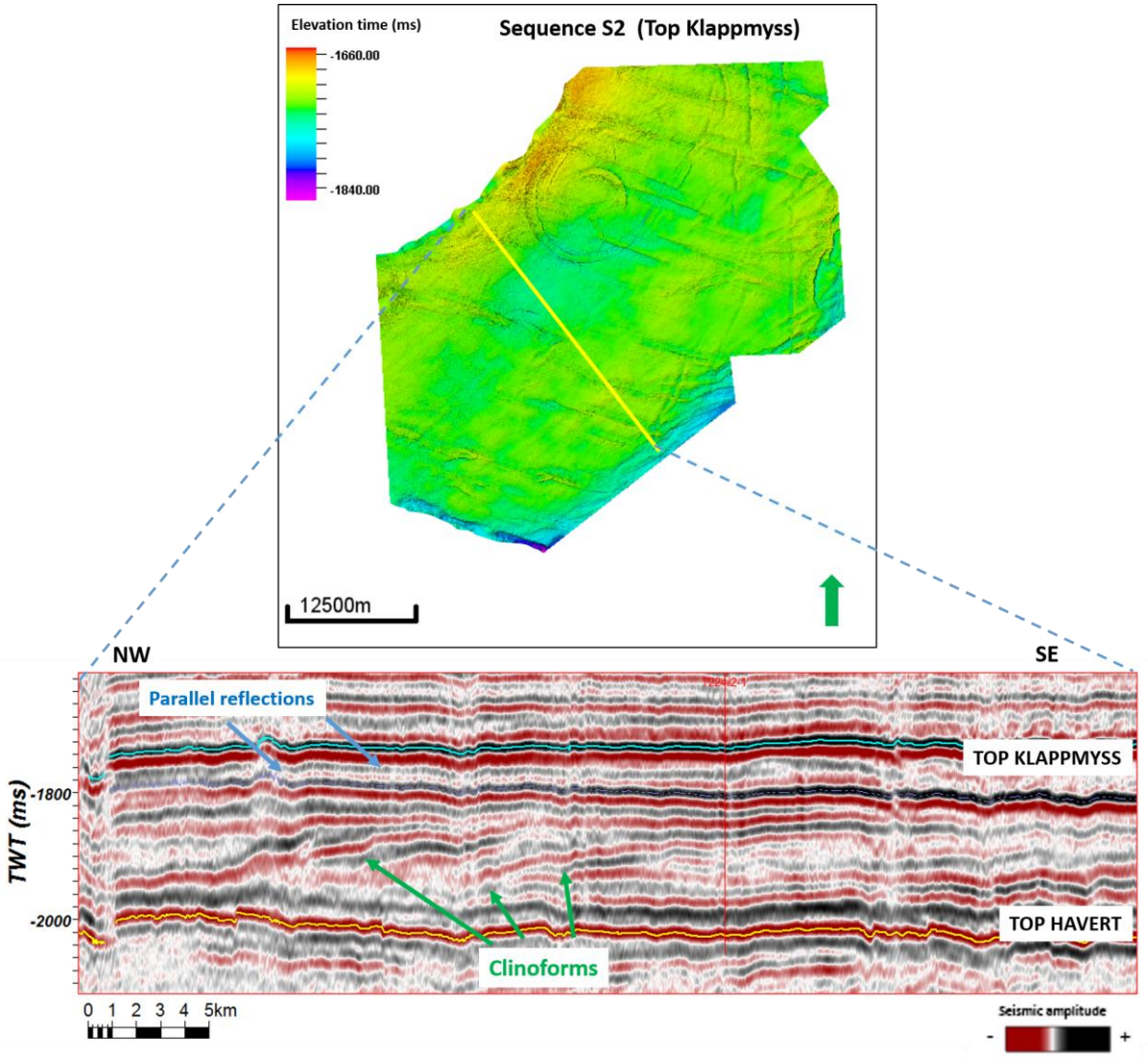

Figure 5-4. *Elevation map of Top Klappmyss (S2) together with seismic section of random line in WIN12003. Green arrows indicating clinoforms, which is interpreted to indicate progratation.*

Interpretation

In the lower part of the formation, the dipping structure against the northeast are interpreted to be clinoforms (chapter 3.3.1, F1). Observations of clinoforms and the decrease in gamma ray values, together with the overlaying sediment package that has continuous, parallel reflectors and an increase in GR values, represents a setting from a low energy environment with shale deposition to a higher energy environment with more sandy depositions. Together, this may indicate an open marine to a marine shelf environment (chapter 3.3.1, F1, F2), with a prograding coastline from east and southeast, probably representing a regressive setting *(Figure 5-5 a)*. The interpretation correlates with earlier studies, where the sequence S2 contains well-developed seismic clinoform belts, prograding from the Fennoscandian Shield (Glørstad-Clark, et al., 2010) *(Figure 3-10)*.

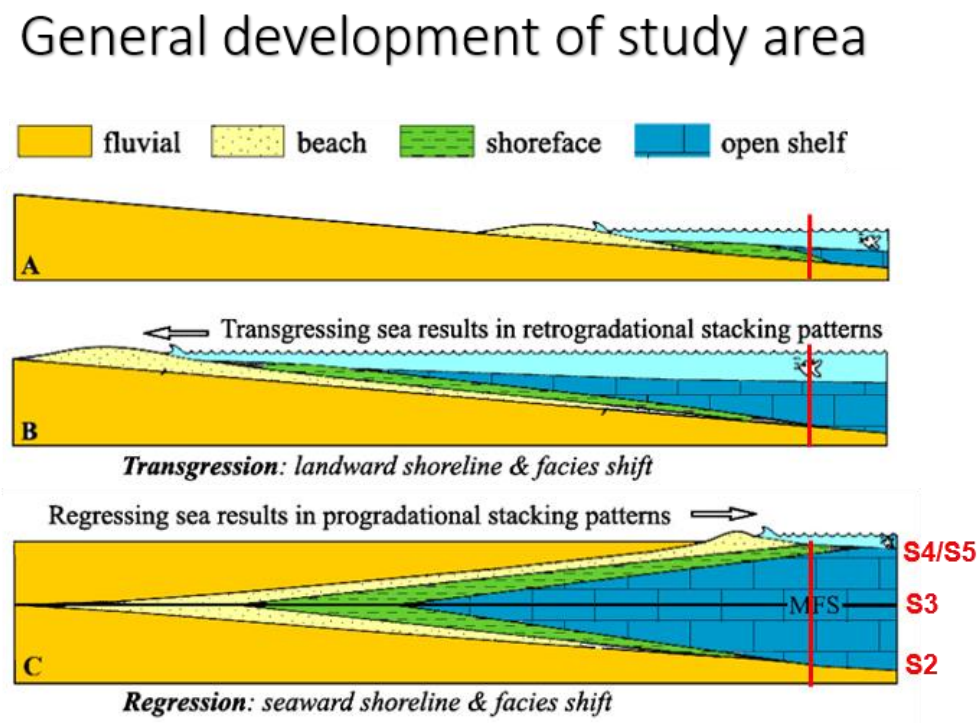

Figure 5-5. *Overall summary of development of the Triassic succession. Red line illustrate hypothetical location of well 7224/2-1. A) Regressive setting as dominant regime in S2, S4 and S5.* ***B)*** *Transgressive setting dominant regime in S3,* ***C)*** *Summary of depositional environment of all sequences.*

Sequence S3

Sequence S3 is interpreted to represent the Kobbe formation (Glørstad-Clark, et al., 2010), bounded by maximum flooding surfaces, with Top Klapmyss formation as lower limit and Top Kobbe formation as upper limit. This sequence showed a significant change in amplitude continuity and amplitude values between the lower and upper part of the sequence (*Figure 5-6).* The lower unit (lower and middle part of the sequence), is represented by a package of parallel, continuous and strong reflections, with stable gamma ray values *(Figure 5-2).* The upper unit is represented by discontinuous, irregular, high and low amplitude reflections, where the gamma ray log shows a small decrease API value.

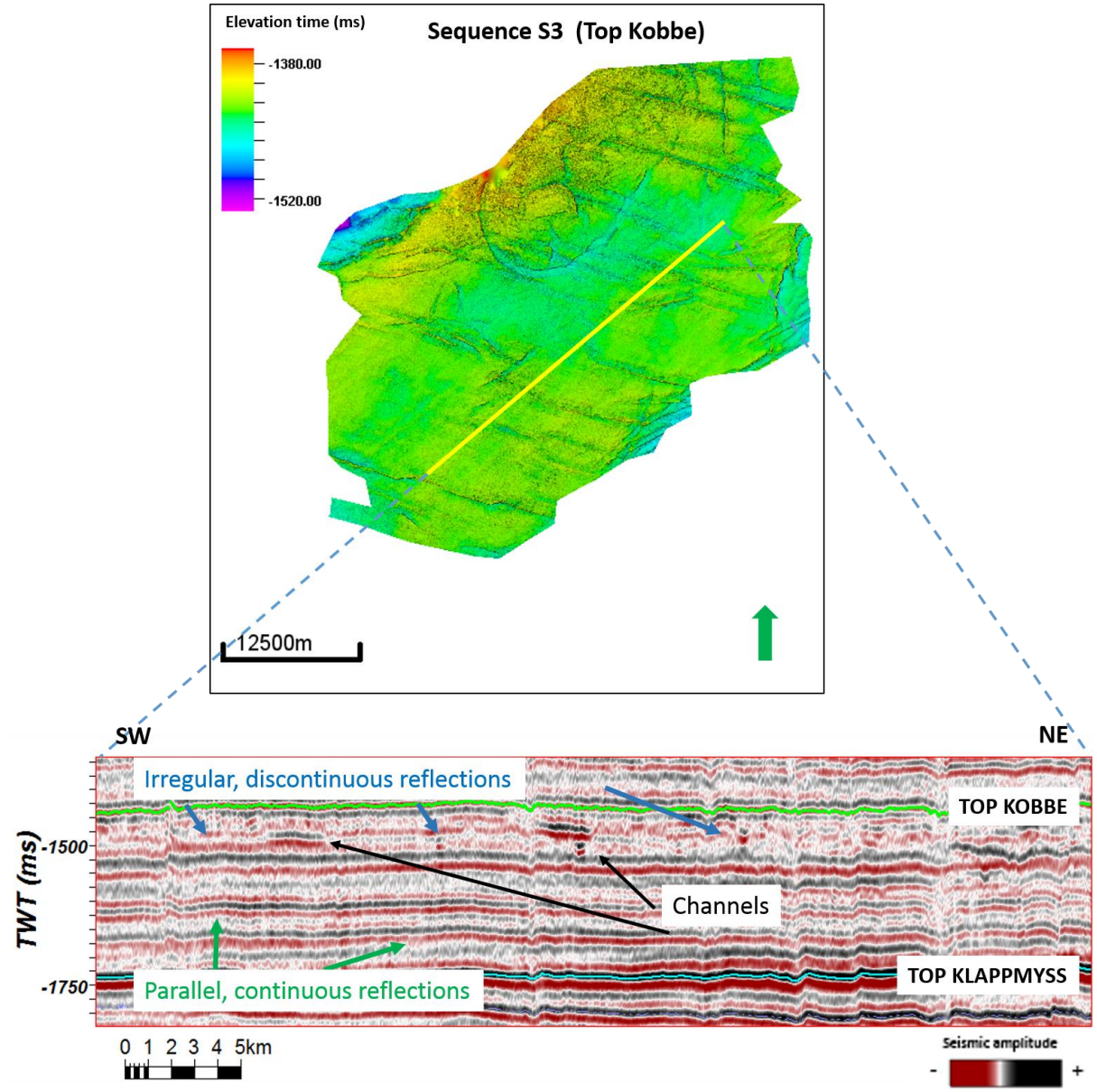

***Figure 5-6**. Elevation map of Top Kobbe (S3) together with seismic section of random line inn WIN12003. Green arrows indicate parallel and continues reflections, interpreted to represent marine environment. Blue arrows show irregular and discontinuous reflections, interpreted to represent a more coastal environment.*

Interpretation

This significant change is seismic facies between the lower and the upper seciton, may suggest a change in the depositional environment. The lower unit is represented by continous, parallel, high amplitude reflections (chapter 3.3.1, F2). Together with a relatively stable gamma ray value, it may indicate a stable marine environment, possibly with an aggrading shoreline *(Figure 5-2)*. The upper part of the unit is represented by irregular, discontinuous, weak amplitude reflectors, with consisting high and low amplitude features. This is interpreted to represent a coastal environment with fluvial channel depositions (chapter 3.3.1, F4). The small decrease in gamma ray value, together with observed channel features supports a sea-level drop in the area. The interpretation correlates with

interpretations by Glørstad-Clark, et al., (2010). The main, lower part of this sequence is shown as continuous, parallel and clear reflectors, interpreted to indicate a quiet marine depositional environment. The upper section of the sequence with its discontinuous, low seismic reflectors with spots of high amplitudes, is interpreted to represent fluvial channels which builds out from the south-east, suggesting a sea level drop. S3 shows downlap geometries closer to the paleo-Loppa High, on top of the high in the south, towards the Svalis Dome and north of 74 degrees N. (Glørstad-Clark, et al., 2010) (*Figure 3-11).*

Sequence S4

Top Kobbe formation represents the base of this unit (Glørstad-Clark, et al., 2010). The upper limit of this sequence is not correlated to any well top. By using the gamma ray log, the top of the sequence may be represented by high API values *(Figure 5-2),* and by a continuous and high amplitude reflection in the seismic profile *(Figure 5-7).* This sequence could roughly be divided in two units, represented by different seismic facies. The reflections observed in the lower part of the unit consists of parallel, continuous and strong amplitudes with low variations. The gamma ray shows stable values *(Figure 5-2).* In the upper unit, the reflections become more discontinuous and irregular, with weaker amplitudes, consisting of some strong high- and low amplitudes in between *(Figure 5-7).* In this interval, the GR log shows alternating high and low values, with some blocks of low values *(Figure 5-2).*

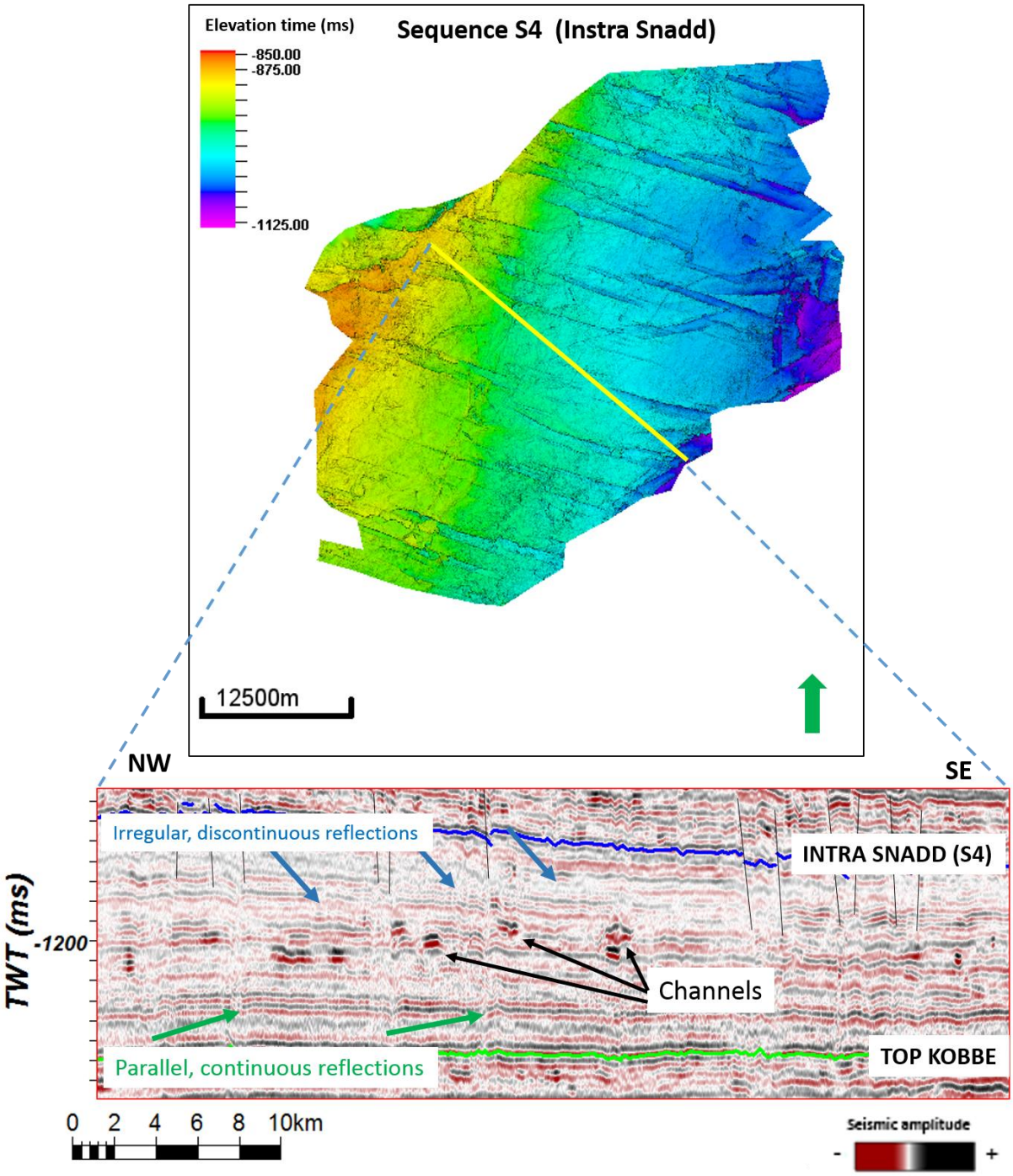

Figure 5-7 . *Elevation map of Intra Snadd (S4) together with seismic section of random line inn WIN12003. Green arrows indicate parallel and continues reflections, interpreted to represent marine environment. Blue arrows show irregular and discontinous reflections, interpreted to be a more coastal environment.*

Interpretation

The top of the unit marked by continuous, high amplitude reflections in the seismic section *(Figure 5-1)*, and represented by a spike in the gamma ray log *(Figure 5-2)*. This can indicate a sea-level rise, where marine sediments have been deposited on land. This boundary is interpreted to represent a maximum flooding surface *(Figure 5-7)*. Glørstad-Clark, et al., (2010) suggests that sequence S4

correlates with the lower part of the Snadd Formation in most wells. In this study, top S4 is interpreted to be located within the middle part of Snadd, interpreted on a maximum flooding surface, where the data show significant spike in the GR log together with strong seismic reflections.

In the lower part of the unit, parallel, continuous and strong amplitudes, together with the stable gamma ray values, was observed. This may indicate a stable marine environment, with a possibility of an aggregating shoreline (chapter 3.3.1, F2). The upper sequence has more irregular and discontinuous reflections, consisting of strong, high and low amplitude features, interpreted to be channels *(Figure 5-1)*. Together with blocks of low values in the gamma ray log in this section *(Figure 5-2),* it may indicate a regressive setting where marine sediments are overlain by land deposits. Altogether, the upper part is interpreted to represent a coastal environment with big influence on fluvial settings (Chapter 3.3.1, F4, F5). The frequent alternating of high and low gamma ray value observed in this unit *(Figure 5-2),* could indicate frequent shifts between transgression and regression in the area. Considering a coastal environment, the rapid changing between transgression and regression regime is likely.

Glørstad-Clark, et al., (2010) states that a transgression represents the onset of S4, which pushed the shoreline significantly further towards the southeast. The interpretation of the depositional environment in the study area is in line with Glørstad-Clark, et al., (2010), where the lower part of the unit is interpreted to mainly represent distal shelfal deposits, and the upper half of the sequence is interpreted to be dominated by mainly continental deposits, with several observed channel features *(Figure 3-12)*. On the Bjarmeland Platform, there is also mapped out an internal maximum regressive surface, making the boundary between Ladinian/Carnian, which probably also is representing the boundary of the lower and upper unit of S4 in this study.

Sequence S5

Sequence S5 is interpreted to represent the upper Snadd formation and Fruholmen formation, bounded by maximum flooding surfaces, with top S4 as lower limit and Top Fruholmen formation as upper limit, in accordance with (Glørstad Clark et. al (2010). In the western part of the study area, a large part of the upper reflections is absent *(Figure 5-8)*. In this work, Top S5 sequence is interpreted to represent Top Snadd Formation, since it was represented by a stronger, continuous reflection easier to track regional than the Top Fruholmen Formation. The sequence is dominated by irregular, discontinuous and weak seismic reflections, with identified high- and low amplitude features. The GR log shows rapid alternating values, with several high and low values *(Figure 5-2).*

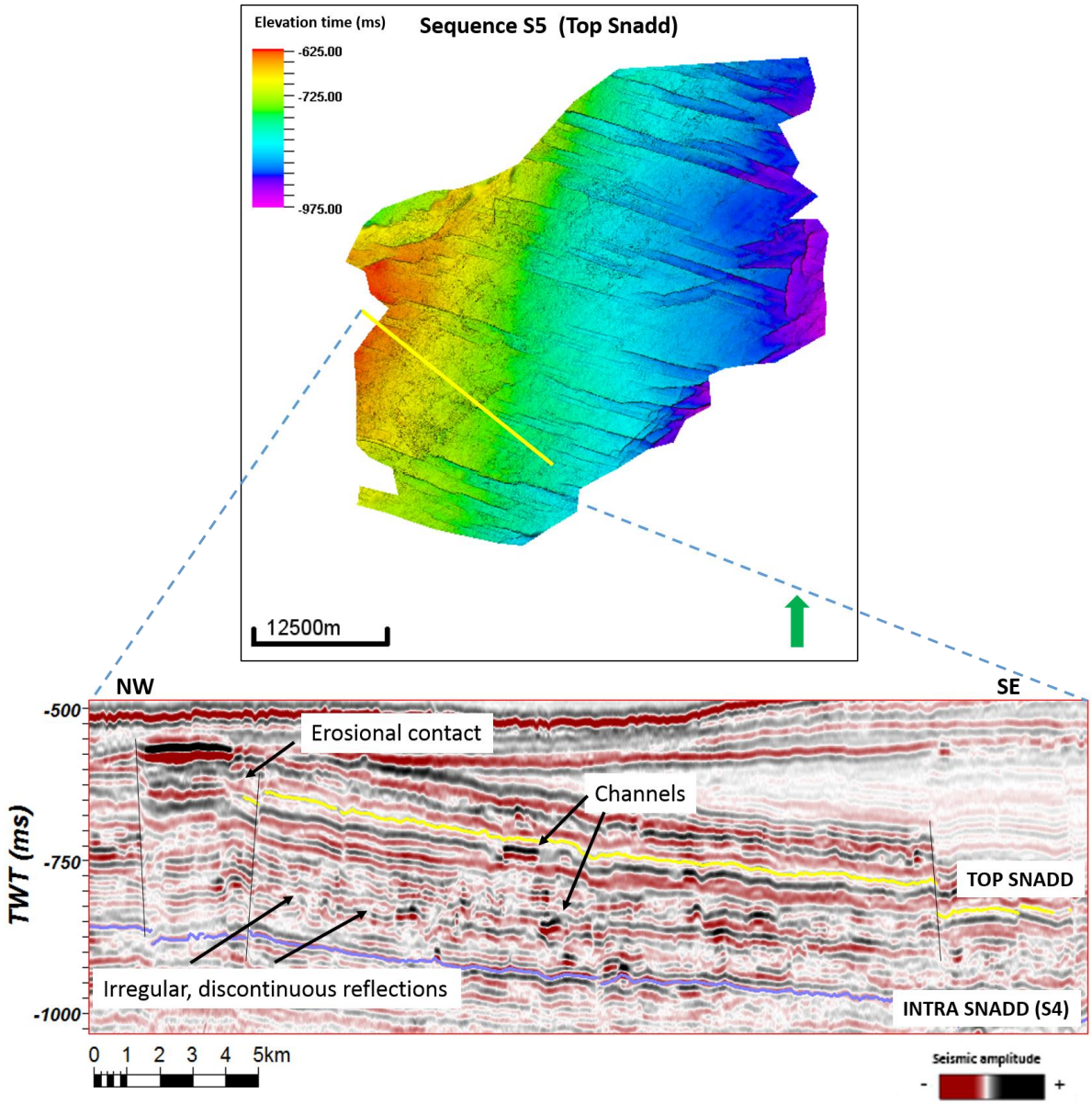

Figure 5-8. *Elevation map of Top Snadd (S5) together with seismic section of random line in WIN12003.*

Interpretation

The irregular, discontinuous and weak seismic reflections are interpreted to represent a coastal plain (chapter 3.3.1, F4), with fluvial and alluvial features, represented by strong high- and low amplitudes in the seismic data. The frequent changes in low and high gamma ray values is suggesting a coastal plain environment with alternating transgression and regression. According to (Glørstad Clark et. al (2010) large parts of the upper limit of S5 has been eroded by the Base Cretaceous Unconformity or the Upper Regional Unconformity (URU). The lower limit represents MFS, based on extent and the observed stratal patterns. The suggested coastal plain environment with alternating transgression and regression in this study, is compliant with (Glørstad Clark et. al (2010) and (Klausen, et al., 2014), where the upper part of Snadd is dominated by non-marine deposits in Carnian succession, followed by a transgressive unit in Early Norian *(Figure 3-13)*.

Time-thickness map *(Figure 5-9 c)* generated between S4 and S5 sequence is indicating a western thickening throughout the area. This is also observed in a seismic section, where the western part of the seismic is clearly thicker than the eastern part *(Figure 5-9 d)*. This could represent a progressively infill of sediments from east to west, with depocenter to the west.

It was further observed that the Triassic succession was a relative continuously unit, with no visible structural interruptions internally in the sequences *(Figure 5-1)* .The seismic data showed different seismic facies, possibly caused by shifting depositional environments described in chapter 5.2. The faults observed in the seismic data is located within the shallow part of the Triassic sequence, also penetrating the Hekkingen formation (Late Jurassic), up to Cretaceous *(Figure 5-1)*. Together with the quiet tectonic observations in the Triassic succession, the faults are interpreted to have been formed by late Jurassic rifting.

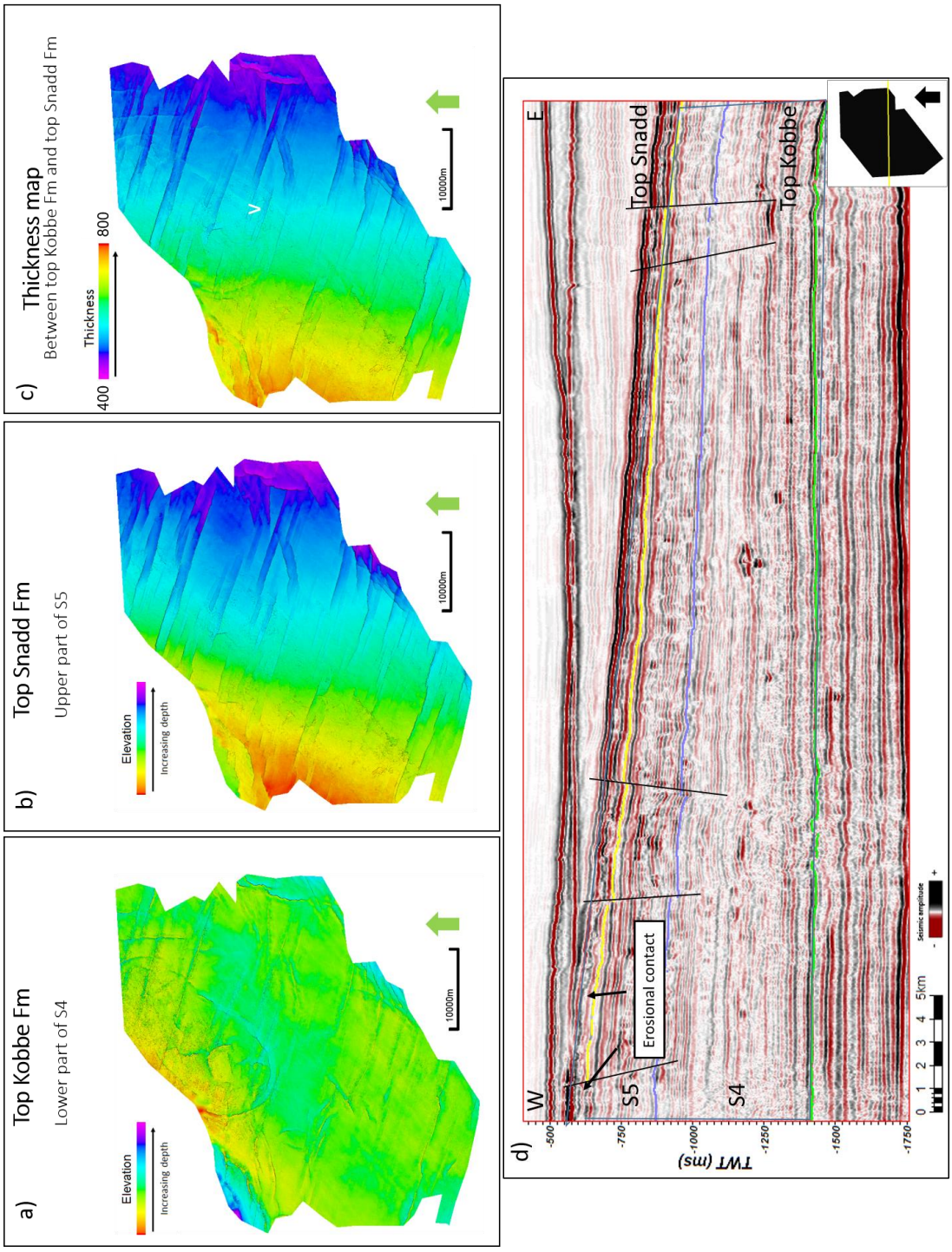

Figure 5-9. A) *Time-structure map of Top Kobbe formation, correlated to lower limit of S4.* ***B)*** *Time-structure map of Top Snadd formation, correlated to Top S5.* ***C)*** *Time-Thickness map between S4 and S5 sequence, indicating a western thickening.* ***D)*** *Vertical seismic section of random line in cube WIN12003 indicating an western thickening in the area.*

5.3 Interpretation of channel systems within the Snadd Formation

The channel systems identified in this work, are characterized and described based on quantitative and qualitative interpretations. The quantitative interpretation involves channel vertical and lateral size, channel sinuosity index and relative channel gradient, while the qualitative interpretation is based on the channel geometry, channel classification and the geological and depositional environment when the channel actively was created. Several channel features of varying size and extent were observed in this dataset, both within Snadd formation and in Kobbe formation. The interpreted channel systems in this thesis are located within the non-marine part of S4 sequence in Snadd formation. There were observed several channel features, where two of them were further analyzed, interpreted and described.

All of the channels were first observed in Petrel, by time slices through generated attribute volumes. By using different attributes described in chapter 4.3.3, the channels were relatively easy to observe on the different time slices, where channel features were distinguished by clear boundaries from the surroundings. The selected channel systems described further, are in this thesis named Channel 1 and Channel 2. They were chosen due to their clear shape, size and continuity, and because they represent different types of channels.

5.3.1 Interpretation of Channel 1

Channel 1 was first observed on a chaos attribute time-slice, where its characteristic channel body was clearly distinguished from its surroundings *(Figure 5-10 A).* It was observed in sequence S4 in the Snadd formation, within the two-way time interval of 1249-1292 ms. The identified feature has an overall orientation from east to west, with some significant river bends throughout the whole channel *(Figure 5-10).*

Based on the sediment infill direction interpreted in chapter 5.2, where the thickness map (*Figure 5-9 C*) and the seismic section *(Figure 5-9 D)* shows a westward thickening, indicating infill from the east, the channel orientation was found. The upper part of the channel system is therefore interpreted to the east, with a flow direction to the west. Further in this thesis, the channel parts will be referred to as the upper and the lower part *(Figure 5-11A).*

The elevation map of the interpreted channel shows a higher TWT value in the upper part of the system, than in the lower part *(Figure 5-11 A).* This means that the upper part of the channel is located deeper down in the seismic than the lower part, which disagrees with the natural water flow direction.

This can indicate that something has occurred in the area after the channel was active, probably uplift of the western areas or subsidence to the west.

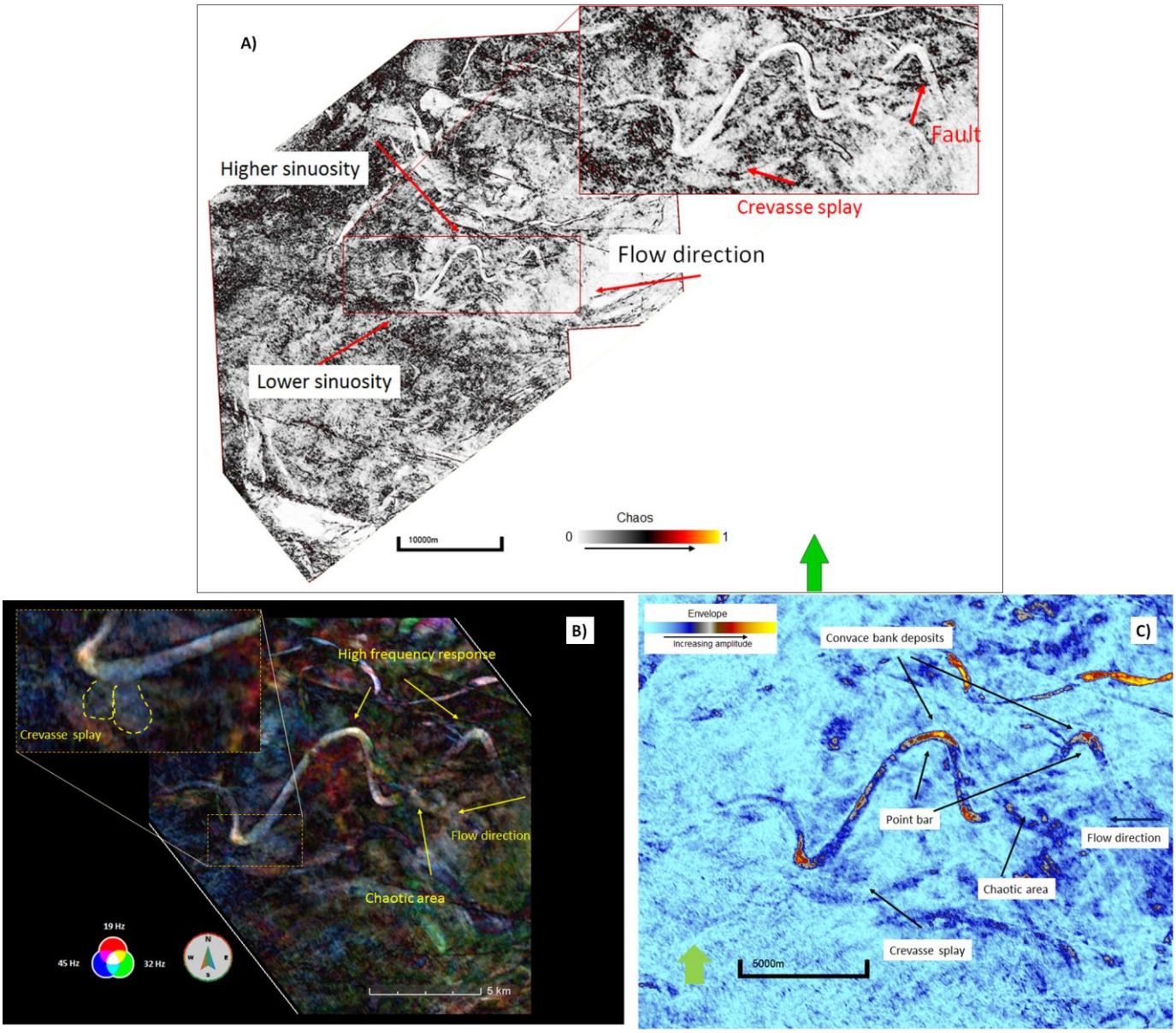

Figure 5-10. ***A****) Chaos attribute map, time-slice 1272. Red arrows indicating limiting faults, crevasse splays and sinuosity.* ***B****) RGB-blend-SO-semblance map of time-slice 1272. Yellow arrows indicating observed features.* ***C****) Envelope attribute map 1272 showing meandering river with several channel features.*

The length of the channel was measured to be approximately 23.9 km with a valley length of approximately 15.5 km. The channel sinuosity was calculated to be 1.55 by using *equation 2* presented in chapter 2.5.6.

The width and vertical thickness of the channel was measured in three separate locations *(Figure 5-11 A).* The depth was found by using the velocity table from the well 7124/2-1 *(Figure 5-11 C),* correlated to the picked TWT at the channel top and base in these locations *(Figure 5-11 D).* The channel thickness was measured to vary from approximately 50 to 72 meters. The deepest part was measured in the meander bend, and the shallowest depth was measured in the lower part of the system. The lateral width of the channel was measured to be between 300-380 meters *(Figure 5-11 B).*. The width to thickness ratio of Channel 1, is calculated to be approximately 5.

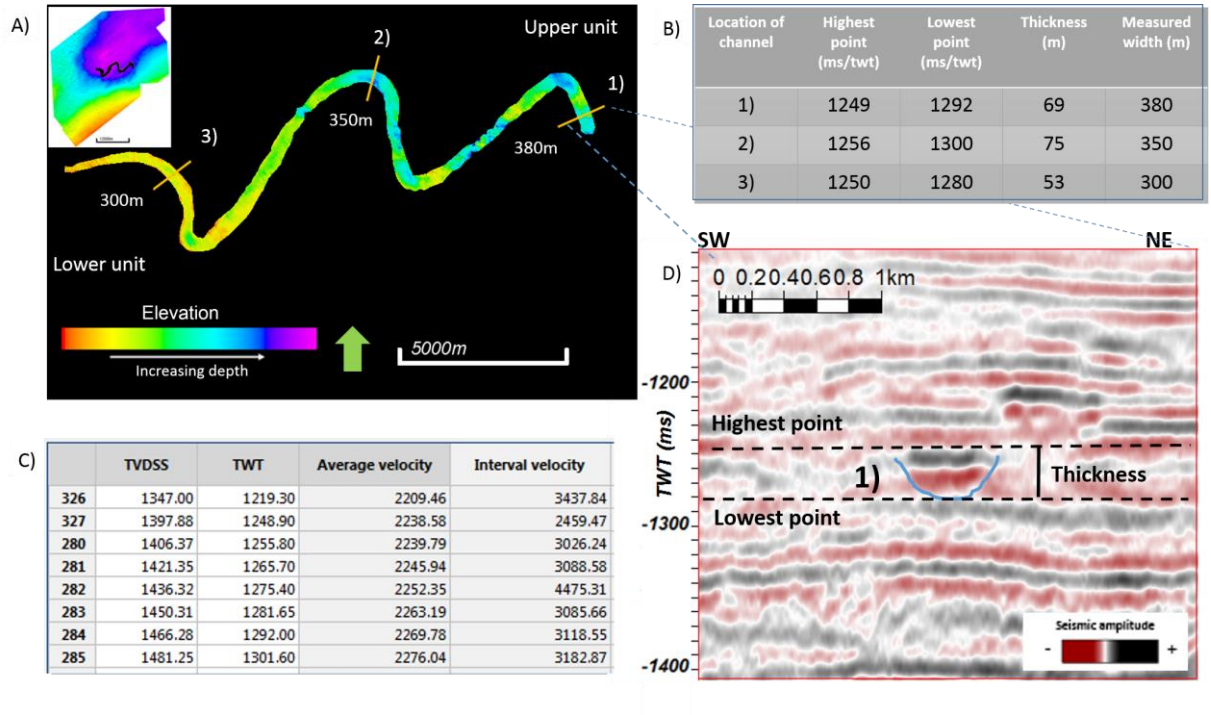

Location of channel	Highest point (ms/twt)	Lowest point (ms/twt)	Thickness (m)	Measured width (m)
1)	1249	1292	69	380
2)	1256	1300	75	350
3)	1250	1280	53	300

	TVDSS	TWT	Average velocity	Interval velocity
326	1347.00	1219.30	2209.46	3437.84
327	1397.88	1248.90	2238.58	2459.47
280	1406.37	1255.80	2239.79	3026.24
281	1421.35	1265.70	2245.94	3088.58
282	1436.32	1275.40	2252.35	4475.31
283	1450.31	1281.65	2263.19	3085.66
284	1466.28	1292.00	2269.78	3118.55
285	1481.25	1301.60	2276.04	3182.87

Figure 5-11 A*) Elevation-map of Channel 1, illustrating location of measurements taken.* ***B****) Tabell with an overview of highest and lowest point, measured width and calculated thickness.* ***C****) VSP log from well 7224/2-1,* ***D)*** *Seismic profile of random line (point 1) in A), showing highest and lowest point, and thickness of Channel 1.*

In a plan view *(Figure 5-10)*, the channel is visualized in the central part of the seismic cube, with a sudden appearance of the channels start and ending points. When investigating the upper part of Channel 1, it is clearly limited by a NW-SE orientated fault, showed in a chaos map (*(Figure 5-10 A).* In the lower part of the system, the channel is gradually disappearing in the time-slices. In a vertical seismic section *(Figure 5-12 B), the* reflectors are slowly tuning out and disappearing due to chaotic dim reflectors. Several high amplitude features are located above this area, causing acoustic masking, making it difficult to further interpret the extent of the channel system. In the seismic section and in the gamma ray log, there are not observed any reflectors or GR API values indicating marine

sediments in this stratigraphic level. There are not observed any other structures that explains the sudden disappearance of the channel. It is therefore thought to extend beyond the interpretation shown in *Figure 5-12 A.*

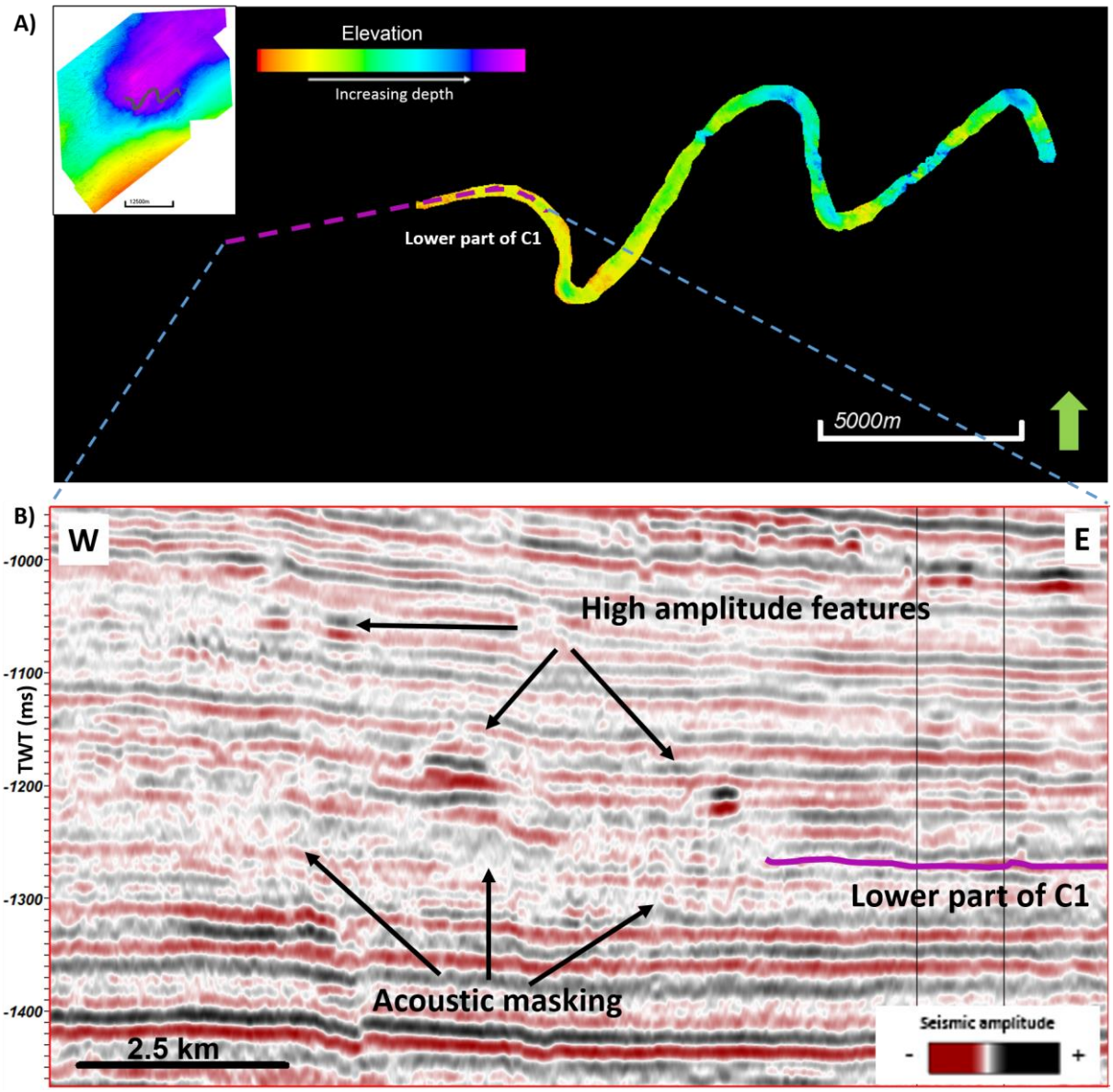

***Figure 5-12** . Elevation map of Channel 1, together with seismic section of random line in cube WIN12003. High amplitude features and acoustic masking makes it difficult to interpret the extent of Channel 1.*

By using some of the seismic attributes described in chapter 4.3.3, a more qualitative investigation was done. To better reveal this channel feature, the seismic data was improved by using three common techniques: Frequency decomposition/RGB-blending, envelope and chaos attribute.

Results from RGB blending method

At time slice 1272 ms (TWT) in the generated RGB output cube, the channel feature was easily observed, with a significant lighter color than the surroundings (*Figure 5-10 B).*The channel bends are dominated with a distinct white color, while the areas in between have a variety of all the RGB colors, and in some areas, significant darker color. By investigating the different channel bends more closely, it appeared that bends with lower sinuosity are dominated with a lighter color in the outer parts of the bends than the inner bends, while in the higher sinuosity bends, the light color are relatively equal on both sides of the bend (*Figure 5-10 B).*According to the design of RGB blending method, the outer bends white color indicates a high response of all three of the frequencies, while the darker color in the inner parts of the bends with low response, could indicate a more massive body (Naseer, et al., 2014).

In the upper part of the channel system, an area with irregular and noisy structure was found, where no specific channel edges were observed (*Figure 5-10 B*). This part related to the rest of the channel feature *(Figure 5-11 A),* but is not clearly revealed in the time-slices. This could be explained by the fact that time slices cut a horizontal line through the seismic cube, while the channel will follow a stratigraphic layer, or because features in this part of the channel appear noisy with the selected RGB settings.

In the lower part of the system, some features with lobate geometries were observed (*Figure 5-10 B).* These features are located outside the concave river bend, and have a distinct blue color, indicating dominance of the high frequencies. The area of this features was measured to be approximately 2 km^2.

Results from the envelope attribute method

The envelope attribute time slice at 1272 ms (TWT) clearly distinguishes the channel body from its nearby material (*Figure 5-10 C*). It is dominated with higher amplitude values (dark blue color) than the surroundings, with some very high values (red/yellow), located in the river bends (*Figure 5-10 B).* With this method, the distribution of high amplitude values in the bends of different sinuosity is revealed, *w*hich also corresponds with the results from the RGB method. It also shows the internal reduction which occurs in the low sinuosity river bends, were the amplitudes goes from higher to lower values when going from the outer to the inner bends.

The observed features with lobate geometries located outside of the channel in the lower part of the system are also visible in the envelope attribute map (*Figure 5-10 B).* They are represented by a dark blue color, similar to the channel body, except for the high amplitudes observed in the channel bends. The amplitude character of these features is lower than the channel bends and higher than the surroundings. This suggests a grain size between the surroundings and the channel bends.

By extracting the envelope values on the interpreted channel *(Figure 5-13 A)*, the internal morphology was easier to interpret. The attribute surface map revealed areas with irregular, elongated and more circular patterns of high values (red color), located in the channel bends. It also shows that in the low sinuosity bends, the high amplitude values are located at the concave meander bends, and decreases towards the convex side *(Figure 5-13 B).* High envelope values often represent high acoustic impedance contrast between layers, and are normally correlated to high porosity (Schlumberger, 2010). In Channel 1, this can indicate that the bends contain sediment accumulation with high porosity and with significant contrast in density and/or velocity compared to the surrounding layers. In the low sinuosity bends, the outer bends is therefore interpreted to consist of significant coarser grains than the inner point bar, due to the fact that high porosity occur in coarser grains contra fine grains. In the high sinuosity bend *(Figure 5-13 C)*, the distribution is more equal through the bend.

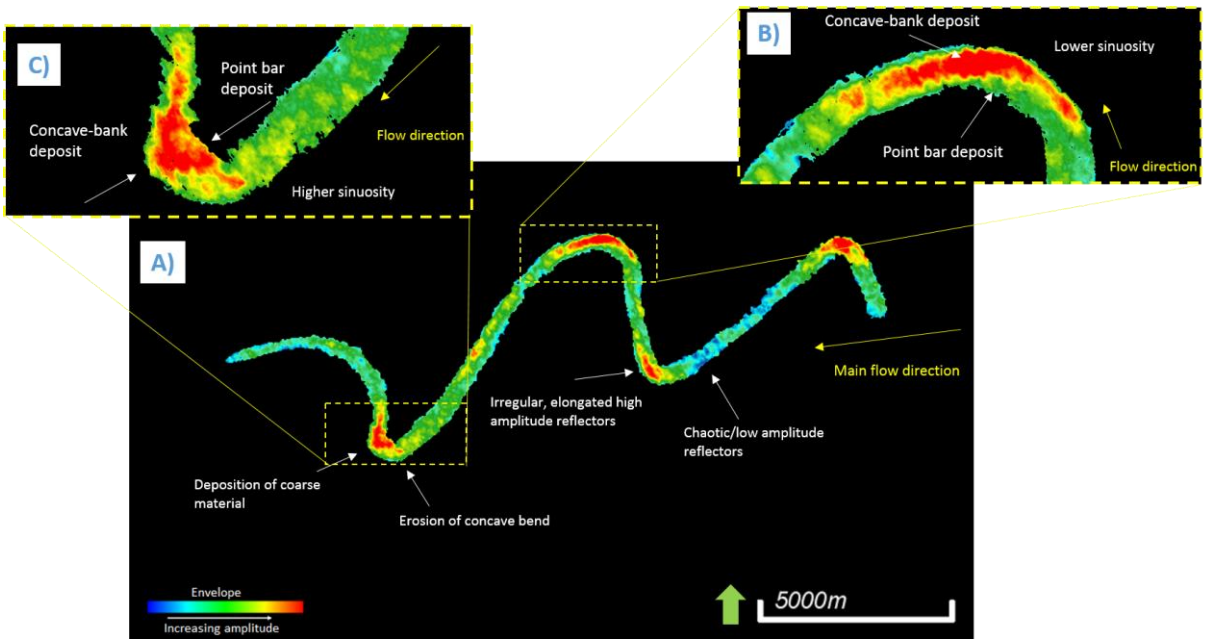

Figure 5-13*. A) Extracted envelope value generated on Channel 1, showing high amplitudes in the channel bends.* ***B)*** *Higher sinuosity bends with a more elongated high amplitude accumulation.* ***C)*** *Lower sinuosity bends showing a more clustered amplitude accumulation.*

By using the RGB results and the attribute map results together, the channel interpretation gets a more solid foundation. In the lower sinuosity bends *(Figure 5-13 B)*, the concave areas are interpreted to consist of thinner sediment packages with high porosity sediments, possible coarser materials, potentially filled with hydrocarbons, due to high acoustic impedance contrast. The convex bends is interpreted to contain point bars, consisting of thicker beds with finer particles *(Figure 5-13 B)*.. The

lobate structures described above are interpreted do be crevasse splays, which consist of a thin sediment layer with relatively similar deposits and grains sizes as the main channel.

In the vertical seismic section *(Figure 5-14 A*), the channel was observed with a significant high amplitude feature compared to the surroundings. The high amplitude channel is truncating the underlying reflectors, and is therefore interpreted to be formed by an erosional process, where it is incised into the underlying deposits. The underlying depositions, which the channel is truncating, are in this area represented by strong, continuous and parallel reflections located in the lower sequence of S4 (*Figure 5-2).* In well 7224/2-1, located close to Channel 1, the GR log curve shows high values in this unit (*Figure 5-2).* These strong reflections and the high gamma ray may indicate that the river has incised in an underlying deposition of marine shelf or prodeltaic depositions, with shale content (chapter 5.2, S4).

The cross section, taken through one of the channel bends *(Figure 5-14 B*) also reveals that the channel has a clearly asymmetric form. The convex part (inner bend) is represented with a shallower area with a more gentle slope against the thalweg, while the convex part (outer bend) is deeper, with a much steeper slope. Cross section through the channel bends also shows a high relief on both flanks of the channel (*Figure 5-14 B).* The shape of this features is similar to a triangle, where the triangle edge closet to the channel is steeper, and gradually becomes less steep against the outer channel. The features have relative high amplitude values, which indicate high acoustic impedance contrast with the surroundings. These features are not observed on the horizontal time-slices. Due to their placement and shape, they are interpreted to be channel levees.

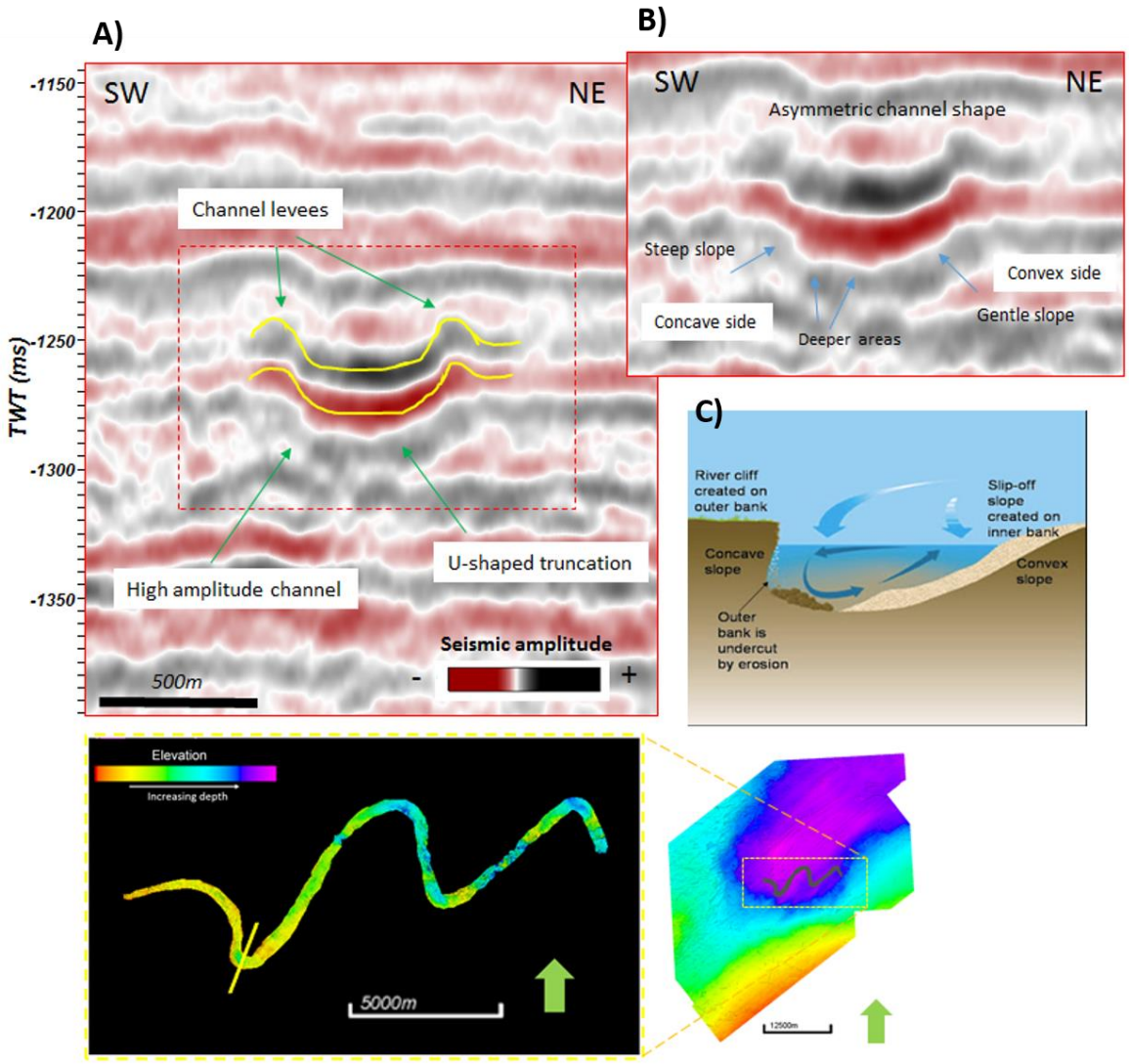

Figure 5-14. ***A)*** *Vertical section of random line through meander bend of Channel 1. Illustrating Channel levees, and u-shape.* ***B)*** *Vertical section illustrating asymmetric shape.* ***C)*** *Illustration of development of asymmetric channel shape.*

5.3.2 Interpretation of Channel 2

This channel feature was observed on a variance time-slice *(Figure 5-15 A)* and located in the time interval 1148-1218 ms TWT, in the non-marine part of the S4 sequence. The channel orientation is interpreted to go in NE-SW direction, due to the interpreted infill direction from east in chapter 5.2.

Channel 2 was observed as a relatively straight channel, with relatively small river bends compared to Channel 1. The length of the channel was measured to be approximately 20.7 km, with a valley length of approximately 20.4 km. The sinuosity was calculated by *equation 2* in chapter 2.5.6 to be 1.01.

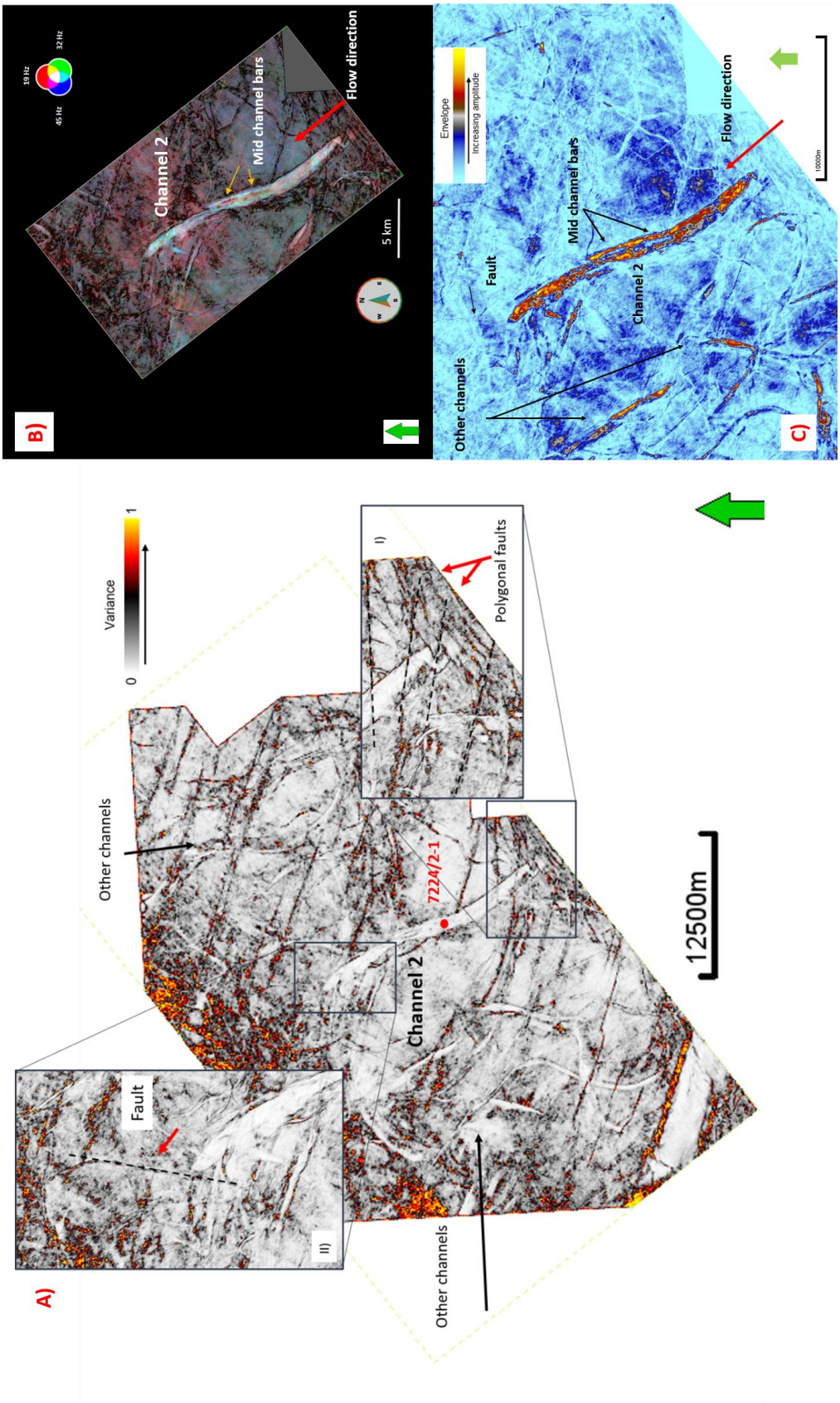

Figure 5-15. A) *Variance map of time-slice 1196 showing Channel 2. Red arrows indicating polygonal faults and other channel systems.* ***B)*** *RGB-color blending map of time-slice 1196 showing Channel 2 and mid channel bars* ***C)*** *Envelope attribute map of time-slice 1196 showing Channel 2 containing mid channel bars.*

The lateral channel width was measured in four separate locations on Channel 2 (*Figure 5-16 B*), and got a value between approximately 780-1550 m. The vertical thickness of the channel was found by using the velocity table from well 7124/2-1 (*Figure 5-16 A*), correlated to the picked TWT at the top and base of the channel in these areas (*Figure 5-16 C*). The channel thickness was measured to vary from approximately 60 to 80 meters (*Figure 5-16 D*). The width to thickness ratio was calculated to be variating from 15.5-25.5.

The elevation map of Channel 2 shows a higher TWT value in the upper part of the system than in the lower part (*Figure 5-16 A*). This implicates tectonic events in the area after the channel was active.

When looking at time-slice 1192 on different attributes *(Figure 5-15)*, both the start and the end of Channel 2 seem to appear suddenly, and in the middle of the seismic cube. When investigating this more closely, the evolution of the channel was observed in time-slices deeper in the seismic, with an origin from east *(Figure 6-2).* On a variance map in slice 1192, it was observed polygonal faults limiting the top of the channel feature *(Figure 5-15 A)*. Channel 2 is therefore thought to extend further to the east than the seismic cube. The lowermost part of the channel is also limited by a fault, observed in the variance map *(Figure 5-15 A)*. In a vertical profile, the western part of the channel is penetrated by several faults, making it difficult to interpret the channel further (*Figure 5-17).* The seismic is also affected by acoustics masking from faults and high amplitudes. Due to the chaotic reflectors and the end of the seismic cube, it is hard to say if the channel systems extended further than this, but when using the gamma ray log, no marine sediments was observed in this stratigraphic layer, and the channel is therefore interpreted to extend further than the slice is showing.

A)

	TVDSS	TWT	Average velocity	Interval velocity
275	1256.60	1162.80	2161.33	2825.74
276	1271.57	1173.40	2167.33	3482.82
277	1286.55	1182.00	2176.90	3291.28
278	1301.53	1191.10	2185.42	2698.03
279	1316.50	1202.20	2190.15	3794.63
325	1337.56	1213.30	2204.83	3146.67
326	1347.00	1219.30	2209.46	3437.84

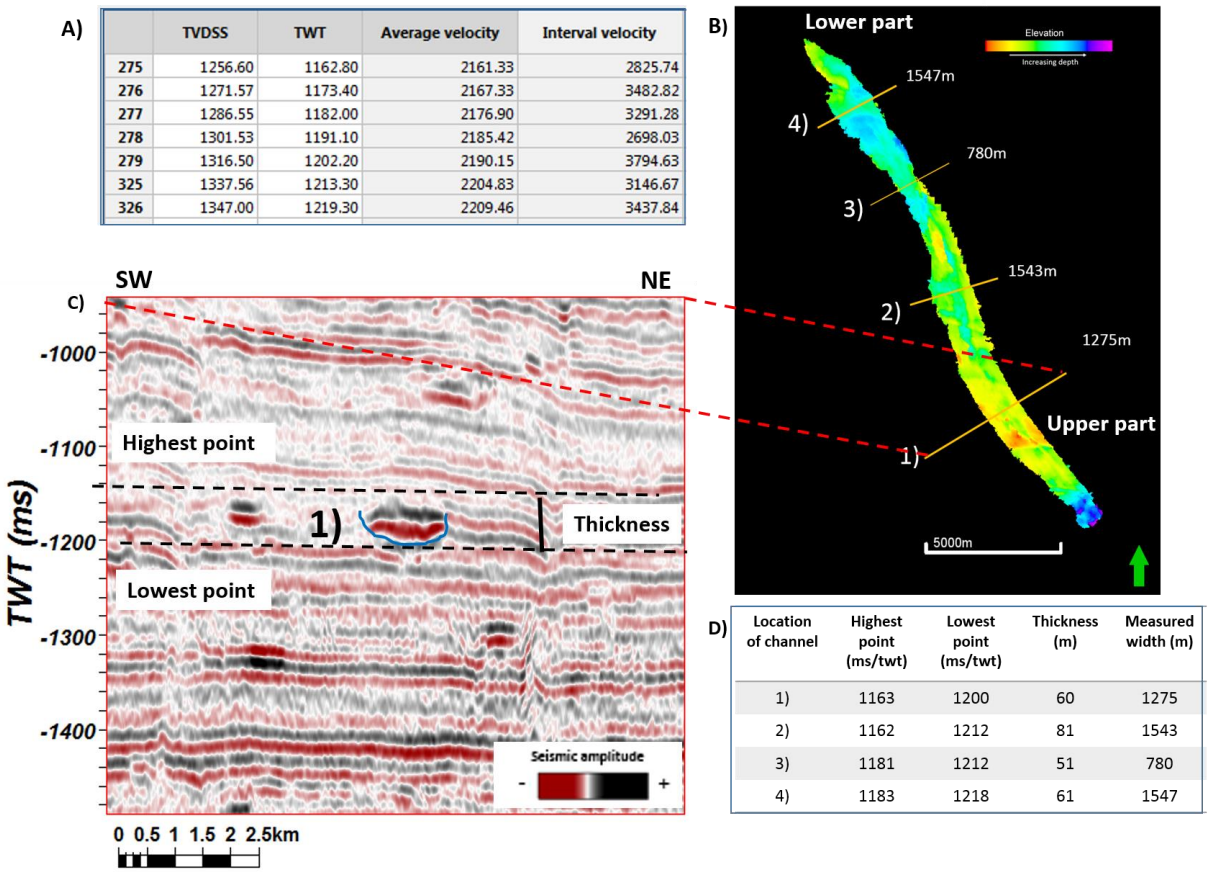

D)

Location of channel	Highest point (ms/twt)	Lowest point (ms/twt)	Thickness (m)	Measured width (m)
1)	1163	1200	60	1275
2)	1162	1212	81	1543
3)	1181	1212	51	780
4)	1183	1218	61	1547

Figure 5-16. A) *VSP time depth table from well 7224/2-1.* ***B)*** *Elevation-map of interpret Channel 2, showing where the different measurements were taken from.* ***C)*** *Vertical section of random line, annoted 1) in cube WIN12003, showing lowest and highest point, and thickness.* ***D)*** *Table showing different measurements done*

To be able to carry out a more qualitative investigation, some of the attributes described in chapter 4.3.3 was used. The method of frequency decomposition/RGB- blending, chaos attribute and envelope were used on this seismic data to better reveal the channel.

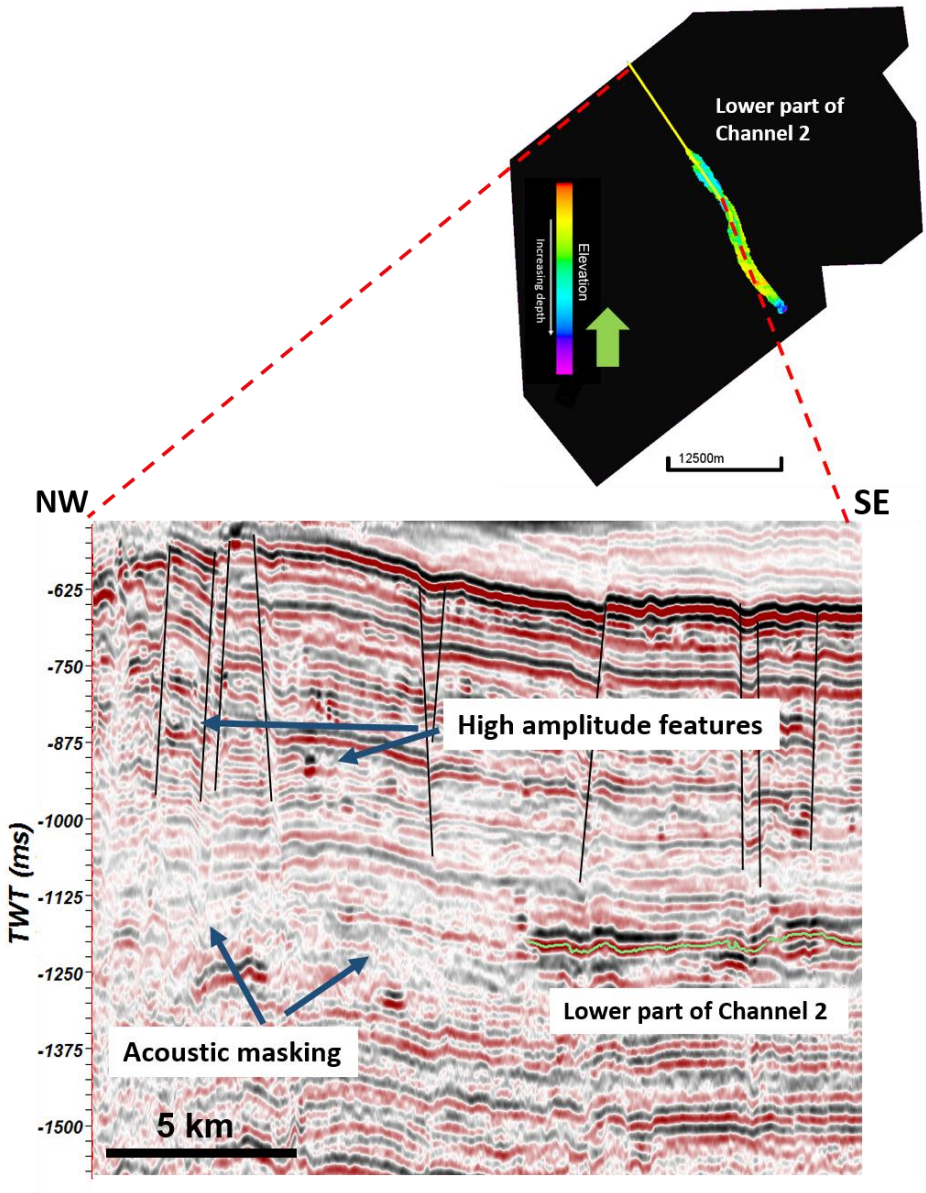

***Figure 5-17**. Elevation map of Channel 2, together with seismic section of random line in cube WIN12003. High amplitude feature, faults and acoustic masking makes it difficult to interpret the extent of Channel 2.*

Envelope attribute

In envelope time-slice 1192 the channel feature is clearly visualized with high reflection strength values (red/yellow color) compared to its surroundings, which have significant lower amplitude values (blue color) *(Figure 5-15 C).* The high envelope values often represent a high acoustic impedance contrast (Schlumberger, 2010), and correlates to high porosity. Based on this, the channel is interpreted to consist of significant coarser grains, than the surroundings.

Some elongated features are observed within Channel 2, with distinct lower amplitudes (blue color) than the main channel. These features have the same low amplitude signature as the dominating

surrounding material outside the channel *(Figure 5-15 C)* ,which may indicate the same type of deposits and/or equal grain size. The low amplitude values observed, may indicate a sediment with less porosity, hence finer particles. The features are orientated parallel to the fluid flow, and measured to be approximately 0.62 km^2 and 0.95 km^2.

RGB - blend

On the RGB time slice, Channel 2 is distinguished with a white and bright color *(Figure 5-15 B)*. The elongated features observed within the channel have a distinct red color. According to the design of RGB blending method, the elongated accumulations observed within the channel with a darker and red color, is interpreted to indicate a more massive body (Naseer, et al., 2014), while the main channel with the white color indicates a high response of all three of the frequencies.

Combining the RGB results with the results from the Envelope attribute value, the elongated features observed in the channel is interpreted to consist of a massive sand body with similar material as the surroundings, containing fine sediments. These features are interpreted to be mid channel bars.

Well 7224/2-1 is penetrating Channel 2. By using the different logs, a more qualitative investigation could be done. In the gamma ray log, the channel bounds have a distinct increase in API values compared to the channel, where the channel body is dominated by stable and low values (*Figure 5-18*), indicating sand sediments. The high API values observed at the limiting top and base of the channel feature may indicate muddy sediments. It is also observed some strong, continuous reflections below and above the channel feature in seismic profile (*Figure 5-16 C*). This together with the gamma ray signature may indicate marine deposits.

The neutron/density log (*Figure 5-18*) was used as an indicator for potential hydrocarbon presence within the channel. As described in chapter 4.4 (well logs), the density log measures the density of the formation including the fluids in the pores. If the formation looks homogenous, meaning that the gamma log is relatively flat, a decrease in the density log might indicate a lighter fluid in the pores. This may again indicate gas or oil as hydrocarbons has lower density than water.

The neutron log measures the amount of hydrogen content in the formation, chapter 4.4. If the neutron log decreases it means that the presence of hydrogens in the pore space has increased. Oil and gas consists of more hydrogen than water, so this might indicate that there are hydrocarbons in the formation. If the density log decreases (goes to the left) at the same time as the neutron log decreases (goes to the right) this is usual a good indication of hydrocarbons present, see the green box in *Figure 5-18*

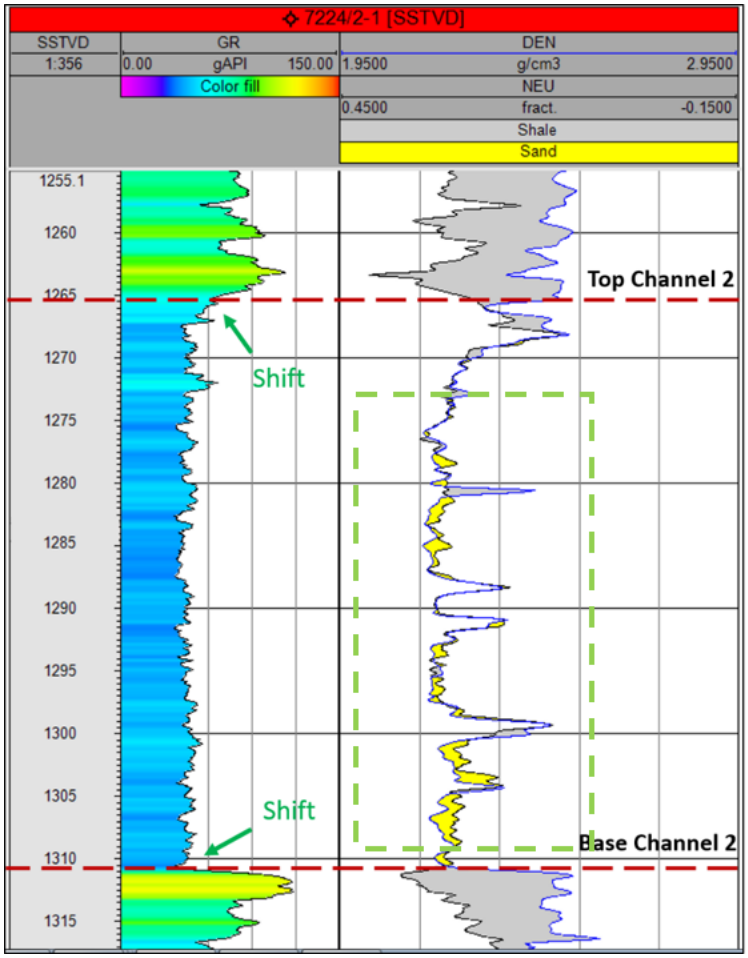

Figure 5-18. *Gamma ray log and neutron/density log from 7224/2-1, trough channel 2. Green arrows indicating a significant shift in Gamma ray values. Green Square indicate a decrease in density together with decrease in neutron, which is a good indicator of hydrocarbons.*

6. Discussion

The depositional environment of the identified stratigraphic units and the mapped channels in this work is interpreted based on the results from the seismic investigations and well log data presented in the previous chapters. The results will primarily be compared to earlier studies by Glørstad-Clark et al., (2010), Klausen et al., (2014) and and Klausen et al., (2015).

6.1 Stratigraphy and area

Vertical sections together with the thickness map *(Figure 5-9)* of the Snadd formation (and Fruholmen) shows an overall thickening to the west. This indicates that the area was progressively filled with sediments from the east and south east over Triassic time, which fits with observations in earlier works. During the Triassic period, the Uralian and the Caledonian orgenies were still active, acting as sediment source. Depositions took place across the western parts of the Barents Sea, due to increased accommodation space and deposition in the western basins (Glørstad-Clark, et al., 2010). The observation of filling from the east and south east also agrees with (Worsley, 2008).

The Triassic section in the area of interest is interpreted to be deposited in a tectonic quiet period, since the reflections within the sequence show few structural interruptions, see *Figure 5-1* . This, together with the observed faults interpreted to have been created by late Jurassic rifting, is in line with the Triassic tectonic description by (Faleide, et al., 1993) and (Gudlaugsson, et al., 1998). Here, Triassic is described as a tectonic quiet period, characterized by regional subsidence and development of local heights, a setting that proceeded to the middle of Jurassic. (Gudlaugsson, et al., 1998), (Faleide, et al., 1993). The uplift of the Paleo-Loppa High and the Pliocene glacial erosion of the Triassic sediments agrees with the interpreted seismic volume. The significant uplift westwards in the study area can be viewed on the Top Snadd elevation map in (*Figure 5-9 B*).

Elevation maps generated for both channels (*Figure 5-11 and Figure 5-16*)show a deeper location of the upper parts of the river systems than the lower parts. This disagrees with the natural water flow, which suggest that uplift in the western part and/or subsidence in the east has occurred in the area after the channels were active.

Sea-level

Figure 5-2 shows blocked gamma ray values throughout section S4, interpreted to represent changes of sea-level, with internal rise and fall. This is supported by the seismic section, which is shifting between seismic facies 2 (chapter 3.3.1), representing shelf deposits, and seismic facies 4 and 5, representing coastal plain with incised channel features. This is in line with Klausen, et al., (2015),

where the Top Ladinian boundary between S4 and S5 in Glørstad-Clark, et al., (2010) is interpreted to correspond with global sea-level changes as a response to changes in the setting of the lithospheric plates. Several channel features were observed within the Snadd formation, *Figure 5-1, 5-10 and 5-15* indicating a non-marine environment.

6.2 Channel systems

6.2.1 Channel 1

The interpretation of Channel 1 can be related to studies of fluvial channel systems and their origin. In this work, the sinuosity of Channel 1 was calculated to be 1.55. The width to depth ratio described in Rosgen (2007) is referred to as the width to thickness in this study, found to be approximately 5 in this channel. By using the classification system defined by Rosgen (2007) presented in chapter 2.5.6, Channel 1 is interpreted to be of type E river, called stable meandering river. This means that this channel probably has followed floodplain development. Channel 1 has low channel width/thickness ratio, and display high channel sinuosity, which leads to this classification. Type E rivers have the highest meander width ratio values of all the described stream types. According to Rosgen (2007), the "E" type river generally occurs in alluvial valleys with low elevational relief characteristics, and develops frequently in low elevated coastal plains.

Considering the interpretation of sedimentation from the east, Channel 1 is interpreted to be located in a very distal area to the source. The meandering shape of the channel may indicate that the observed channel is located in the middle or in the lower part of the channel system (chapter 2.2). Since the landscape is flatter in this part of the system (*Figure 6-1*) and the energy in the river is lower it tends to go sideways. Due to less energy the heavy sediments are already dropped, as there is not enough energy to keep them moving in the water. Channel 1 was observed with a relative constant thickness throughout the observed channel area, which is typical for meandering rivers (Rosgen, 2007).

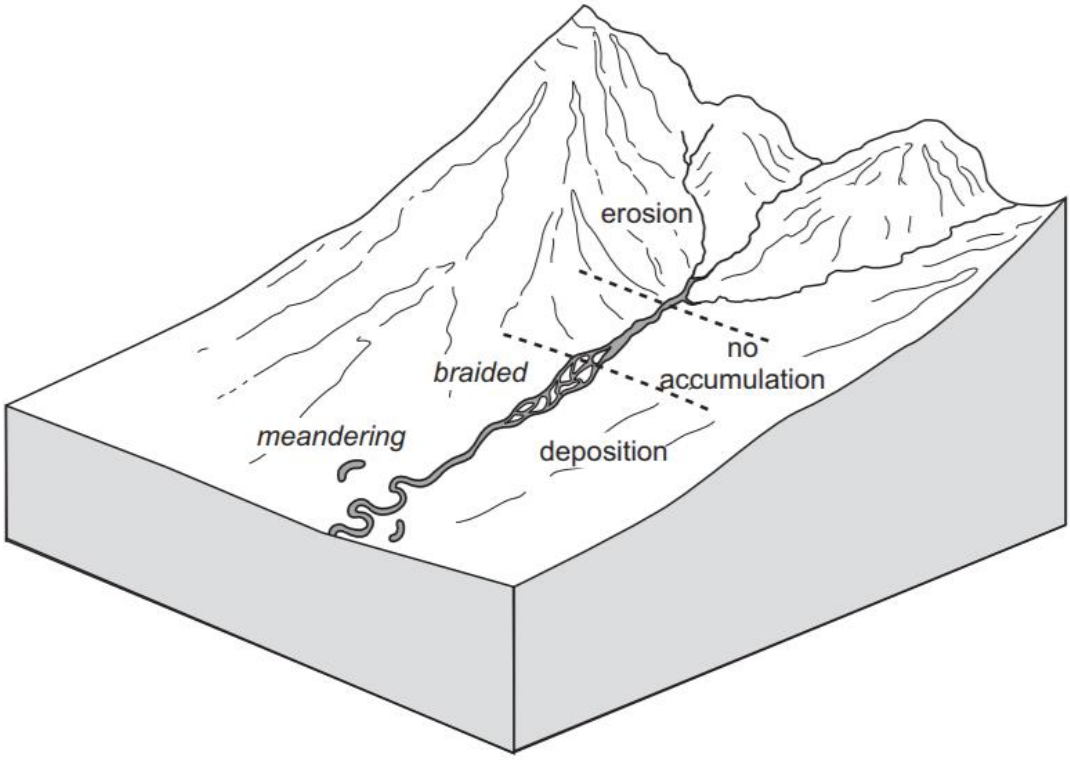

Figure 6-1. *Geomorphical zones within fluvial and alluvial systems. Braided rivers are often found in more proximal areas, while meandering rivers are found further down steam. (Nichols, 2009).*

The observed channel is truncating the lower unit of S4 (*Figure 5-14* A), which is represented with relatively continuous, parallel and strong amplitude reflections. This unit was connected with high gramma ray values in the nearby well 7224/2-1. This may indicate a channel, eroding in underlying shelf marine or prodeltaic sediments. This may be in line with the interpretation done in chapter 5.2, where the lower unit of S4 is interpreted to represent a marine environment, and corresponds to (Glørstad-Clark, et al., 2010), which supports the interpretation of marine deposits, underlying continental deposits containing channel features, limited by the maximum regressive development within this sequence.

Due to no available core photo in the nearby well, the exact fluvial deposition within the channel was relatively hard to find. By using the amplitude distribution, and knowledge of meandering streams and depositions, an assumption was done. The seismic shows contrasts, and since the background is interpreted to be mud or shale deposits the, the channel body contrast could be interpreted to be sandy. In the envelope map *(Figure 5-10 B),* the Channel 1 is clearly distinguished from its surroundings, indicating an acoustic impedance contrast in material. This means that the channel feature most likely consist of another material than its surrounding marine deposits. According to Einsele (1992), the deposition of meandering river consists of fine grained sediments, such as sand, silt and mud. Due to

the significant acoustic impedance contrasts found in the river bends, which indicated a material coarser than the rest of the channel, the river bends are interpreted to consist of medium sand to coarse sand, while the rest of the channel is interpreted to consist of very fine sand to fine sand.

When validating the interpretation of Channel 1, it is important to understand the interaction between the river velocity, the river geometry and the sediment behavior in the river. The asymmetric shape observed in the cross-section trough the meandering bends in Channel 1 *(Figure 5-14 B)* is in line with the characteristic of meandering rivers, where the meandering bend apex normally has an asymmetric geometry (Figure 5-14 C) (Dey, 2014). The maximum flow velocity in a meandering river occurs in the outer part of the bend, the concave area, causing erosion, makings the river deeper, while the water velocity would drop significantly in the inner part of the river, causing sedimentation. These mechanisms cause the asymmetric shape observed in Channel 1*(Figure 5-14 B)*. Sinuous channels grow more asymmetric in the downstream translation and lateral expansion, leading to continuous preservation of point bar and concave-bank deposits.

The fluvial channel migration pattern discussed here predicts grain-size distribution along the curved segments of fluvial channels. Higher velocity and turbulent stream implies that the coarsest sediments erode and are transported from the outer bend near the bend apex. When moving from the outer part to the inner part of the bend, velocity will decrease. This implies that the coarser grains will be deposited in the outer part of the bend, since the inner part of the river does not have enough capacity to transport the coarse sediments. In *Figure 5-13 B* it is also visualized that in the low sinuosity curve, the coarser grains (red color) is interpreted to be located significant closer to the outer bends than the inner bends, where more finer grains is deposited. In the high sinuosity bends, this difference is less clearer.This is believed to be because the flow more quickly looses power in these sharp bends compared to the low sinuosity bends, causing the coarser grains to deposit more rapidly. Here, the distribution appears to be more equal through the bends.

Continued erosion of the outer bank and deposition of bedload on the inner bank leads to migration of channel bends as the water flow scours deeper along the outside of the bend apex, which is closest bank to thalweg. In Channel 1, maximum thickness near meander bends has been interpreted to be located at the closest bank to the thalweg (*Figure 5-14 B*).

The observed, interpreted channel levees has a triangle shape, where the inner edge is steeper than the outer edge. The coarsest sediments is deposited along the channel flanks, grading into finer sediments into the floodplain, due to decrease in flow velocity further from the channel. This agrees with Weschenfelder, et al., (2010) who suggest that sandstone thickness and sediment grain

size is decaying when moving away from the channel body (Figure 2-14 A). Channel-levee deposits are commonly divided into two main facies; mud- and sand rich sediments (Kane, et al., 2007). Sand rich deposits occur close to the channel. Due to the proximal placement of the observed levees and the observed high amplitudes, the deposits are interpreted to represent very fine sand to fine sand, same as the dominant sand deposits in Channel 1 (chapter 2.6.1). This may indicate high flow velocity with high deposition rate (Kane, et al., 2007).

In times of high energy in a river, the flow potentially cuts through the channel levees, forming crevasse splays on the floodplain, transporting coarser grains across the floodplain (Bridge & Demicco, 2008). This is also observed in Channel 1, where the interpreted lobate crevasse splays is suggested to consist of a thin sediment layer with coarser grains than its surroundings.

As mention, Channel 1 was deposited during the S4 Triassic succession. The seismic features found in Channel 1 (meandering bends, levees, crevasse splays) fits well with the theory that the upper part of this sequence is being dominated by continental deposits (Chapter 5.3, S4).

6.2.2 Channel 2

The interpretation of the morphology of Channel 2 can be related to the classification system defined by Rosgen (2007) presented in chapter 2.5.6. The sinuosity of Channel 2 was found to be 1.01, with a width to thickness ratio varying from approximately 15 - 25. Based on these calculated parameters, Channel 2, as it occur in the seismic data, does not have a good match with any of the described rivers in Rosgen (2007). Due to the sinuosity and the observed mid channel bars, the channel is closest to be interpreted as a braided channel, classified as type D. The calculated width to thickness will then be too small, according to Rosgen. This mismatch could probably be caused by Channel 2 consisting of smaller outer parts below vertical resolution. Another source of error could be over-estimated vertical channel depth.

Compared to Channel 1, the straight shape of Cannel 2, could indicate a more energetic flow. According to (Ferguson, 1993), braided rivers are distinctive due to high stream power and subsequent high rates of erosion and deposition compared to other river types *(Figure 6-1*). Channel 2 was interpreted to consist of coarser material than the surroundings and the interpreted mid channel bars. This is due to the high amplitude values observed on the envelope map (*Figure 5-15 C*) and described in chapter 5.3. This interpretation is also is in line with Nichols (2009), where the coarsest material will be transported between the bars, where the flow is strongest, and the material deposited on the channel floor. The gamma ray log, together with the neutron density log from well 7224/2-1 *(Figure 5-3)* indicate sand deposits in Channel 2. Since braided channel fills are dominated by coarse-grain,

with little suspended-load material, due to the high streaming power (Ferguson, 1993), Channel 2 is interpreted to consist of coarse sand deposits.

The gamma ray also reveals a sufficient difference in values within and outside the channel. The value is significant higher in the outer parts, which represents a higher shale-content deposition. This is interpreted to represent marine deposits, probably from transgression, where marine sediments is overlain by land sediments.

The elongated features observed in Channel 2 are interpreted to be mid channel bars, which forms in times with high discharges. The high energy water flow may produce a distinct braided channel pattern, as much as different periods of climatic stability may produce a single, straight channel (Bridge, 1993); (Whited, et al., 2007). The mid channel bars in Channel 2 appear to be longitudinal bars due to their shape. The red color observed in the RGB map (*Figure 5-15 B)* indicate a massive sediment body. The envelope map reveals the same lower amplitude value in the bars as the surrounding material outside the channel, probably muddy sediments. Braided channels are typical wide rivers, with content of bars in different size and shape (Nichols, 2009).

When investigating the development of the channel, the use of several time-slices was useful, since it could give a better understanding of the development of the channel system *(Figure* **5-15** *6-2*). The time-slices indicate that Channel 2 has developed over time with integration and connection of several channel systems, see *Figure 6-2*.

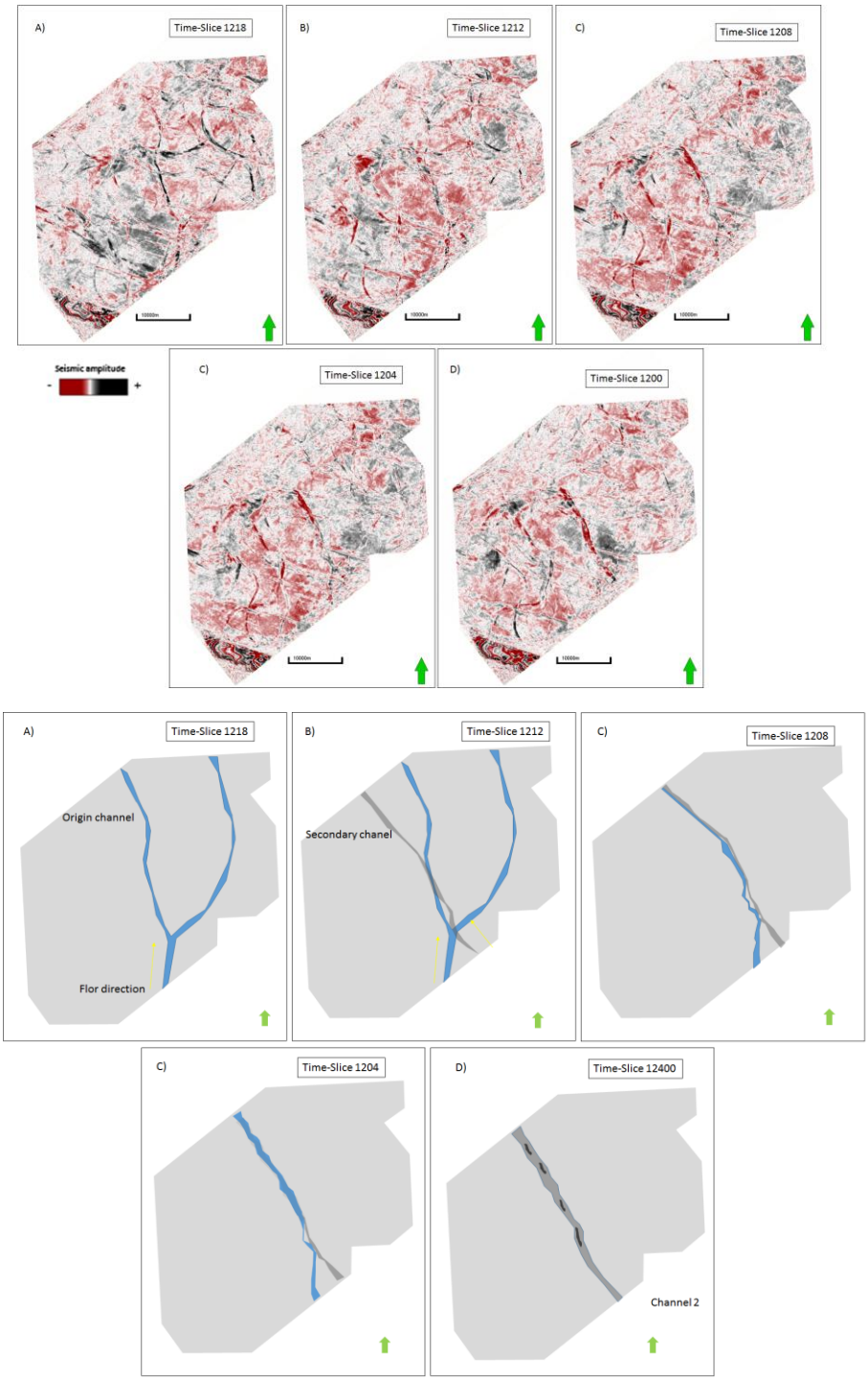

Figure 6-2. A) *The interpretation of the deeper stratigraphic level shows a clear channel feature from south-east, separating by two northwest and northeast oriented channel-arms. B) When moving further up in the seismic time-slice, another stream is observed from east, passing through the original channel in a southeast-nortwest direction. C) Further up in the seismic section, it seems like the main channels meet, and flow next to each other, separated with braids. The secondary channel changes direction to a more southeast-northwest D) The channel seems to be fully connected with a common direction against northwest, with the parts that were separating described above, as bars.*

Channel 2, explorational well target

While interpreting Channel 2 and comparing it with the Kvaltann prospect, which was the secondary target of exploration well 7224/2-1, it appears to be the same channel system. According to Wintershall, this secondary target was a positive amplitude anomaly identified within the middle to upper Snadd Formation channels (NPD, 2017). The system turned out to be dry, apparently because of lacking trap, which also was predicted to be the main risk of the prospect. The Kvaltann channel came in as predicted with respect to quality reservoir sandstones as "blocky" sandstone units with high porosity (NPD, 2016).

The interpreted Channel 2 was estimated to have a channel body thickness varying between 51-81 meters (Figure 5-16 D)

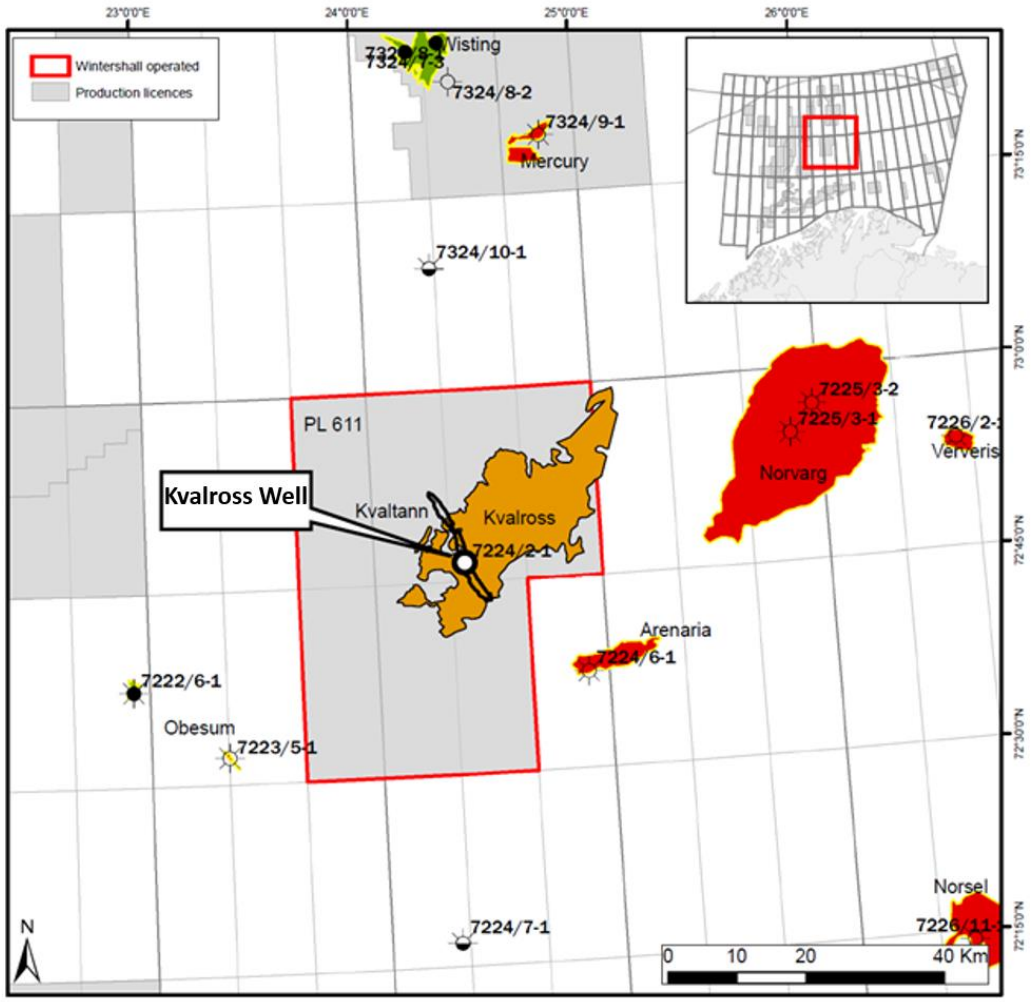

Figure 6-3. *Prospect map of well 7224/2-1 including main target Kvalross and secondary target Kvaltann. Modified from(Faroe, 2015)*

Meandering river observed in the same area as braided river

Braided rivers tend in general to occur in more proximal areas and meandering rivers occur further downstream (Nichols, 2009). This study shows an interpreted meandering rivers and a river what is believed to be braided in the same area. The high sinuosity channel is often found in lowlands, where the area is flat, and the flow has less energy, while braided river is frequently found closer to the mountains where slope is steeper and the flow has more energy. One explanation is that something has happened in the area between the appearances of the different channels. Three possible theories are carried out to explain the presence of a braided river in the same area as a meandering river. For the transition from a meandering landscape to a braided steam environment, the slope of the land has become steeper, and river suddenly receive significant more energy from the source area.

The first theory is that this increase in slope happened as a result of a tilt in the area, after the meandering river was buried. The landscape became steeper and the water flood had more energy creating a straight braided river. The second theory that could explain the presence of different channel types in the same area, is a drop in the sea-level after the meandering river was deposited. When the sea-level drops, the land is prograding into the ocean, changing the channel position from a more distal to a more proximal area, which could explain the presence of a braided river in the same area. The third reason that could cause a braided stream environment, is a sudden climate change, effecting the river discharge to suddenly create more energy.

Time slices of the braided channel shows smaller, neighboring and more sinuous channel systems, appearing to be meandering *(Figure 5-15 C).* According to Rosgen (2007), meandering rivers generally occur in alluvial valleys with low elevational relief characteristics and in low elevated coastal plains. It is therefore not believed that the braiding is caused by uplift or tilting. This interpretation is also supported by the quiet tectonic history in the area in Triassic, when the river system was active.

Due to this, the interpretation leans towards that Channel 2, because of sea level drop has been added more energy from the hinterland and received enough capacity to become a braided stream, where coarser grain has been transported.

According to Klausen, et al., 2014, several channel fill sandstone bodies that occur clustered together might be considered as indicative of a braided rive system. Also work by (Lane, 1957) and (Leopold & Wolman, 1957) indicate that there is a gradient or discharge threshold above which river tends to be braided. Experimental work reported by (Schumm & Germanoski, 1993) shows that rivers that are situated close to the meandering-braided threshold should have a history that is characterized by transition in morphology from braided to meandering and vice versa.

7. Summary and conclusions

- Interpretation of the 3D seismic survey WIN12003 correlated to exploration well 7224/2-1, located in the north-eastern part of the Loppa High, has revealed channel systems in the middle to late Triassic succession.

- Two channels, Channel 1 and Channel 2 were mapped out in the Ladinian-early Carnian (S4) sequence, which is correlated to lower Snadd formation and clearly bounded by maximum flooding surfaces.

- The interpretation of the two fluvial channel bodies show consistency with the westwards propagation of siliclastic sediments sourced from Caledonian and Uralian orogeny during Triassic.

- The sinous Channel 1 body shows typical meandering river geomorphic features, including channel-levee, point bar, crevasse splay and concave-bank deposits. Lateral migration of Channel 1 shows accretion and preservation of concave bank deposits, where the maximum thickness of the coarse-grained depositions is locaded at the closest bank to the thalweg.

- The characteristic asymmetric geometry of meandering rivers is observed in the cross-section trough the meandering bends of Channel 1, including the point bar and concave-bank deposits caused by the downstream translation and lateral expansion of this channel. The channel shows grain-size distribution typical for meandering rivers.

- Channel 2 was interpreted to be formed by high energy water flows that has produced a distinctly braided channel pattern, related to the river classification system by Rosgen (2007). The observed sinuosity and with to depth ratio have mismatch with the Rosgen classification, possible due to resolution issues and measurement insecurities, which could be investigated further.

- Channel 2 has elongated features interpreted to be mid channel bars which is visualized as massive sediment body by and interpreted to have been formed in times with high discharges.

- Interpretation shows neighboring sinuous channels to Channel 2 in the same stratigraphic level. Rivers that are situated close to the meandering-braided threshold could be characterized by transition in morphology from braided to meandering in continuous processes, controlled by discharge and gradient.

- Channel 1 and channel 2 represent what is believed to be meandering and braided rivers in the same area, where braided channel is younger than the meandering river, located higher up in the S4 unit. Meandering river overlain by braided river could indicate sea level drop.

8. References

Andreassen, K., Nilssen, E. G. & Ødegaard, C. M., 2007. *Analysis of shallow gas and fluid migration within the Plio-Pleistocene sedimentary succession of the SW Barents Sea continental margin using 3D seismic data.* s.l.:Springer-Verlag.

Ashutosh, B., Das, U., Pant, D. & Rakesh, R., 2013. *Application of Multi-Attributes and Spectral Decomposition with RGB blending for understanding the strati-structural features: A Case study,* New Delhi: Corporate Exploration Centre-ONGC Group,.

Bennett, A., n.d. *River Processes: erosion, transportation and deposition & Hjulström Curve.* [Online]
Available at: http://www.alevelgeography.com/the-long-profile-changing-processes-types-of-erosion-transportation-and-deposition/
[Accessed 09 November 2017].

Bilat, J., 2005. *Some considerations on the interpretation of seabed images based on commercial 3D seismic in the Faroe-Shetland Channel,* Edinburgh: Blackwell Publishing Ltd..

Bjarnadôttir, L. R., Winsborrow, M. C. & Andreassen, K., 2013. *Deglaciation of the central Barents Sea,* s.l.: Elsevier.

Bjorlykke, K., 2010. *Petroleum Geoscience- From Sedimentary Environments to Rock Physics.* s.l.:Springer-Verlag Berlin Heidelberg.

Bridge, J. & Demicco, R., 2008. *Earth Surface Processes, Landforms and Sediment Deposits.* s.l.:Cambridge University Press.

Bridge, J. & Lunt, I., 2006. Depositional Models of Braided Rivers.. In: I. A. o. Sedimentologists, ed. *Braided Rivers. Process, Deposits, Ecology and Management.* s.l.:Blackwell Publishing.

Bridge, J. S., 1993. *The interaction between channel geometry, water flow, sediment transport and deposition in braided rivers.* s.l.:Department of Geological Sciences, State University of New York, Binghamton, New York, 13902-6000, U.S.A. .

Bridge, J. S., 1999. *Alluvial architecture of the Mississippi valley: predictions using a 3D simulation model,* s.l.: Geological Society of London.

Bristow, C. & Best, J., 1993. Braided rivers: perspectives and problems. In: *Braided Rivers Vol 75.* s.l.:Geological Society, Special Publications.

Browne, G., 2004. *Downstream Fining and Sorting of Gravel Clasts in the Braided Rivers of mid-Canterbury, New Zealand.* s.l.:New Zealand Geographer.

Brunke, M. & Gonser, T., 1997. The ecological significance of exchange processes between rivers and groundwater. In: *Freshwater Biology, Volume 37.* s.l.:Wiley-Blackwell, pp. 1-37.

Bryhni, I., Hallenstvedt, A., Askheim, S. & Hoel, A. H., 2017. *Barentshavet.* [Online]
Available at: https://snl.no/Barentshavet
[Accessed 22 10 2017].

Bryhni, I., Ramberg, I. B., Nøttvedt, A. & Rangnes, K., 2013. *Landet blir til.* 2 ed. Trondheim: Norsk geologisk forening.

Chopra, S. & Marfurt, K. J., 2005. *Seismic attributes — A historical perspective,* s.l.: Society of Exploration Geophysicists.

Chopra, S. & Marfurt, K. J., 2012. *Seismic attribute expression of differential compaction.* s.l.:SEG Las Vegas 2012 Annual Meeting.

Clark, J. D. & Pickering, K. T., 1996. *Architectural elements and growth patterns of submarine channels; application to hydrocarbon exploration.* s.l.:AAPG Bulletin. American Geological Institute..

Collinson, J., 1996. Alluvial Sediments. In: H. Reading, ed. *Sedimentary Environments, Processes, Facies and Stratigraphy.* s.l.:Wiley-Blackwell, pp. 37-81.
Dalrymple, R. W., 2010. Introduction to siliciclastic facies models. In: D. R. James N.P., ed. *Facies Models 4.* s.l.:Geological Association of Canada.
Dey, S., 2014. Fluvial processes: Meandering and brading. In: *Fluvial Hydrodynamics. Hydrodynamics andSediment Transport phenomena.* Berlin : Springer .
Donselaar, M., Gozalo, M. C. & Moyano, S., 2007. Avulsion processes at the terminus of low-gradient semi-arid fluvial systems: Lessons from the Río Colorado, Altiplano endorheic basin, Bolivia. *Elsevier,* Volume 283, pp. 1-14.
Dorê, A., 1994. *Barents Sea Geology, Petroleum Resources and Commercial Potential,* s.l.: The Arctic Institute of North America.
Duncan, G. & Harding, J. S., 2007. *Braided river ecology. A literature review of physical habitats and aquatic invertebrate communities.* s.l.:Science & Technical Publishing.
Einsele, G., 1992. *Sedimentary Basins: evolution, facies, and sediment budget.* s.l.:Springer-Verlag Berlin Heidelberg.
Ellen Wohl, M. K. M. A. O. A. K. M. F. S. L. K. R. W. L. T.-L. N. B. J. T. P. H. T. a. F. B. V., 2013. Synthesizing the Scientific Foundation for Ordinary High Water Mark Delineation in Fluvial Systems. *US Army Corps of Engineers,* pp. 1-217.
Faleide, J. I., Gudlaugsson, S. T. & Jacquart, G., 1984. Evolution of the western Barents Sea. In: *Marine and Petroleum Geology.* Oslo: Elsevier, pp. 123-150.
Faleide, J. I., Vågnes, E. & Gudlaugsson, S. T., 1993. *Late Mesozoic-Cenozoic evolution of the south-western Barents Sea in a regional rift-shear tectonic setting,* Oslo: Elsevier.
Ferguson, R., 1993. *Understanding braiding processes in gravel-bed rivers: progress and unsolved problems.* s.l.:Geological Society, London, Special Publications, 75..
Formel, S., 2007. *Local seismic attributes,* s.l.: Society of exploration geophysicists.
Frick, J., 2014. *Colour blending in GeoTeric.* [Online]
Available at: http://www.geoteric.com/blog/wordpress/2014/02/06/colour-blending-in-geoteric
[Accessed March 2018].
Frick, J., 2015. *Enhancing your stratigraphic features on RGB color blends.* [Online]
Available at: http://www.geoteric.com/blog/wordpress/2015/11/05/enhancing-your-stratigraphic-features-on-rgb-color-blends
[Accessed 13 January 2018].
Galloway, W. E. & Hodbay, D. K., 1996. Alluvial Fans. In: *Terrigenous Clastic Depositional Systems.* s.l.:Springer-Verlag Berlin Heidelberg.
Gay, A. et al., 2005. Isolated seafloor pockmarks linked to BSRs, fluid chimneys, polygonal faults and stacked Oligocene–Miocene turbiditic palaeochannels in the Lower Congo Basin. In: *Marine Geology. Vol 226.* s.l.:Elsevier, pp. 25-40.
Gernigon, L. et al., 2014. Crustal and basin evolution of the southwestern Barents Sea: From Caledonian orogeny to continental breakup. *Tectonics,33 - An agu journal*, 7 April, pp. 347-373.
Glørstad-Clark, E., Faleide, J. I., Lundschien, B. A. & Nystuen, J. P., 2010. Triassic seismic sequence stratigraphy and paleogeography of the western Barents Sea area. In: *Marine and Petroleum Geology.* Oslo: Elsiver, pp. 1448-1475.
Gonzalo, V. D., Apalletti, L. A. & Flint, S. S., 2007. Anatomy of a Fluvial Lowstand Wedge: The Avilé Member of the Agrio Formation (Hauterivian) in Central Neuquén Basin (Northwest Neuquén Province), Argentina. In: E. W. C. P. Gary Nichols, ed. *Sedimentary Processes, Environments and Basins: A Tribute to Peter Friend.* s.l.:International Association of Sedimentologists, pp. 341-365 .

Grabau, A. W., 1920. *A Textbook of Geology.* Boston: Heath & Co..
Gradstein, F. M., Ogg, J. G., Schimtz, M. & Ogg, G., 2012. The Chronostratigraphic Scale. In: *The Geologic Time Scale.* s.l.:Elsevier, p. 32.
Grenfell, M. C., 2012. *Dynamics and Morphodynamic Implications of Chute Channels in Large, Sand-Bed Meandering Rivers.* s.l.:University of Exeter.
Gudlaugsson, S. T., Faleide, I. J. & Breivik, A. J., 1998. Late Palaeozoic structural development of the South-western Barents Sea. In: *Marine and Petroleum Geology.* Oslo: Elsevier, pp. 73-102.
Gulliford, A. R., Flint, S. S. & Hodgson, D. M., 2017. Crevasse splay processes and deposits in an ancient distributive fluvial system: The lower Beaufort Group, South Africa. *Elsevier,* Volume 358, pp. 1-18.
Hajek, E. & Edmonds, D., 2014. Is river avulsion style controlled by floodplain morphodynamics?. *Geological Society of America,* Volume 42, pp. 199-202.
Hayes, C., n.d. *Shutterstock, River system diagram..* [Online]
Available at: https://www.shutterstock.com/image-vector/river-system-diagram-465543794
[Accessed 17 Desember 2017].
Henriksen, E. et al., 2011. Tectonostratigraphy of the greater Barents Sea: implications for petroleum systems. In: *Arctic Petroleum Geology.* s.l.:Geological Society of London, pp. 163-195.
Holdaway, K. R., 2016. *erived Seismic Attributes Underpin Reservoir Characterisation in Data-Driven Methodologies,* s.l.: Sosiety of petroleum engenieers.
Hubbard, S. M. et al., 2011. *Seismic geomorphology and sedimentology of a tidally influenced river deposit, Lower Cretaceous Athabasca oil sands, Alberta, Canada.* s.l.:AAPG Bulletin.
Hudson-Edwards, K., 2007. Fluvial environment. In: *Environmental Sedimentology.* s.l.:Blackwell Publishing.
Janocko, M., Nemec, W., Henriksen, S. & Warchol, M., 2012. The diversity of deep-water sinuous channel belts and slope valley-fill complexes. In: *Marine and Petroleum Geology. Vol 41.* s.l.:Elsevier, pp. 7-34.
Jones, H. & Hajek, E., 2007. Characterizing avulsion stratigraphy in ancient alluvial deposits. *Elsevier,* 202(1-2), pp. 124-137.
Kane, I. A., Catteral, V., McCaffrey, W. D. & Martinsen, O. J., 2010. *Submarine channel response to intrabasinal tectonics: The influence of lateral tilt.* s.l.:The American Association of Petroleum Geologists. AAPG Bulletin..
Kane, I. A. et al., 2007. Anatomy of a submarine channel–levee: An example from Upper Cretaceous slope sediments, Rosario Formation, Baja California, Mexico. In: *Marine and Petroleum Geology. Vol 24.* s.l.:Elsevier.
Kearey, P., Brooks, M. & Hill, I., 2002. *An Introduction to Geophysical Exploration.* 3. ed. s.l.:Blackwell Science Ltd.
Keylock, C., 2014. Reviewing the Hjulstroms curve. *Geography Review,* 17(Phillip Allan publisher), pp. 16-20.
Klausen, T. G. et al., 2014. Spatial and temporal changes in geometries of fluvial channel bodies from the Triassic Snadd Formation of offshore Norway. *Journal of Sedimentary Reaserch,* Volume 84, pp. 567-585.
Klausen, T. G. et al., 2015. Regional development and sequence stratigraphy of the Middle to Late Triassic Snadd Formation, Norwegian Barents Sea. *Elsevier,* pp. 102-122.

Lane, E., 1957. *A study of the shape of channels formed by natural streams flowing in erodible material.* s.l.:U.S. Army Engineers Division, Missouri River, Corps of Engineers, Omaha, Nebraska.
Langbein, W. B. & Leopold, L. B., 1968. *River Channel Bars and Dunes - Theory of Kinematic Waves,* Washington: U.S.G.S. Prof.
Leeder, M., 2011. River and Fan Deltas. In: *Sedimentology and Sedimentary Basins, From Turbulence to Tectonics.* s.l.:Wiley-Blackwell, pp. 386-412.
Leopold, L. B. & Wolman, M. G., 1957. *River Channel Patterns: Braided, Meandering and Straight.* s.l.:U.S. Geological Survey Professional.
Lin, D. A. T., 2012. *Seismic Stratigraphy.* Taoyuan City: National Central Univ., Department of Earth Sciences.
Makaske, B., 2000. *Anastomosing rivers: a review of their classification, origin and sedimentary products.* s.l.:Elsevier.
Marshak, S., 2005. Streams and Floods: The Geology of Running Water. In: *Earth portrait of a planet.* s.l.:W. W. Norton & company.
McArdle, N. et al., 2010. *Spits, channels and beaches: advanced imaging and delineation of Jurassic and Triassic stratigraphic targets.* [Online]
Available at: https://www.geoteric.com/hubfs/uploads/downloads/PETEX_2010.pdf
[Accessed 13 February 2018].
Miall, A., 1992. Alluvial Deposits. In: *Facies models: response to sea level.* s.l.:St. John's, Nfld. : Geological Association of Canada.
Miller, M. B., n.d. *Alluvial Fans.* [Online]
Available at:
http://www.seddepseq.co.uk/DEPOSITIONAL_ENV/Fluvial/Alluvial/AlluvialFan.htm
[Accessed May 2018].
Mjos, R., Walderhaug, O. & Prestholm, E., 1993. *Crevasse Splay Sandstone Geometries in the Middle Jurrasic Ravenscar Group of Yourkshire, UK,* Stavanger, Nowray: Rogaland Research Institute.
Mosaselim, A., 2015. *SEDIMENTARY DEPOSITIONAL ENVIRONMENTS.* [Online]
Available at:
https://www.emaze.com/@ALRRWRRC/sedimentarydepositionalenvironments-120204112837-phpapp02.pptx
[Accessed 21 November 2017].
Nainggolan, H., 2014. *2 D HIGH RESOLUTION MARINE SEISMIC DATA PROCESSING BY USING SEISMIC UNIX: PART- 2: TRACE EDITING.* [Online]
Available at: http://totalcorner.blogspot.no/2014/05/2-d-marine-seismic-data-processing-by.html
[Accessed 10 October 2017].
Naseer, T. M. et al., 2014. *Application of Seismic Attributes for Delineation of Channel Geometries and Analysis of Various Aspects in Terms of Lithological and Structural Perspectives of Lower Goru Formation, Pakistan,* s.l.: International Journal of Geosciences.
Nichols, G., 2009. *Sedimentology and Stratigraphy.* 2nd ed. s.l.:Wiley-Blackwell.
Nichols, G., Williams, E. & Paola, C., 2007. *Sedimentary Processes, Environments and Basins: a Tribute to Peter Friend.* s.l.:Blackwell Publishing.
North, C. P. & Warwick, G. L., 2007. FLUVIAL FANS: MYTHS, MISCONCEPTIONS, AND THE END OF THE TERMINAL-FAN MODEL. *Journal of Sedimentary Research,* Volume 77, pp. 693-701.
NPD, 2012. *NPD.* [Online]
Available at:

http://factpages.npd.no/FactPages/default.aspx?nav1=survey&nav2=PageView|Finished|2012&nav3=7615
[Accessed 06 January 2018].
NPD, 2017. *Doubling the resource estimate for the Barents Sea, NPD.* [Online]
Available at: http://www.npd.no/en/news/News/2017/Doubling-the-resource-estimate-for-the-Barents-Sea/
[Accessed 25 January 2018].
NPD, 2017. *NPD.* [Online]
Available at:
http://factpages.npd.no/ReportServer?/FactPages/PageView/wellbore_exploration&rs:Command=Render&rc:Toolbar=false&rc:Parameters=f&NpdId=7870&IpAddress=195.88.107.70&CultureCode=nb-no
[Accessed 14 April 2018].
NPD, 2017. *NPD.* [Online]
Available at:
http://factpages.npd.no/ReportServer?/FactPages/PageView/wellbore_exploration&rs:Command=Render&rc:Toolbar=false&rc:Parameters=f&NpdId=7870&IpAddress=195.88.107.70&CultureCode=nb-no
[Accessed 03 January 2018].
NPD, 2018. *NPD.* [Online]
Available at:
http://factpages.npd.no/ReportServer?/FactPages/PageView/discovery&rs:Command=Render&rc:Toolbar=false&rc:Parameters=f&NpdId=20441001&IpAddress=195.88.107.70&CultureCode=en
[Accessed 03 May 2018].
NPD, n.d. *Fact maps, Norwegian Petroleum Directorate.* [Online]
Available at: 2018
[Accessed 13 January 2018].
NPD, n.d. *Factapages, Norwegian petroleum directorate.* [Online]
Available at:
http://factpages.npd.no/FactPages/default.aspx?nav1=discovery&nav2=PageView%7CAll&nav3=45026
[Accessed 13 February 2018].
Perry, C. & Taylor, K., 2007. Environmental Sedimentology: Introduction. In: *Environmental Sedimentology.* s.l.:Blackwell Publishing, pp. 1-31.
Posamentier, W. H. & Walker, R. G., 2006. *Faciees Models Revised.* s.l.:SEPM Society for Sedimentary Geology.
Press, F. & Siever, R., 1986. *Earth.* 2nd ed. New York: W.H. Freeman and Co.
Rider, M. & Kennedy, M., 2011. *The Geological Interpretation of Well Logs.* Sutherland: Rider-French Consulting Limited.
Riis, F. et al., 2008. *Evolution of the Triassic shelf in the northern Barents Sea region,* Stavanger: Norsk Polarinstitutt.
Ritzmann, O. & Faleide, I. J., 2007. Caledonian basement of the western Barents Sea. *Tekconics, 26 - An agu journal*, 10 Oktober.
Rogers, D. J., 2008. *CHAPTER FOUR: HISTORYOF THE NEW ORLEANS FLOOD PROTECTION SYSTEM,* s.l.: New Orleans Levee Systems. Hurricane Katrina.
Rosgen, D. & Silvey, H., 1996. *Applied River Morphology.* s.l.:International Journal of Geosciences.

Sambrook Smith, G. H. et al., 2006. *Braided Rivers: Process, Deposits, Ecology and Management.* s.l.:Blackwell Publisher.
Schlumberger, 2010. *Attribute Matrix, Petrel,* s.l.: Schlumberger.
Schmidt, I., Paton, G. S. & Lacaze, S., 2013. *Spectral Decomposition and Geomodel Interpretation - Combining Advanced Technologies to Create New Workflows.* [Online]
Available at:
https://www.researchgate.net/publication/266633652_Spectral_Decomposition_and_Geomodel_Interpretation_-_Combining_Advanced_Technologies_to_Create_New_Workflows?enrichId=rgreq-5ce7dcc53d03d4acc805aa3b1f1315c9-XXX&enrichSource=Y292ZXJQYWdlOzI2NjYzMzY1MjtBUz
[Accessed 10 February 2018].
Schumm, S. A., 2005. *River variability and complexity. Cambridge.* s.l.:University Press, Cambridge.
Schumm, S. & Germanoski, D., 1993. Changes in Braided River Morphology Resulting from Aggradation and Degradation. In: *The Journal of Geology, Vol 101.* s.l.:The University of Chicago Press, pp. 451-466.
Smelror, M., Petrov, O. V., Larssen, G. B. & Werner, S., 2009. *Geological History of the Barents Sea.* Trondheim: NGU.
Stanford, J. & Ward, J., 1988. *The hyporheic habitat of river ecosystems.* s.l.:Nature, international journal of science.
Steel, G., 1980. *Clastic Depositional Environments..* [Online]
Available at:
http://www.uwosh.edu/faculty_staff/hiatt/Teaching/314/Clastic_Environs1.html
[Accessed 13 February 2018].
Stemmerik, L., 2000. Late Palaeozoic evolution of the North Atlantic. *Palaeogeography, Palaeoclimatology, Palaeoecology*, 31 July, pp. 95-126.
Sylvester, Z., Primez, C. & Cantelli, A., 2010. A model of submarine channel-levee evolution based on channel trajectories: Implications for stratigraphic architecture. In: *Marine and Petroleum Geology. Vol 28.* s.l.:Elsevier, pp. 716-727.
Taner, M. T., 2003. *Attributes Recisited,* s.l.: Rock solid images.
Technical Supplement, 3., 2007. *Rosgen Stream Classification Technique—Supplemental Materials.* s.l.:National Engineering Handbook.
The Environment Agency, 2010. *Environment Agency, Fluvial Ecology.* [Online]
Available at: http://evidence.environment-agency.gov.uk/FCERM/en/FluvialDesignGuide/Chapter4.aspx
[Accessed January 2018].
Van Djiik, W., Van de Lageweg, W. & Kleinhans, M., 2012. *Experimental meandering river with chute cutoffs.* s.l.:JOURNAL OF GEOPHYSICAL RESEARCH, VOL. 117.
Weschenfelder, J., Stalliciere Corrêa, I. C., Aliotta, S. & Baitelli, R., 2010. *Paleochannels related to late quaternary sea-level changes in Southern Brazil.* s.l.:Brazilian Journal of Oceanography.
Whited, D. et al., 2007. *Climate, hydrologic disturbance, and succession: drivers of floodplain pattern..* s.l.:Division of Biological Sciences, The University of Montana.
Woessner, W. W., 2000. *Stream and Fluvial Plain Ground Water Interactions: Rescaling Hydrogeologic Thought.* s.l.:Groundwater, Volume 38.
Wooster, J., 2002. *A Braided River System in a Glacial Environment, the Copper River, Alaska.* s.l.:s.n.

Worsley, D., 2008. *The post-Caledonian development of Svalbard and the western Barents Sea,* Sætre, Norway: Polar Research.